To the Graduate Council :

I am submitting herewith a thesis written by Lawrence Mancil Garrett entitled "The Design and Prototyping of a Four Degree of Freedom, Low-Cost, High-Speed, Cartesian-Motion Robot." I have examined the final copy of this thesis for form and content and recommend that it be accepted in partial fulfillment of the requirements for the degree of Master of Science, with a major in Mechanical Engineering.

Frank Speckhart, Major Professor

We have read this thesis

and recommend its acceptance:

Ray W. Holland

Clement C. Wilson

Accepted for the Council:

Vice Provost

and Dean of the Graduate School

THE DESIGN AND PROTOTYPING OF A FOUR DEGREE OF FREEDOM, LOW-COST, HIGH-SPEED, CARTESIAN-MOTION ROBOT

A Thesis

Presented for the

Master of Science

Degree

The University of Tennessee, Knoxville

Lawrence Mancil Garrett

May 1989

Copyright © Lawrence Mancil Garrett, 1989
All Rights Reserved

ACKNOWLEDGEMENTS

There are many people who deserve recognition for their contributions during the development of this project. I wish to thank International Business Machines for their involvement in the Technical Interchange Program, without which the project would have never existed. Their reviews and technical support of the project were essential.

I am very grateful to my major professor, Dr. Frank Speckhart, for involving me in this project. His patience and insight in helping me solve problems was invaluable.

I also wish to thank my committee members, Dr. Clem Wilson, for his consistent interest in the robot's development, and Professor Ray Holland, for his help in supplying molding techniques.

Mr. Mark Granger deserves recognition, not only for designing the first prototype of the robot, but for the patient manner in which he brought me up to date at the beginning of the project.

It was also very educational and a pleasure to work with Mr. Siak Yeo, the designer of the robot's software and controller, Mr. Daniel Graham, the machinist for the prototype, and Mr. Dennis Higdon, the senior electronic technician for the department.

I wish to thank Linda Stooksbury, the senior accounting clerk for the department, for her efficient handling of all the paperwork involved in this project.

Fred Baes, a biologist a Oak Ridge National Laboratory, deserves recognition for his software support and assistance in producing this document.

Finally, I wish to thank my fiancee, Karen Hostetler, a mechanical engineer at the Tennessee Valley Authority, for her understanding and editing of this report.

ABSTRACT

Today's robots are expensive, highly accurate, and use complex control techniques. However, industry lacks low-cost robots that can perform medium accuracy assembly operations and material handling. International Business Machines, through the Technical Interchange Program, supported the development of a low-cost, high-speed, cartesian motion robot to fill this niche. Several design requirements were specified; the most important was a total cost of $600. High speed was the next most important consideration. Stepper motors with open-loop control were specified. Four degrees of freedom were required: three translations, and one yaw rotation. The design also required modularity and ease of manufacture. The high volume production model will need to use plastic injection molded parts wherever possible to achieve minimal cost per part. Timing belts were required to minimize backlash, cost, and maintenance, and to increase reliability. An error detection/recovery capability was needed so that the robot could periodically recalibrate itself. The payload specified was three pounds. One possible application of the prototype is in an IBM circuit board manufacturing facility.

A first prototype which performed only horizontal positioning, was developed as a master's thesis by Mark Granger, in the Department of Mechanical Engineering, at the University of Tennessee, Knoxville. For this second prototype, the bearings were replaced with rolling element bearings to increase its reliability. PVC plastic that has been bonded together is used to model the injection molded parts. This second prototype had a vertical arm that can also rotate. The cost of the proposed design has a projected cost of $1066 per robot, based on production of 200,000 robots. A maximum horizontal speed of the arm is 48 in/sec with an average velocity of 28 in/sec for a 12 inch move.

This thesis discusses the design overview and methodology of the robot, projected performance and performance testing of the prototype, assembly instructions, failure modes and their correction, an analysis of the critical tolerances, a cost analysis and recommendations.

TABLE OF CONTENTS

CHAPTER PAGE

1. INTRODUCTION....1
   1.1 Background....1
   1.2 Design Goals and Requirements....2
   1.3 Scope....2
   1.4 Technical Changes Made During The Design Process....3

2. DESIGN OVERVIEW....4
   2.1 Method of Operation: X-Y Plus horizontal Positioning Mechanism....4
   2.2 Method of Operation: Vertical Translation And Yaw Rotation....5
   2.3 Robot Frame Features....5
   2.4 Robot Electronics and Control....8

3. DESIGN METHODOLOGY....9
   3.1 Plastic Molding Considerations....9
   3.2 X-Y Plus System Changes....9
   3.3 Z Platform Assembly....11
   3.4 Z Arm Guide Tube and Yaw Rotation....14

4. PROTOTYPE DESIGN AND CONSTRUCTION....16
   4.1 Z Platform Prototyping....16
   4.2 Z Arm Guide Tube and Yaw Rotation....17
   4.3 X-Y Plus System....17
   4.4 Robot Frame....18

5. THEORETICAL CONSIDERATIONS....19
   5.1 Projected Performance; X-Y Plus and Z Arm....19
   5.2 Accuracy Analysis of Critical Tolerances....22
   5.3 Binding Analysis: X-Y Plus System Binding....29
   5.4 Binding Analysis: Z Arm Binding....30
   5.5 Frame Analysis....32
   5.6 Z Arm Guide Tube Groove Analysis....34

6. PERFORMANCE TESTING OF PROTOTYPE....39
   6.1 Repeatability Test....39
   6.2 Z Arm Settling Time....39
   6.3 Cyclic Testing....45
   6.4 Failure Modes....47
   6.5 Prototype Performance Data....48

7. COST ANALYSIS....50

CHAPTER PAGE

8. RECOMMENDATIONS....53
8.1 Possible Molding Considerations....53
8.2 Parts To Be Upgraded....56

LIST OF REFERENCES....58

APPENDICES....59
A Analysis of Critical Tolerances....60
B Binding Analysis For Z Arm....69
C Frame Analysis....72
D Z Arm Groove Analysis....78
E Repeatability Test....84
F Z Arm Settling Time Test....86
G PVC Pull Test....100
H Prototype Pictures....103
I Vendors and Price References....110
J Robot Assembly Procedures....113

VITA....120

LIST OF FIGURES

FIGURE PAGE

2.1 X-Y Plus horizontal positioning mechanism....4
2.2 Assembled view of the Z Platform assembly....6
2.3 Assembled view of the low-cost robot....7
3.1 Redesigned Slider for the X-Y Plus system....10
3.2 Isometric views of the Z Platform....12
3.3 Exploded view of the Z Platform assembly....13
3.4 Exploded view of the Z Arm assembly....15
5.1 Maximum average velocity versus horizontal travel....19
5.2 Optimum pulley radius for horizontal moves....20
5.3 Maximum average velocity versus upward travel....21
5.4 Optimum pulley radius for vertical moves....21
5.5 Inaccuracy due to corner bracket misalignment....23
5.6 Case of non-orthogonal control tubes....24
5.7 Corner bracket elevation effects....25
5.8 Horizontal bearing clearance contributions....26
5.9 Vertical bearing clearance contributions....27
5.10 X-Y Plus system binding....29
5.11 Free body diagram of Z Arm during upward travel....30
5.12 Z Arm efficiency with increased force offset distance using various friction coefficients....31
5.13 Two dimensional model of frame....32
5.14 Stiffness of 2-D frame model with increasing frame arm inertia....35
5.15 Relative volume of 2-D frame model with increasing frame arm inertia....36
5.16 Insert pull-out force for increasing groove depth using selected applied torques....38
6.1 Impulse response of unloaded Z Arm and subsequent integrations....40
6.2 Displacement specification envelope....41
6.3 Dual channel output of motor pulse duration and Z arm acceleration....42
6.4 Z Arm residual vibration without payload....43
6.5 Residual vibration of Z Arm with 3.5 lb payload....44
8.1 Possible methods of timing belt attachment to sliders....54
8.2 Present design of corner bracket....55

LIST OF PLATES

PLATE	PAGE
(1) Z Platform	In pocket
(2) Slider	In pocket
(3) Z Arm Tubes	In pocket
(4) Z Arm Drive Components	In pocket
(5) Z Platform Mast	In pocket
(6) Tube Mount	In pocket
(7) Z Platform Prototype	In pocket
(8) Z Platform Prototype Bosses	In pocket
(9) Slider Prototype	In pocket
(10) Frame Legs	In pocket
(11) Frame Arms	In pocket
(12) Assembled View of Z Platform With Parts List	In pocket

CHAPTER 1

INTRODUCTION

1.1 Background

In the Fall of 1986, IBM Charlotte contracted with the University of Tennessee, Knoxville to design a high-speed, low-cost, cartesian motion robot. The robot would be used for low-accuracy, light-weight assembly operations, such as handling circuit boards in an IBM manufacturing facility. An inexpensive design was an essential requirement. The robots that are currently available are more sophisticated than necessary, and are therefore not cost effective.

The robot required five degrees of freedom: three translations, and two rotations. Other criteria were a modular design, a stepper motor/open loop control, and an error detection/recovery capability. Through the Technical Interchange Program (TIP), Mr. Mark Granger, a mechanical engineering graduate student at the University of Tennessee, Knoxville, developed a method for performing the horizontal translations and a program for modeling stepper motor performance.

The horizontal motions are achieved by the "X-Y Plus" system. Two horizontal shafts lie at right angles to one another and are free to move horizontally, relative to each other, along outer guide shafts. Four corner brackets support the robot, house the motors and idler pulleys, and hold the four outer guide shafts in an orthogonal position. The tubes are actuated by a timing belt/pulley arrangement that is powered by four stepper motors. Both ends of each tube are attached to a slider bracket that houses a bearing and serves as the attachment point for a timing belt. The timing belt is driven by a stepper motor. A platform is attached at the point of intersection of the two translating tubes, enabling the platform to move anywhere in the X-Y plane.

The motor program finds the optimum ramp function to accelerate/decelerate the stepper motor, compensating for the influence of friction, gearing, and mass of the members to which the motors drive. A ramp function is a set of delay times between motor steps, which are read by a controller program that converts the ramp data into phase signals. The phase signals are sent to the stepper motor

driver, which supplies power to the motors.

The software and the controller for the prototype were developed by Mr. Siak Yeo, an electrical engineering graduate student at the University of Tennessee, Knoxville. The drivers for the robot's motors are modified IBM Proprinter circuit boards.

1.2 Design Goals and Requirements

Low cost is the main criteria for the robot design. Production is to be based on a quantity of 200,000 robots in five years. The functional requirements are similar to those of existing industrial robots, but with some relaxations in order to reduce cost. The details of the IBM requirements for function and design are listed below.

Functional Requirements

Rectilinear workspace
Cartesian motion
Four degrees of freedom: 3 linear, 1 rotary
39 inches per second average velocity over 12 inches
Positional accuracy within 0.118 inches (3 mm)
Maximum settling time of 0.1 second to within 0.118 inches
Limited number of predefined moves
Payload of 3 pounds

Design Goals

Low Cost: $600 maximum for parts, labor, and overhead
High speed
Modular design
Design for assembly
Stepper motor open-loop control
Error detection/recovery capability

1.3 Scope

This project includes the building of a single prototype, consistent with the ultimate goal of mass production of the robot. This includes the design and prototyping of an arm to perform the vertical translation/rotation and interface with the "X-Y Plus" design for horizontal positioning. Because open-loop stepper motor control cannot detect when the motor misses a step, the design needs to include a means for the robot to recalibrate itself periodically. Also included in this work will be a redesign of the

"X-Y Plus" design. The first prototype used sleeve bearings having a sliding coefficient of friction. The friction forces made binding likely if a misalignment occurred between the ends of the control tube.

This thesis will cover a design overview and projected performance, design and performance testing of the prototype, an analysis of the critical tolerances, a cost analysis, recommendations and assembly procedures.

1.4 Technical Changes Made During Design Process

After meeting with IBM engineers on April 7-8, 1988, the X-Y Plus system was redesigned with linear ball bushings to reduce the friction dependence of the device. The original sleeve bearings had excessive friction and could produce binding forces that would stall the motors. The stiffness of the control tubes was also reduced to help solve the binding problem. A more flexible control tube would allow the motor to deflect the tube to overcome an obstacle, such as grit, or a bend in the tube itself. Steel was selected as the tube material, based on its wear resistance as a bearing surface.

The sliders and the Z Platform were machined out of plastic for the prototype. This provides a means for testing plastic performance, since it is intended to use injection molding for mass production of parts. The original constraint against violating the area above the workspace was relaxed, and the functional requirement for pitch rotation was deleted.

Various methods of performing the vertical translation were discussed in the meeting. The use of a power screw to actuate the vertical arm was considered. A high cost ball screw would be required to limit backlash. The efficiency of a power screw is not high, and a power screw does not provide modularity if the length of travel is changed. Also, the life of a power screw is not infinite and must be readjusted to account for wear. Therefore, this method was abandoned.

The method chosen for performing the vertical translation was a timing belt arrangement. This design is both inexpensive and simple. There is no need for adjustment after assembly, and timing belts have proven to be very reliable and durable.

CHAPTER 2

DESIGN OVERVIEW

2.1 Method of Operation: X-Y Plus Horizontal Positioning Mechanism

The horizontal positioning mechanism (X-Y Plus system) has two components that will be made of plastic, the corner brackets and the sliders. These are shown in Figure 2.1 (4). The four corner brackets hold the outer guide shafts in an orthogonal position. One corner bracket mounts two 2.1 amp stepper motors, another holds two idler pulleys. The remaining two corner brackets hold one motor and one idler pulley. The corner brackets attach to the frame that elevates the robot above the workspace. All of the corner brackets are designed to come out of the same mold.

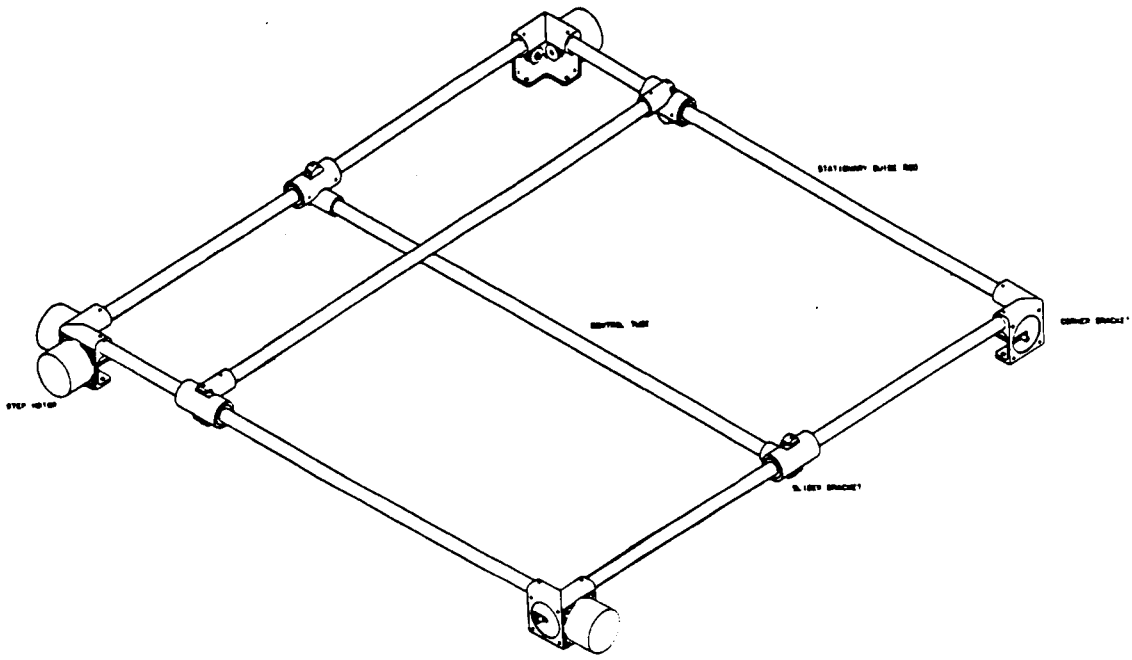

Figure 2.1: X-Y Plus horizontal positioning mechanism (4).

The sliders are mounted on each end of the two control tubes, and serve as the attachment point for the timing belt. The sliders also house the bearing that rides on the stationary guide shafts. The four sliders are identical, but are separated into pairs, one pair for each control tube. One pair of sliders is inverted with respect to the other pair. This creates a space between the orthogonal control tubes, and allows uninhibited movement of each tube. The four sliders are designed to grip the timing belt from either orientation, so that all four sliders are identical.

2.2 Method of Operation: Vertical Translation and Yaw Rotation

The vertical translation is performed by the Z Arm, which is a reciprocating tube attached to a timing belt. The belt moves the tube up and down between the motor and an upper idler pulley attached to a leaning mast. Figure 2.2 shows the assembled view of the Z Platform mechanism. A plastic platform holds the mast, the vertical arm's linear ball bushings, the bushings that ride on the horizontal control tubes, and the 2.1 amp stepper motor that drives the vertical timing belt. The yaw rotation is driven by a direct drive from a 1.1 amp stepper motor mounted on top of the vertical guide tube. The vertical guide tube does not rotate, but houses an inner drive tube that transmits the rotation to a vertical spindle located at the end of the vertical guide tube. The spindle is the attachment point for a wrist adaptor, or a tool mount.

2.3 Robot Frame Features

The frame elevates the robot above the workspace and holds the corner brackets a set distance apart. The frame is essentially a box made of steel. The vertical legs of the frame are made of square tubing. These tubes are connected at the top and bottom by equal-leg angle iron. The corner brackets bolt onto the frame with two bolts at each corner of the frame. Adjustable rubber feet are attached on the bottom of the frame to keep it level and stationary. The frame bolts together to facilitate moving the robot or changing the dimensions of the frame, should either be desired. A view of the entire robot is shown in Figure 2.3.

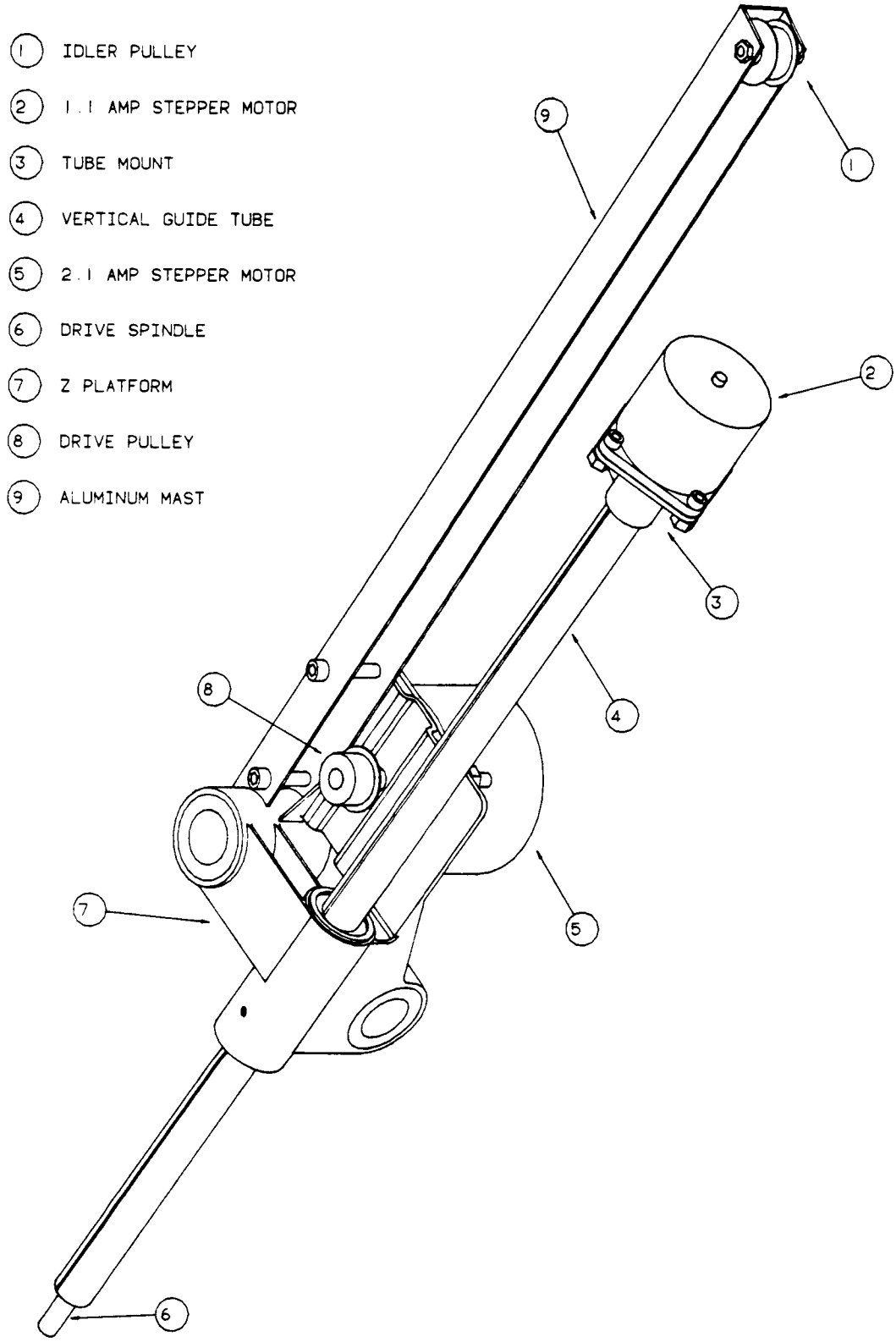

Figure 2.2: Assembled view of Z Platform assembly.

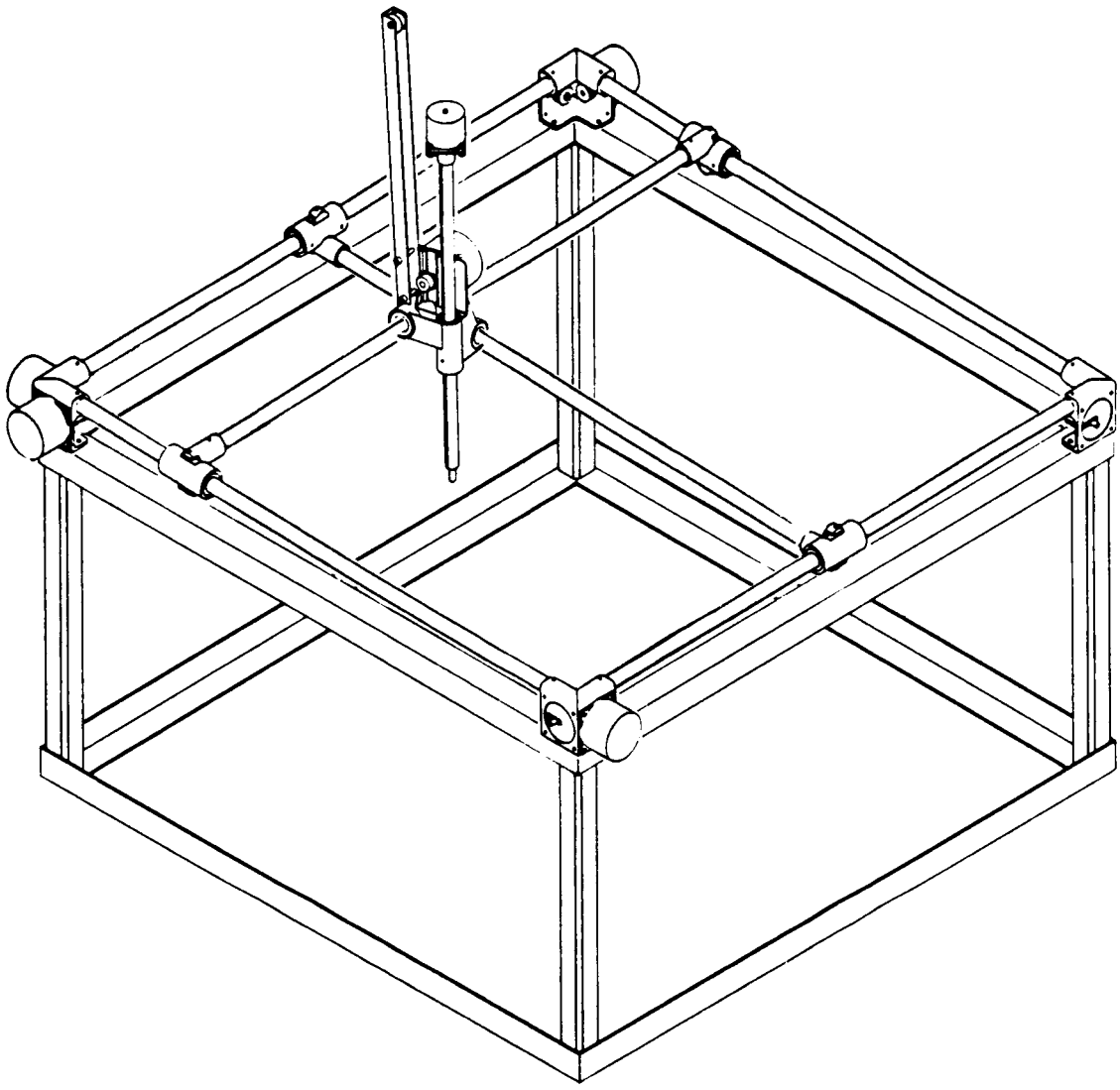

Figure 2.3: Assembled view of the low-cost robot.

2.4 Robot Electronics and Control

The electronics that actuate the robot consist of a controller and driver for each stepper motor. The computer downloads to the controller the ramps to accelerate and decelerate the motors, the move file that the robot is to perform, and the number of desired repetitions. The controller then sends the phase signals to the motor drivers that power the motors and send timed pulses of current to the appropriate phases to turn the motor. Proprinter circuit boards were provided by IBM to be used as the motor drivers. The boards were modified to run the larger 2.1 amp stepper motors by changing the voltage comparator circuitry. Two of the chips that control the printer were removed. Selected pins were then wired to the controller.

The ramps are essentially the time delays for the current pulses to the motors. Ramping up is a shortening sequence of delays that will accelerate the motor. Conversely, ramping down is a lengthening sequence of time delays that decelerates the motor. Both sets of delays are needed to control the motors, and are referred to as the ramp function. The designing of the robot's ramp function is contained in Reference (4).

Error detection is also a feature of the robot. Since the robot uses open-loop control for its motors, there is no way for the robot to know if one of its motors misses a step. Therefore, a home position is defined at one corner of the robot's workspace. Home positions also exist for the vertical arm and the yaw spindle. All of the home positions are detected by a photosensor. When the photosensor supplies a signal, the motors are reinitialized. The software controls the frequency that the robot will report home. This is the simplest form of error detection/correction, since the robot does not know when it fails but will periodically recalibrate itself whether it has missed steps or not. The software and electronics for the photosensors are still in the development stages and are not yet operational.

CHAPTER 3

DESIGN METHODOLOGY

3.1 Plastic Molding Considerations

Since the ultimate goal for the robot is high volume production with the lowest possible cost, it is desirable to use injection molding wherever possible. When designing for injection molding, one of the most critical factors is uniform wall thickness. Non-uniform wall thickness can cause dimensional instability and warpage. Strengthening a part is accomplished by the addition of ribs. Guidelines exist for the maximum wall thickness, rib design, fillets, and radii (2). There are also certain limitations in the design of holes. Blind holes are limited in their depth, and through holes that are not in line with the parting line of the mold can increase molding costs substantially. Therefore, it requires a considerable amount of experience to design a part properly for the injection molding process.

There are six different parts on the robot that should be molded. Some preliminary work has been done on the parts by using the design criteria mentioned above. More work is needed before the parts are fully suitable for molding.

3.2 X-Y Plus System Changes

The sliders, which hold the control tubes and serve as the attachment point of the horizontal timing belts, were revised only slightly from the first prototype. Figure 3.1 shows the redesigned slider. Linear ball bushings were used instead of the teflon fiber bushings for movement along the outer guide shafts. The bushings are press-fit into place. The use of the linear ball bushings made the sliders much shorter. The shorter length makes the system more prone to bind, but the extremely low friction in the bearings makes this phenomena negligible. This result agrees with the binding analysis performed on the first prototype by Mr. Granger (4). A shorter slider also slightly increases the work area of the robot. The vertical spacing between the control tubes was reduced from 0.689 inches on the first prototype of to 0.125 inches. The spacing between the tubes was decreased to make the design of the Z Platform more compact. Ribs were added to stiffen the slider after its thickness was reduced to one that could

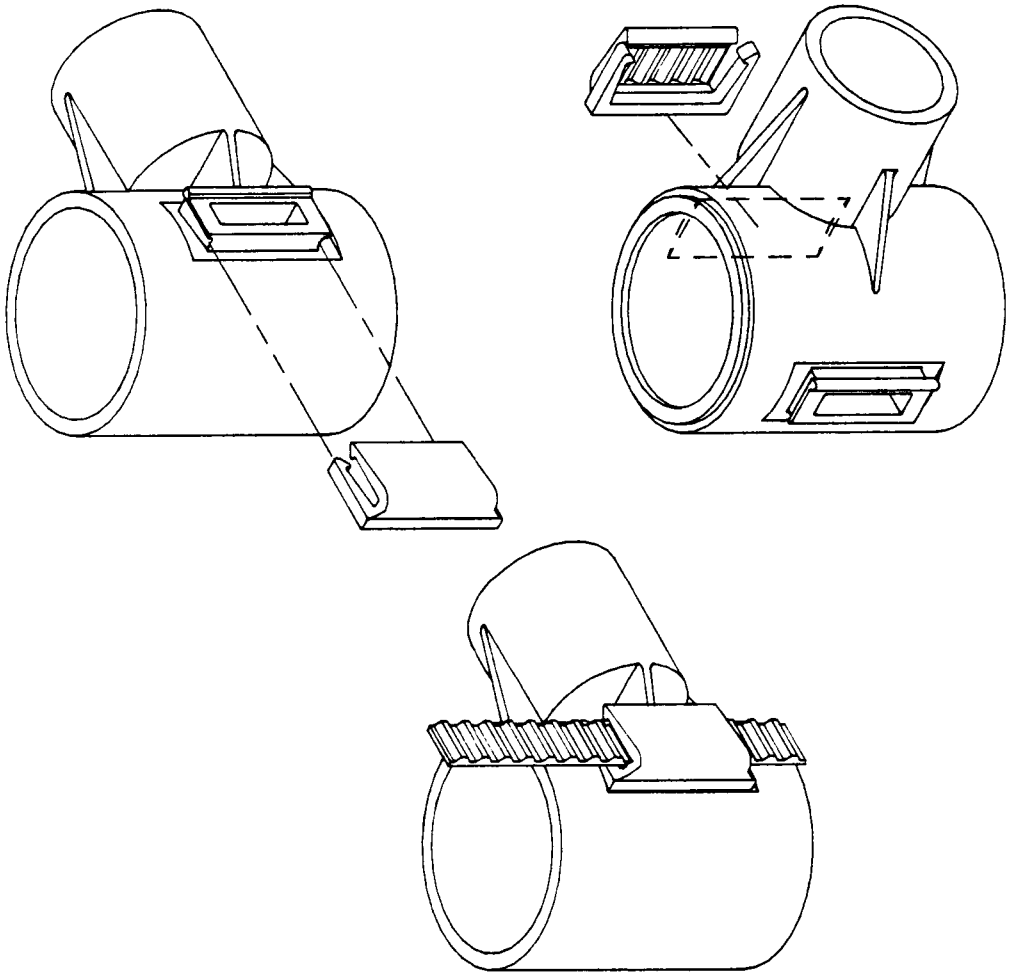

Figure 3.1: Redesigned slider for the X-Y Plus system.

be molded. The method of securing the timing belt to the slider is an item that needs further study, and is discussed in the Recommendations section.

The original method of tensioning the timing belts was changed. The earlier design tensioned the belts by pulling on the idler pulley axle along a slot in the corner brackets. This arrangement proved unsatisfactory because the tightening action of the idler axle tended to loosen the belt. The new design incorporates a small turnbuckle that grips the belt on each end by two teeth and allows it to be tensioned. A small wire is threaded through the turnbuckle to prevent it from loosening.

3.3 Z Platform Assembly

After the method of performing the vertical translation was chosen, the platform that interfaces with the X-Y Plus system, holds the vertical arm, and accommodates the linear ball bushings was designed. The first step in the conceptual design of the platform was to create a library of the motor, bearings, mast and pulleys on CADAM. CADAM (Computer Augmented Design and Manufacturing) is a CAD package provided by IBM, Charlotte. Once a library of the known components for the platform was created, these parts were arranged as closely to one another as possible without interferences. The closer the components were together, the closer the center of mass of the Z Platform would be to the intersection of the control tubes. From a plot of this general configuration, a clay model was made to understand the three dimensional geometry of the Z Platform. The next stage was another iteration with the CADAM library to define the dimensions and geometry of the platform. The results of this were shown to Mr. Matt Galatha, an IBM design engineer. His instructions were to make the platform more uniform in thickness so it would be suitable for injection molding, and to use corrugation and more ribbing to increase stiffness. Again, to help in the visualization process, a refined clay model was created. The motor mount surface was corrugated to increase its inertia with a constant thickness of 0.118 inches (3 mm). This is close to the maximum recommended thickness to which plastic should be molded to avoid sinks and warping. The cylinders that retain the ball bushings were attached with ribs and bosses. The clay model was drawn on CADAM and revised to a form suitable for injection molding. Figure 3.2 shows isometric views of the front and back of the Z Platform. An exploded view of the Z Platform assembly is shown in Figure 3.3.

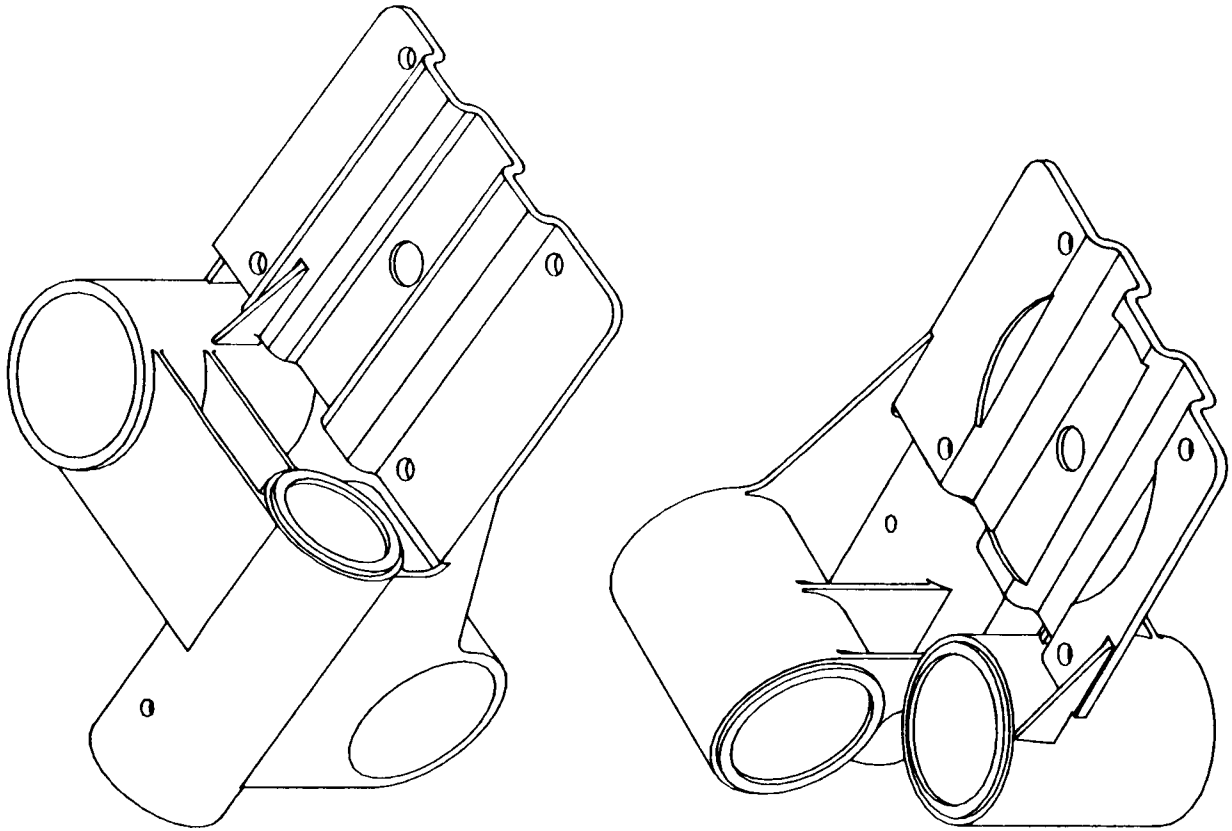

Figure 3.2: Isometric views of the Z Platform.

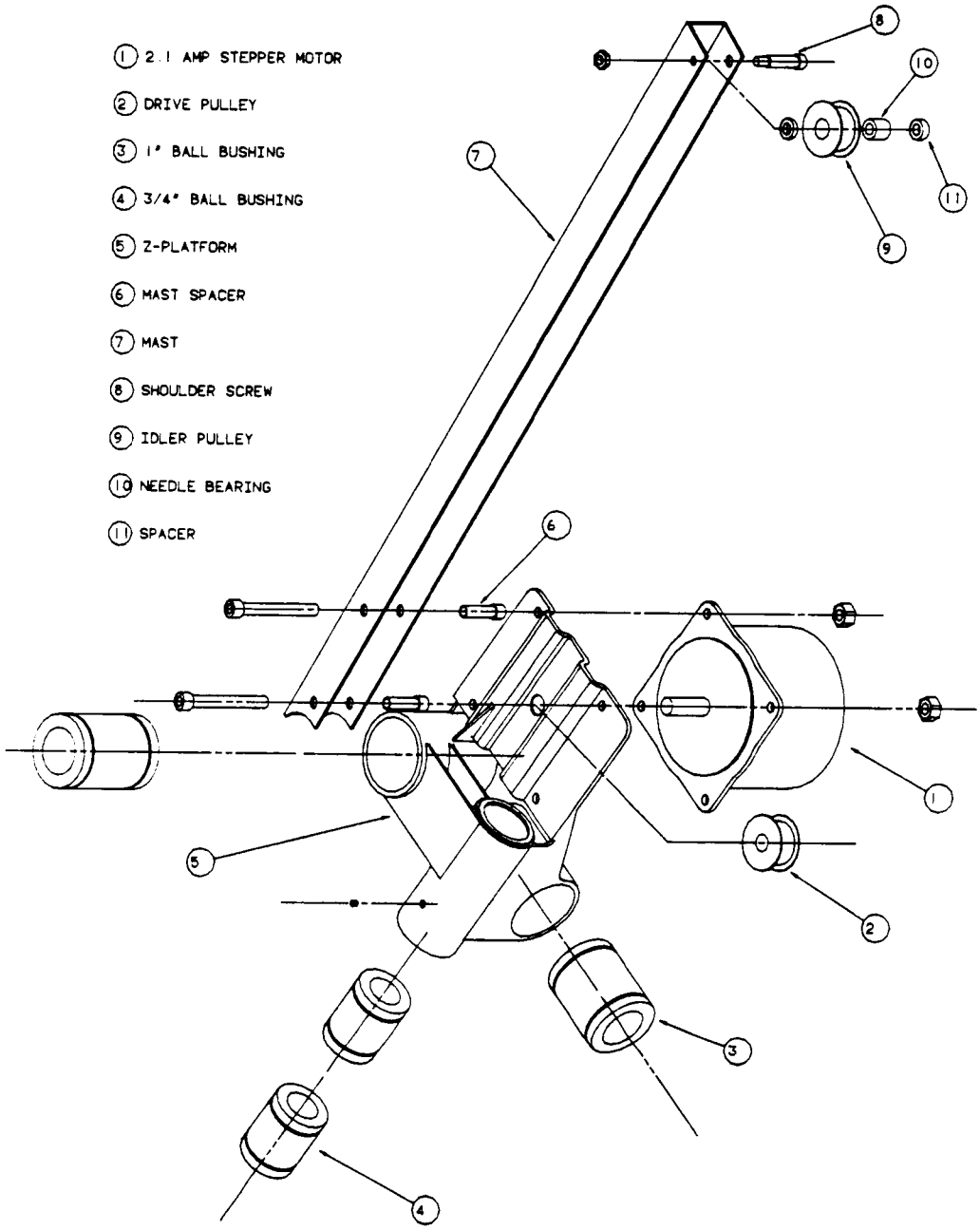

Figure 3.3: Exploded view of the Z Platform assembly.

3.4 Z Arm Guide Tube and Yaw Rotation

The design of the vertical guide tube was centered on using self-aligning, recirculating ball Thomson bushings. This requirement restricted the tube material to steel in order to provide a durable bearing surface. A smaller bearing, with a housing bore of 3/4 of an inch was used. Because the bearings are self-aligning, they have approximately one degree of clearance. Therefore, two bearings were needed to travel in tandem to reduce the movement at the end of the guide tube. The guide tube is a thin-walled, stainless tube used as a bearing surface. The tube has two grooves that are 180° apart, and 0.008 inches deep. These grooves restrict rotation of the guide tube. This is accomplished by using the feature of the self-aligning ball bushings that allow a ball track to be driven inward by a set screw into the grooves. This arrangement locks the bearing onto the tube, thus allowing only translation with no relative rotation. Since there are two bearings, one groove is used for each bearing, which increases the maximum torque that the tube can withstand without rotating.

The design of the mechanism to perform the yaw rotation was discussed in an August 3rd, 1988 design review in Charlotte, where IBM stated that a resolution equal to the stepper motor's rotational accuracy of 1.8° per step was sufficient. This change made the design much simpler, since no gearing or belting was required. Figure 3.4 shows an exploded view of the Z Arm. The 1.1 amp stepper motor is mounted onto the top of the vertical guide tube with its spindle extending into the outer guide tube. The motor rotor is rigidly coupled to a thin-walled, aluminum, 1/2 inch drive tube. A spindle at the other end of the tube is attached through a tongue/groove drive that isolates it from the drive tube. Therefore, the only axial load on the motor is the small constant weight of the drive tube. The yaw spindle is supported by two radial ball bearings, which are held in place by a spacer and two internal snap rings. The end of the spindle protrudes out of the lower end of the vertical guide tube so that a wrist adaptor or tool may be attached.

The motor mount for the yaw motor is also injection molded. This part also holds the Z Arm guide vertical tube and grips the vertical timing belt in the same manner as the sliders.

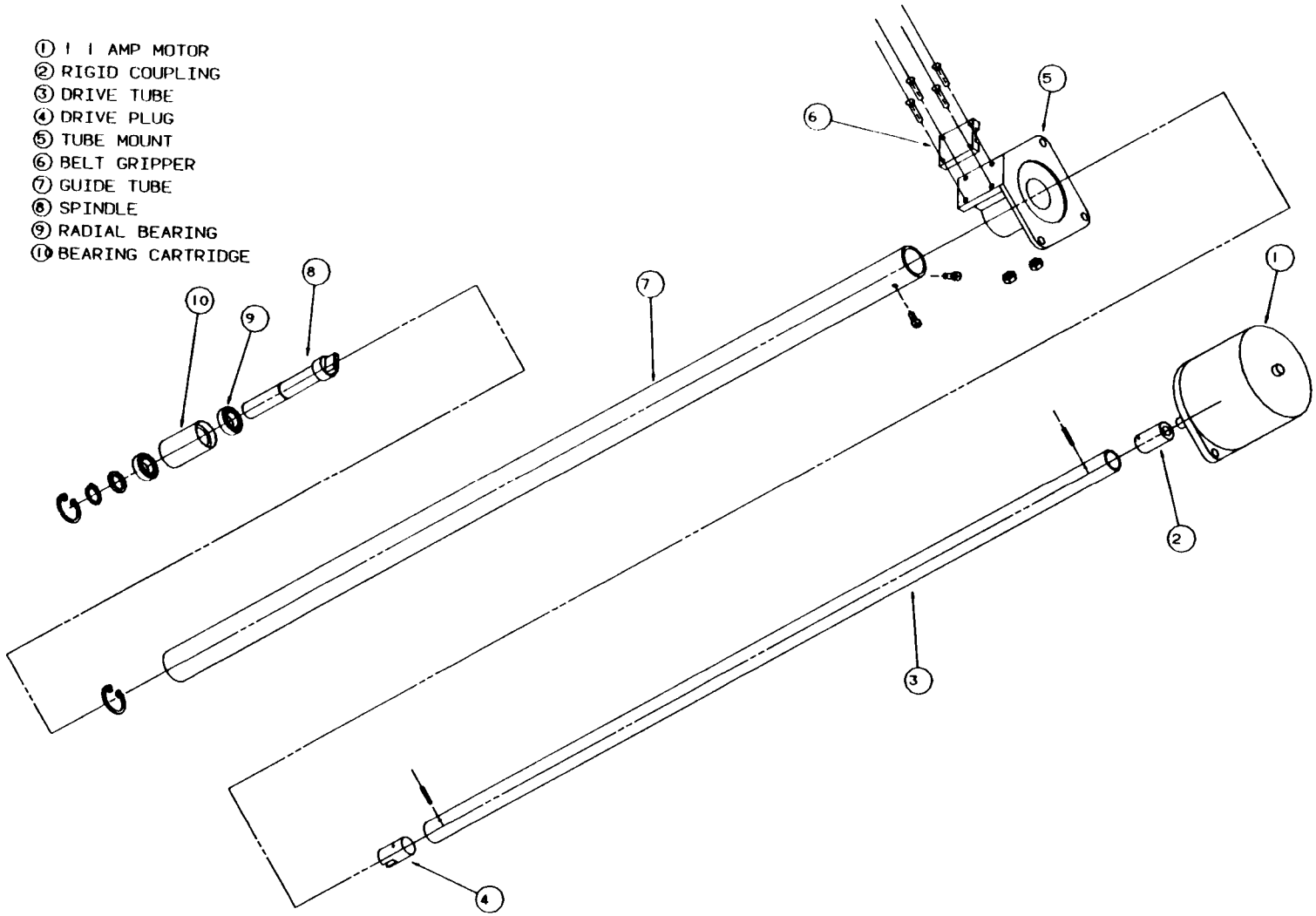

Figure 3.4: Exploded view of the Z Arm assembly.

CHAPTER 4

PROTOTYPE DESIGN AND CONSTRUCTION

4.1 Z Platform Prototyping

From the developed design of the Z Platform, a working prototype was made. It was desirable to use plastic for the prototype in order to try and replicate the injection molded part as closely as possible. This presented a problem; a block of suitable plastic (nylon, polycarbonate, etc.) large enough to be milled out to form the platform was not available, nor do proper adhesives exist to bond these plastics together. A discussion with materials science engineers led to the suggestion of using PVC to make the parts of the platform and bond them together, since advanced adhesives exist for this type of plastic. This idea was accepted by IBM in the August 3rd design review. A tensile test was performed to test the adhesive's strength. Six samples, three lap joints and three butt joints, were bonded with heavy bodied PVC cement and pulled axially until failure. The stresses that the joints withstood were higher than the expected operating stresses of the robot, so the recommendation of bonding the parts together was used. The data obtained from this test is located in appendix G.

The Z Platform part was broken up into machinable pieces and bonded together. The ribs and bosses were made thicker than the design for injection molding in order to increase the glued area, and therefore the strength. The motor mount was not corrugated in order to increase the stiffness of the part and to simplify machining. The one inch ball bushings for horizontal movement were press-fit into place. The two vertical ball bushings are self-aligning; therefore, a sliding fit was used. Overall, the prototype part is still very similar to the molded design.

For the vertical guide tube to resist rotation, set screws were used to hold the ball tracks of the 3/4 inch self-aligning ball bushings in the tube's grooves. It was undesirable to thread the outer plastic tube of the platform that houses the vertical bearings; therefore, an internally threaded, self-broaching insert was used. The insert is headed on the inside of the tube, so that it cannot pull through. It is held in place by the broaching action it exhibits when it is pressed into an undersized hole in the tube.

4.2 Z Arm Guide Tube and Yaw Rotation

A stainless steel tube with a 0.049 inch wall was used for the prototype of the vertical guide tube. The length of the tube was determined after deciding on a 15 inch vertical move. This length of the vertical move was based on having a move of more than one foot, but less than the length at which the 3/4 inch tube would become excessively compliant.

The tube mount for the yaw motor was made from PVC for the prototype; this part will also be injection molded. This piece grips the vertical timing belt, by having an aluminum belt gripper with threaded studs to mesh with timing belt and bolt onto a flat surface of the part (Figure 3.4).

The mast that holds the upper idler pulley for the vertical timing belt is constructed out of aluminum channel with one inch sides and a 1/16 inch wall thickness. The mast bolts directly onto the z axis motor with the Z Platform sandwiched in between. Spacers are used in the mast to prevent it from deflecting when the bolts are tightened (Figure 3.3).

There are two photocells attached to the Z Platform assembly so that its position may be periodically checked. One photocell is used to locate a slit on a thin aluminum disk that is press-fit onto the back of the yaw motor rotor. The other photocell is attached to the Z Arm. This cell is triggered when the arm passes a flag that is attached to the mast.

The wires from the motors and the photocells are kept clear of the Z Arm by attaching them to a 3/16 inch diameter tube that extends 12 inches outward from the top of the mast. The tube is supported by a mount made of Valox plastic that allows the tube to pivot while the robot is moving.

4.3 X-Y Plus System

The original prototype of the X-Y Plus system was altered slightly for the second prototype. The dimensions of the prototype were reduced to one meter per side after IBM engineers suggested that the first model was too large for a prototype. The sliders were redesigned to use Thomson linear ball bushings, and the injection molded parts were modeled with PVC. The cylinder that houses the linear ball bushings was bonded to the orthogonal cylinder that holds the end of the control tube. Two side ribs and a vertical rib were also bonded on to increase the part's stiffness. The belt mounting for the prototype is different from the production model; self broaching studs were used to secure the belt

hanger and timing belt.

The original corner brackets were used for the second prototype. The prototype brackets were machined out of aluminum, but were designed by Mr. Granger as injection molded parts.

4.4 Robot Frame

The main criteria in designing the frame was to minimize material and therefore cost. Steel was chosen for the structure, rather than aluminum, because of its low cost. Steel was also preferred over aluminum because of its higher density, which will make the frame heavier and provide a damping effect for high frequency vibration of the system. The frame is a box that supports the robot. The corner brackets are bolted on at each corner of the frame. One alternative considered was using the X-Y Plus system itself as part of the frame; this option was rejected due to the difficulty that would arise in adjusting the X-Y Plus system during assembly.

CHAPTER 5

THEORETICAL CONSIDERATIONS

5.1 Projected Performance: X-Y Plus System and Z Arm

The performance of the horizontal positioning mechanism was modeled in Mr. Granger's work (4). This particular curve, shown in Figure 5.1, is based on a motor moving a 12 pound load, over various lengths under the influence of friction. By using the curve shown in Figure 5.1, the maximum average velocity for a specific move can be obtained. The friction coefficient used is 0.2. This value is the friction coefficient of the plastic bushings used on the first prototype. Both the 2.1 amp stepper motor and the 1.1 amp motor have been modeled. The gear radius is not constant on this curve. The optimum pulley radius that the motor should use to obtain these velocities for a given move is obtained by reading Figure 5.2. To project the performance of the X-Y Plus system for a 24-inch move, for example, this

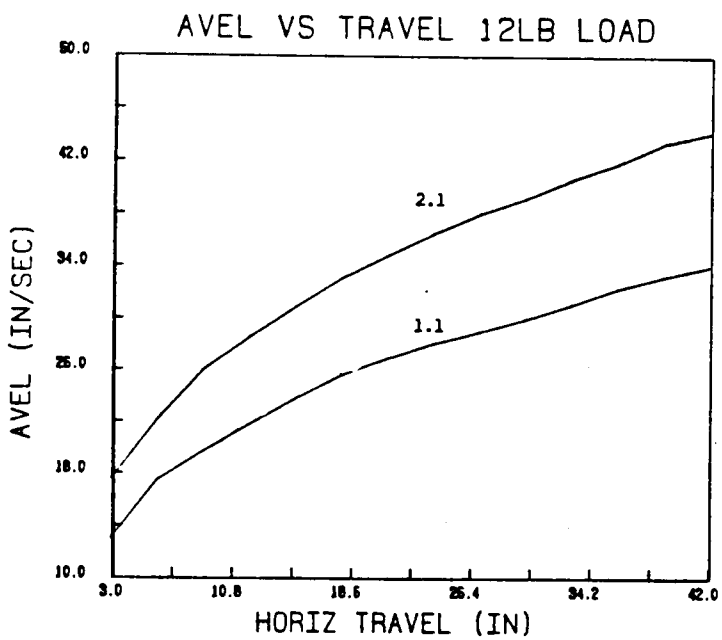

Figure 5.1: Maximum average velocity versus horizontal travel.

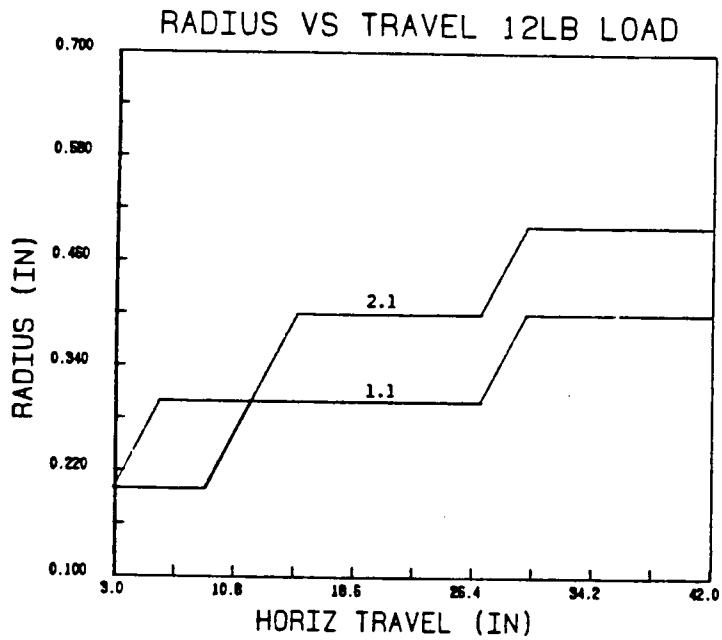

Figure 5.2: Optimum pulley radius for horizontal moves.

distance is selected on the abscissa of Figure 5.1 and the corresponding velocity of 34 inches per second is read from the ordinate of the graph for the 2.1 amp stepper motor. To find the optimum pulley radius for this move, Figure 5.2 is used. For a 24 inch move the pulley radius should be 0.4 inches.

The performance of the Z Arm can also be projected with Mr. Granger's work. Figure 5.3 is a plot of average velocity versus travel for the 2.1 amp and 1.1 amp stepper motors based on lifting a 4 pound load. It is desired to see what average velocity the 2.1 amp motor can produce for a 12 inch move. By locating this value on the abscissa a corresponding velocity of 31 inches per second is obtained. There is a separate plot to find the optimum pulley radius for the upward motion, shown in Figure 5.4. Again the desired move is 12 inches and the 2.1 amp motor is to be used. This move requires a pulley radius of 0.4 inches (4).

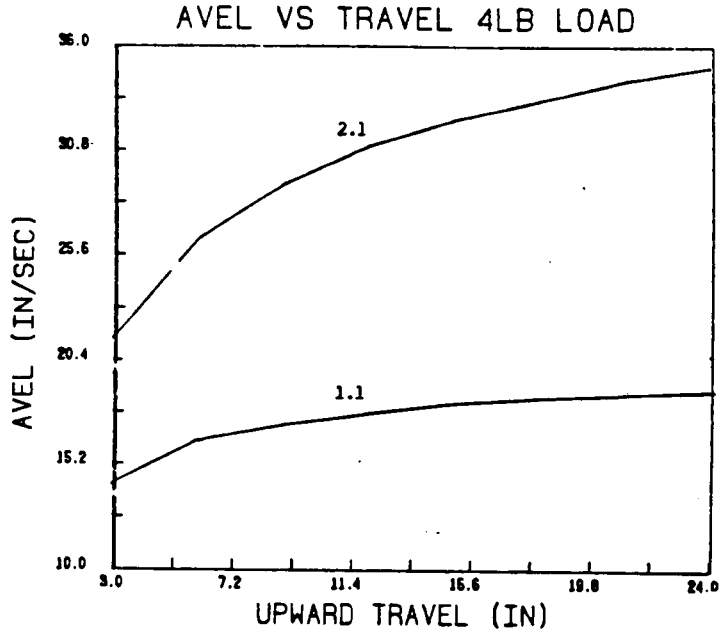

Figure 5.3: Maximum average velocity versus upward travel.

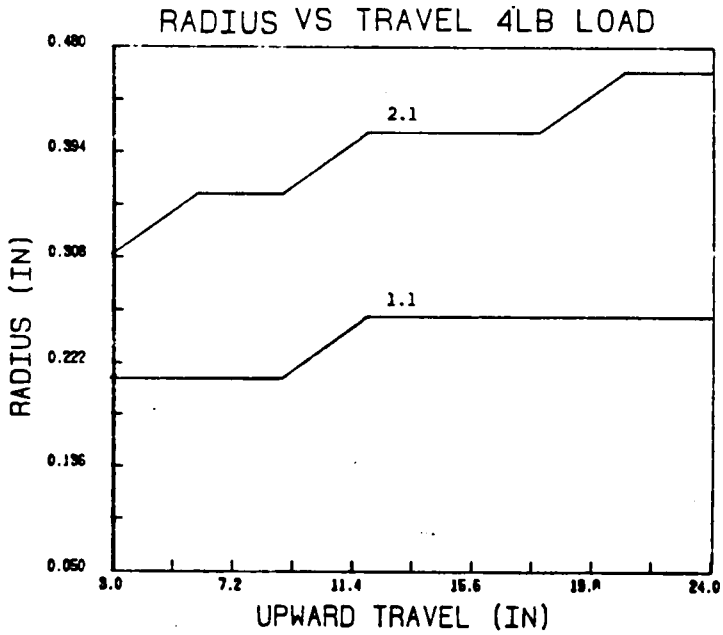

Figure 5.4: Optimum pulley radius for vertical moves.

5.2 Accuracy Analysis of Critical Tolerances

All of the members of the robot contribute to the accuracy of the end effector. A misalignment of the frame, for instance, will be reflected through the X-Y Plus system, to the Z Platform, the vertical guide tube, and then to the end effector. Since the contributions of the individual members are small, they can be added linearly to find the total misalignment at the end of the arm. The analysis considers misalignment in only one dimension for each of the cases considered. The first case of inaccuracy is shown in Figure 5.5, where the corner brackets are not square, that is, the outer guide shafts form a parallelogram. This creates an inaccuracy in the y-direction when the platform moves along the control tube in the x-direction.

The next component that will contribute to positional error in the y-direction is a slider bracket that does not position the control tube in an orthogonal position with respect to the outer guide shafts. Figure 5.6 demonstrates that as the platform moves in the x-direction, the misaligned control tube in the y-direction forces an undesirable movement in the Z Platform in the y-direction.

The next four cases are due to vertical misalignments that tend to tilt the platform, which will produce horizontal and vertical errors at the end of the vertical arm. The first scenario is shown in Figure 5.7, where one of the corner brackets is higher than the other. This has the effect of raising the platform as it moves in the y-direction.

The clearance in the bearings also contributes to the positional accuracy of the end effector. This is seen first in the sliders, where the clearance in the bearings allows the control tube to slant downward. This happens again at the horizontal bearing on the platform. Figure 5.8 illustrates both of these cases simultaneously. The clearance in the vertical bearings that the Z Arm rides on are also contributors to overall inaccuracy. This effect is shown in Figure 5.9

The last contributor to the horizontal and vertical positioning of the end effector is the stepper motors. These are accurate to ± 3% of a step. Therefore, with a timing belt pulley radius of 0.4775 inches, this converts to a linear accuracy of ± 0.00045 of an inch. For the vertical motor, with its 0.637 inch diameter pulley, this number is reduced to ± 0.0003 of an inch. The total positional accuracy of the robot is the addition of all the cases presented.

The areas of inaccuracies described vary in significance. The values of the bearing inaccuracies

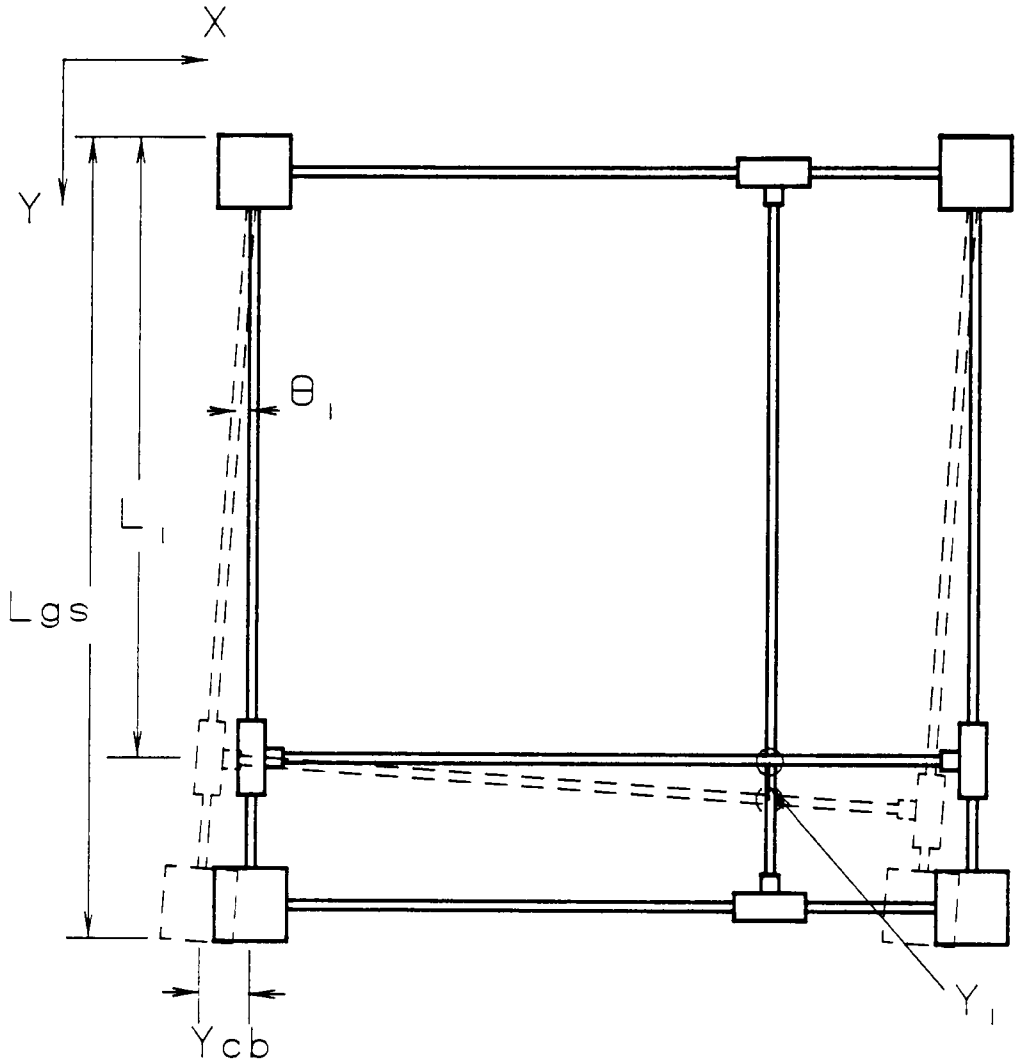

Lgs = Length of guide rod from corner to corner
Ycb = Distance of corner bracket misalignment
L_1 = Position of midpoint of upper platform bearing measured from corner
Y_1 = Inaccuracy of platform in y-direction due to corner bracket misalignment

Figure 5.5: Inaccuracy due to corner bracket misalignment.

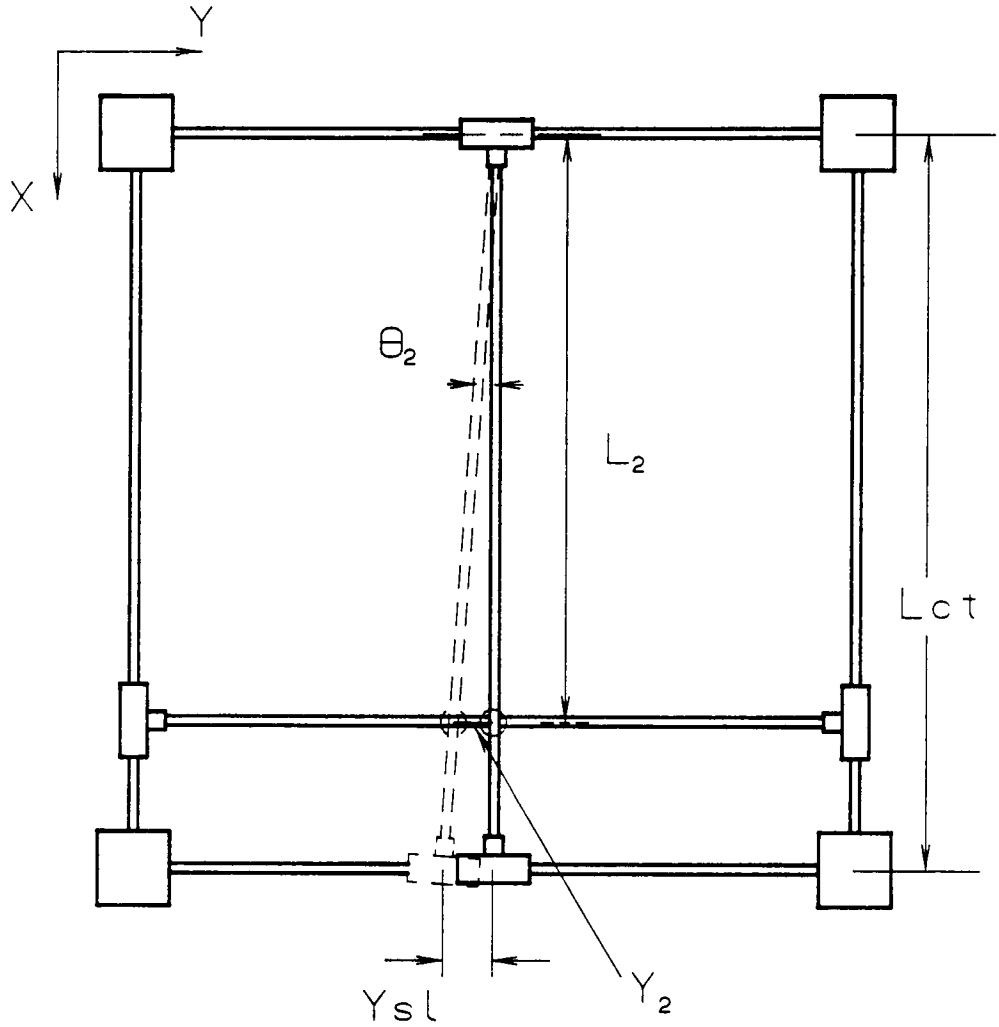

Lct = Distance between control tubes
Ysl = Slider misalignment
L_2 = Position of platform measured from control tube
Y_2 = Platform misalignment in y-direction due to non-orthogonal control tube

Figure 5.6: Case of non-orthogonal control tubes.

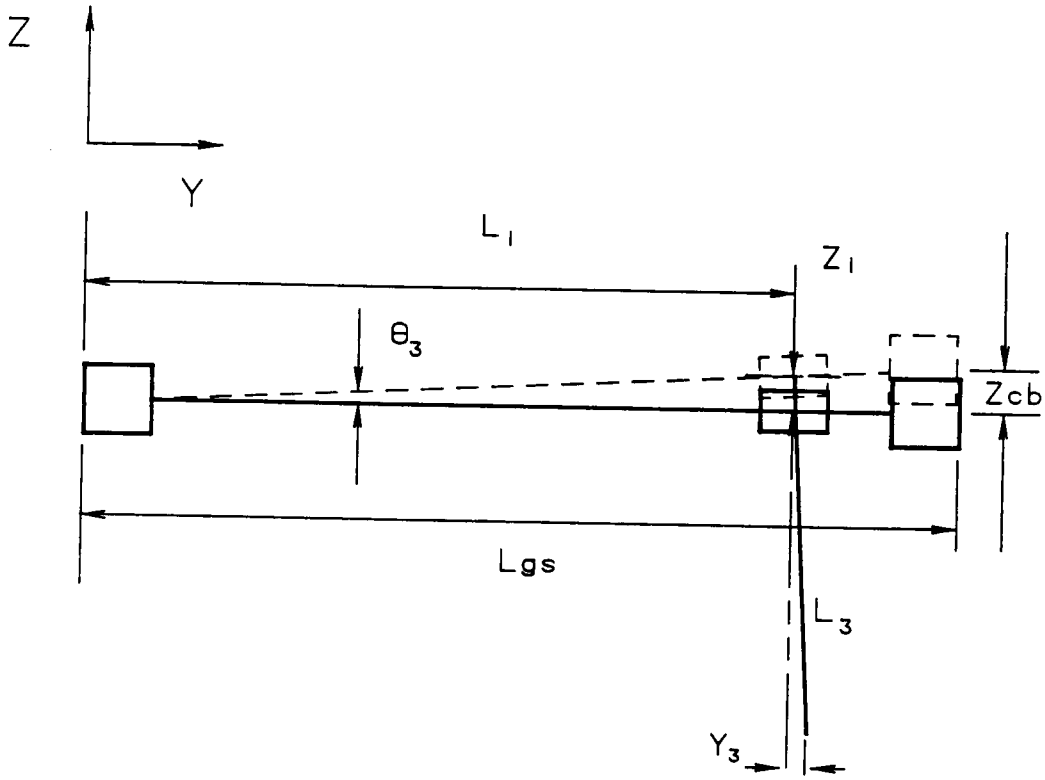

Lgs = Length from corner to corner
L_1 = Length from corner to midpoint of upper platform bearing
L_3 = Length from center of upper platform bearing to end of arm
Zcb = Vertical misalignment of corner bracket
Z_1 = Vertical misalignment of end of arm
Y_3 = Horizontal misalignment of arm in y-direction

Figure 5.7: Corner bracket elevation effects.

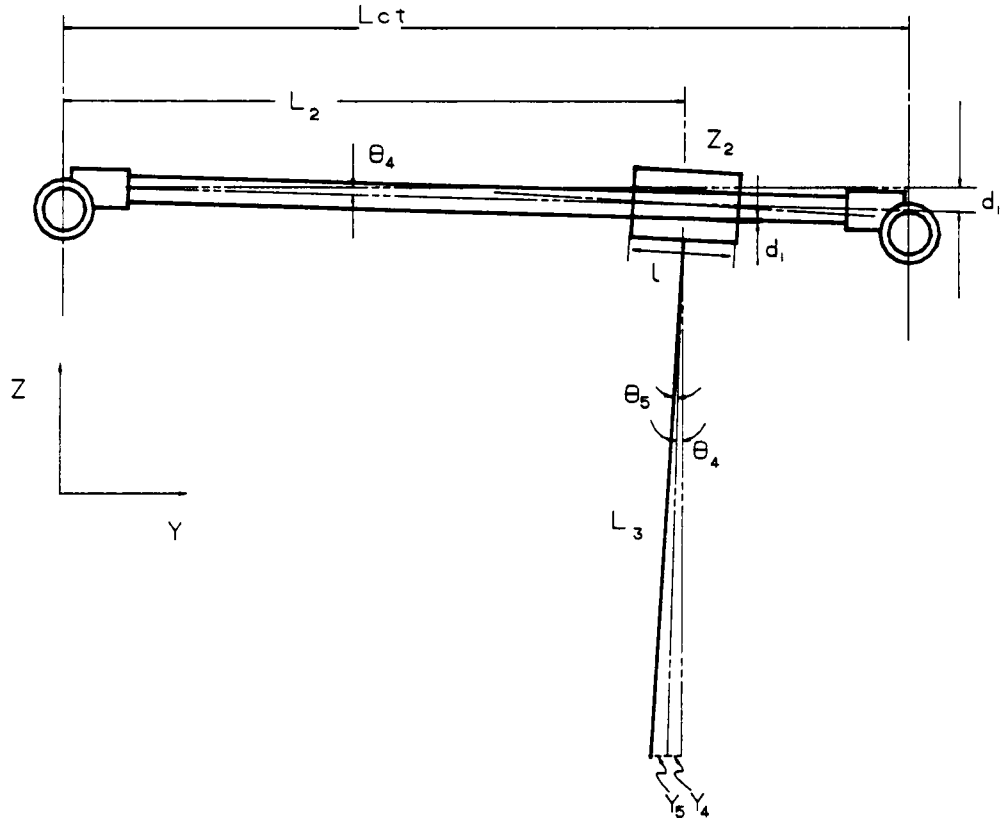

Lct = Length between control tube centers
L_2 = Position of midpoint of platform upper bearing measured from control tube
L_3 = Length of vertical guide tube measured from center of upper platform bearing
d_1 = Diametral clearance of 1" ball bushing
l = Length of bearing contact for 1" ball bushing
Y_4 = Horizontal misalignment of arm in y-direction due to slider bearings
Y_5 = Horizontal misalignment of arm in y-direction due to platform bearings
Z_2 = Vertical misalignment of platform at midpoint of upper bearing

Figure 5.8: Horizontal bearing clearance contributions.

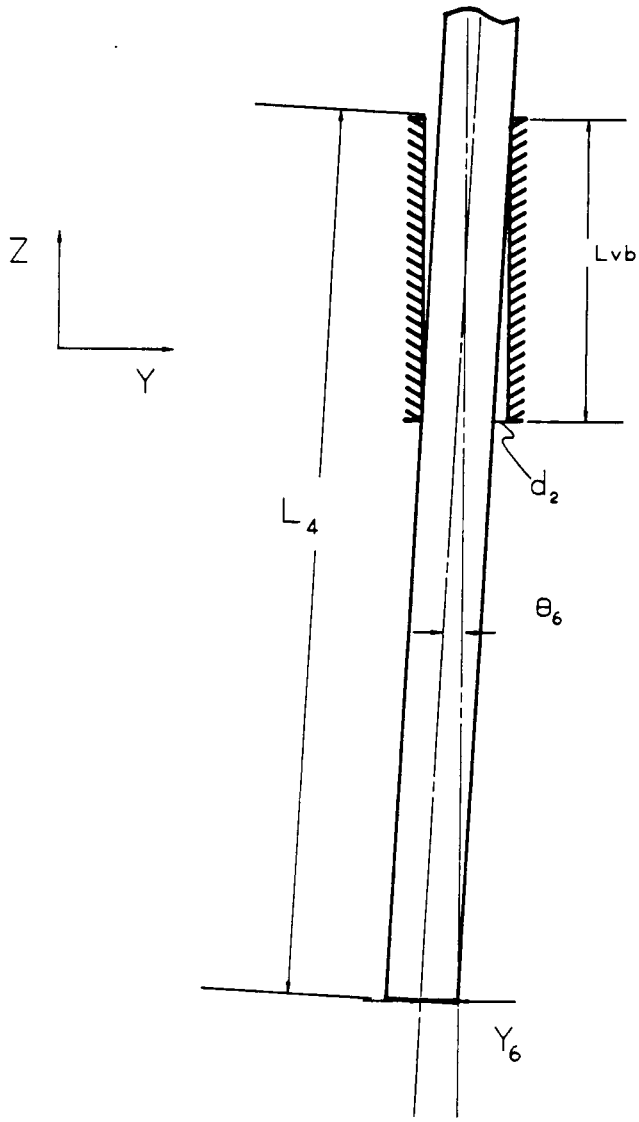

L_4 = Length of vertical arm measured from top of upper vertical bearing
Lvb = Sum of length between bearings and of bearing contact distance
d_2 = Diametral clearance of 3/4" self-aligning ball bushing
Y_6 = Horizontal play of arm in y-direction due to vertical bearing play

Figure 5.9: Vertical bearing clearance contributions.

for the prototype may be calculated and are given below. Each value was calculated with the robot at the worst possible position.

(1) Slider bearing effect on free clearance of arm

horizontal clearance = 0.0008 inches

vertical clearance = 0.0013 inches

(2) Z Platform bearing effect on free clearance of arm

Horizontal Bearings

horizontal clearance = 0.02 inches

vertical clearance = 0 (insignificant)

Vertical bearings

horizontal clearance = 0.0575 inches

vertical clearance = 0 (insignificant)

Total horizontal clearance due to bearings = 0.0783 inches

Total vertical clearance due to bearings = 0.0013 inches

For the horizontal accuracy of the robot to be 0.118 inches, the remaining three contributors to inaccuracy must add up to 0.0392 inches. These contributors are the first three cases presented, where either the outer guide shafts or the control tubes are out of alignment. These tolerances were specified in order to preserve the initial accuracy requirement. Each value of misalignment was weighted by taking the percentage of its contribution to the inaccuracy to that of the total inaccuracy for the three different cases. This percentage was then multiplied by the total allowable inaccuracy of 0.0392 inches to obtain the maximum permissible inaccuracy at the end effector in each situation. The maximum allowable misalignment for each case is shown.

horizontal corner bracket distance = 0.0131 inches

horizontal control tube distance = 0.0129 inches

vertical corner bracket distance = 0.0347 inches

A rotational error exists in the Z Arm due to a 0.002 inch clearance between the tongue of the drive spindle and the groove of the drive plug. This clearance produces a rotation positional error of ± 0.0015 inch at the edge of the wrist adapter. Another source of rotational error is the 1.1 amp motor used for the yaw rotation. This motor has the same accuracy as the 2.1 amp motors. The motor error creates a ± 0.0014 inch error at the edge of the wrist adapter. The total rotation positional error of the Z Arm at the periphery of the wrist adapter is the sum of these two cases, or ± 0.0164 inches.

These values are only pertinent to the prototype. If the dimensions of the robot were changed, the empirical equations would have to be used to find new tolerance values. These are derived and given in appendix A.

5.3 Binding Analysis: X-Y Plus System Binding

The first prototype of the X-Y Plus positioning mechanism was very prone to binding because of high friction forces caused by the plastic sleeve bearings. A binding analysis of the X-Y Plus system was performed by Mr. Granger in his work (4). The model used for the analysis is shown in Figure 5.10. For the system not to bind,

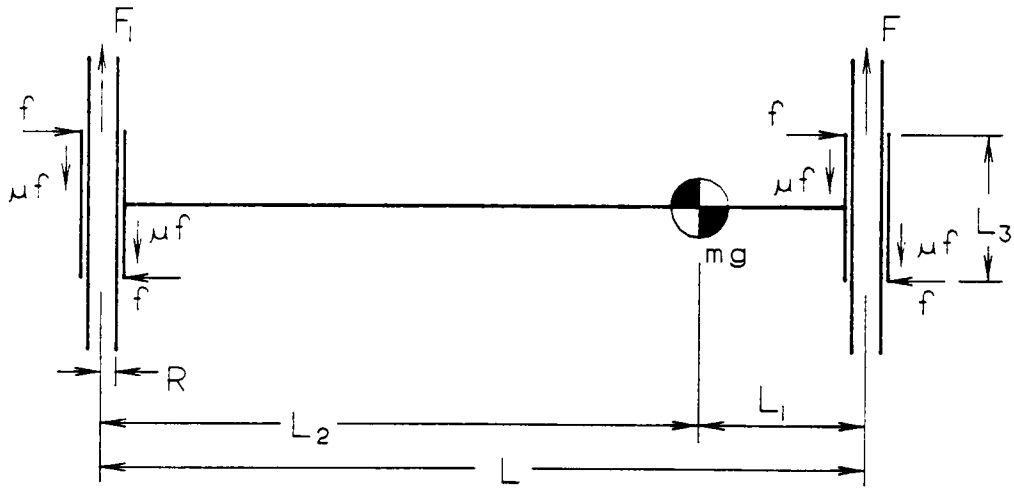

Figure 5.10: X-Y Plus system binding.

$$F + F_1 > 2\mu(F_1L_2 - FL_1)/(\mu L_2 - \mu L_1 - L_3)$$

This equation breaks down into two possibilities. The first case is when the platform is in the middle of the control tubes ($L_2 = L_1$) and the force on each end of the control tube is equal ($F_1 = F$). This situation will produce no binding. For any other position of the platform, the system will not bind when:

$$L < L_3/\mu$$

For the second prototype, L_3 = 1.5 inches and μ_{max} = 0.004 (3). Therefore, for no binding, L must be less than 31 feet. The derivation of this work is found in reference (4).

5.4 Z Arm Binding

The geometry of the Z Arm is such that the point of attachment of the timing belt is offset from the vertical guide tube bearings. When the Z Arm is moved up or down, the offset vertical force creates horizontal binding forces at the bearings as shown in Figure 5.11. If the friction coefficient of

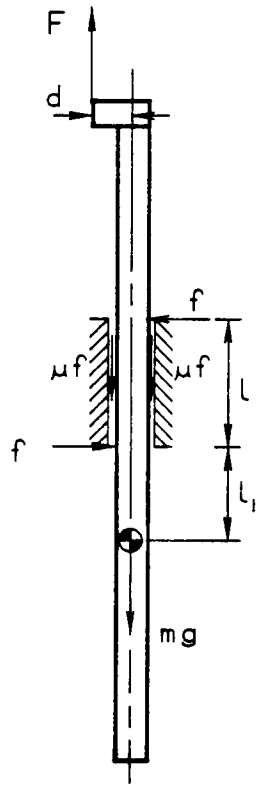

Figure 5.11: Free body diagram of Z Arm during upward travel.

the bearings is too high, the offset distance "d" too large, or the distance "l" between the bearings too small, the mechanism will bind. The required acceleration was found by summing forces vertically and summing moments around the center of mass. The ratio of accelerations with and without friction is a measure of efficiency. The force offset distance influences the mechanism's acceleration efficiency for various friction coefficients, as shown in Figure 5.12. Six different friction coefficients, that varied from 0.004 to 0.1, were used. The plot shows that the efficiency decreases linearly with increasing force offset distance. The slope of the line becomes more negative with an increase in the friction coefficient. The maximum published (3) friction coefficient for the prototype, with the linear ball bushings, is 0.004 and the force offset distance is 1.25 inches. Therefore, the device is very efficient and the force offset distance will not produce binding. Appendix B contains the details of this analysis.

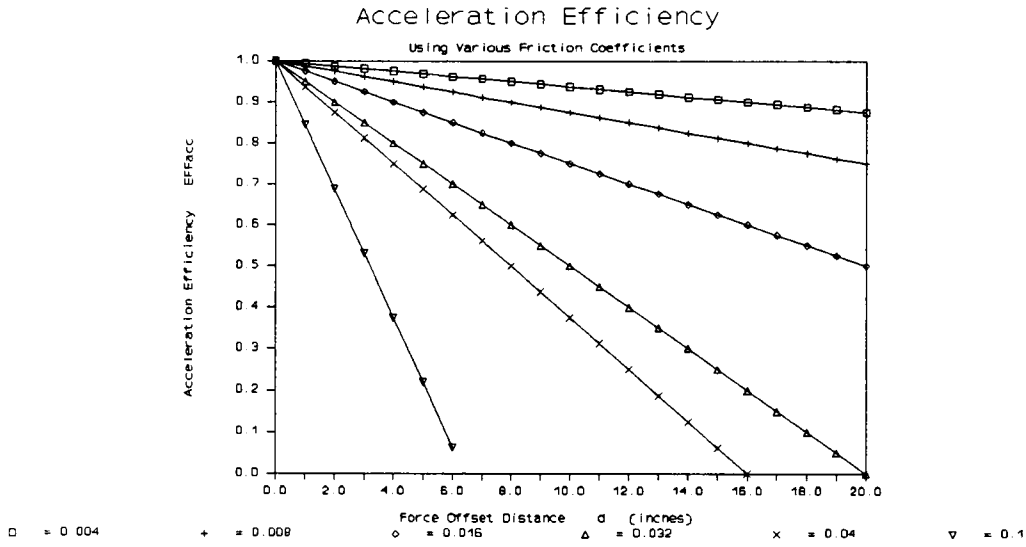

Figure 5.12: Z Arm efficiency with increased force offset distance using various friction coefficients.

5.5 Frame Analysis

Once the general geometry of the frame was selected, a stiffness analysis was performed on the frame. The objective of the stiffness analysis was to minimize the amount of material while still providing adequate rigidity. The analysis was simplified to the two dimensional case. Figure 5.13 shows a side view of the frame with a horizontal load "P". The dashed lines denote the exaggerated deflections of the

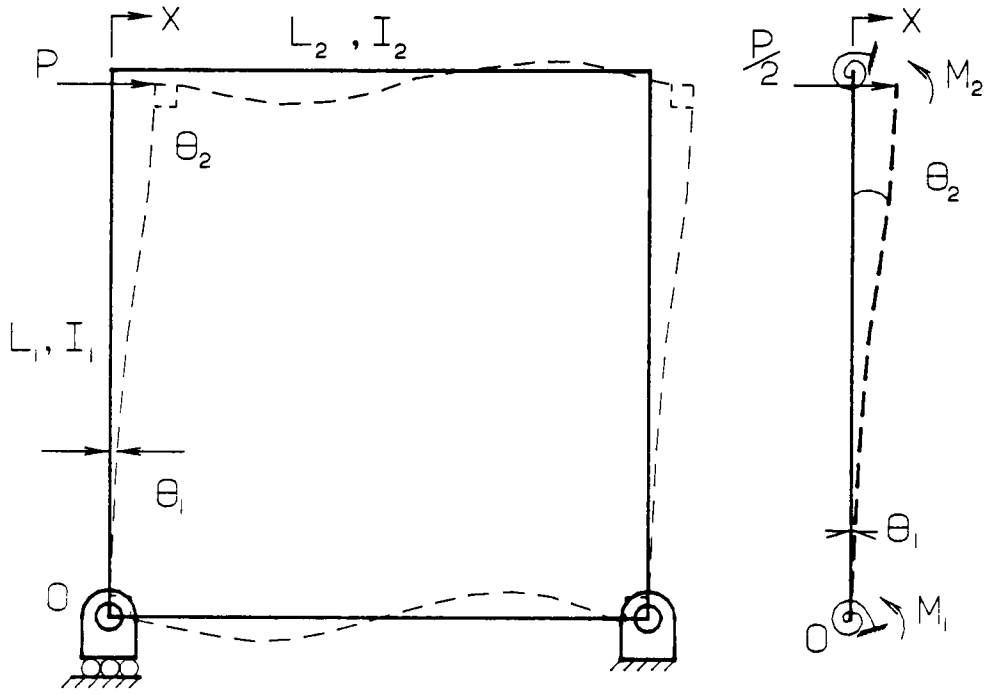

Figure 5.13: Two dimensional model of frame.

members. Only one side of the frame was considered; the other horizontal cross members were assumed to provide no rigidity. This assumption simplified the analysis, but still gave information on how the two different members contributed to the overall stiffness. The load on the frame was assumed to be a 20 pound horizontal load,"P", acting on the side of the frame. The 20 pound load was used as an estimate of the force on the frame when the robot is under an inertial load of approximately two G's.

The analysis proceeded by looking at the subsequent horizontal deflection of the vertical legs. Since the frame is symmetric, the loading and subsequent deflections are symmetric. Therefore, for the 2-D case, each vertical member shares the 20 lb load equally. The contribution of the horizontal members is a restoring moment at each end of the vertical leg. The restoring moments are equal to the angle of rotation Θ of the vertical leg at each end, times the stiffness K of the horizontal members. This is modeled as a torsional spring attached at each end of the vertical leg. The total deflection of the vertical leg at the point of the load is the sum of the contributions of the load itself, and the restoring moments.

$$X = P(L_1)^3/3EI_1 + \Theta_1 L_1 - K\Theta_2(L_1)^2/2EI_1 \qquad (1)$$

Summing moments about point "O",

$$\Sigma M_o = PL_1 - K\Theta_1 - K\Theta_2 = 0 \qquad (2)$$

The horizontal arm's stiffness K was modeled as a pinned beam with a moment on one end. Due to the symmetry of the loading, there is no moment at the middle of the horizontal member; thus, the length used in determining K is only half the length of the horizontal members. Therefore, the final equation for the stiffness is,

$$K = 6EI_2/L_2$$

The angle of rotation at the point of the load is represented by,

$$\Theta_2 = P(L_1)^2/2EI_1 - K\Theta_2 L_1/EI_1 + \Theta_1 \qquad (3)$$

Combining equations (1), (2), and (3) into matrix form gives the relationships for the angles of rotation and the deflection at the point of the load, in terms of the frame geometry, stiffness, and loading.

$$\begin{bmatrix} 1 & -L_1 & K(L_1)^2/2EI_1 \\ 0 & K & K \\ 0 & -1 & (1+KL_1/EI_1) \end{bmatrix} \begin{bmatrix} X \\ \Theta_1 \\ \Theta_2 \end{bmatrix} = \begin{bmatrix} P(L_1)^3/3EI_1 \\ PL_1 \\ P(L_1)^2/2EI_1 \end{bmatrix}$$

A BASICA program was written to vary the lengths of the sides of the horizontal arm members (equal-leg angle iron), with a fixed cross-section of the vertical leg (square tubing). The program calculates the area, volume, and inertia of the members, and the horizontal deflection of the vertical

leg at the point of the load. A deflection of five thousandths of an inch was chosen as the maximum acceptable deflection. Figure 5.14 shows the frame model's deflection as the length of the sides of the horizontal arm member increases. For each size of the vertical leg there is a size of the horizontal arm member that will provide adequate stiffness for a 0.005 inch deflection. The horizontal arm member size is given as the length of the equal-leg angle iron. Each geometry that provides the required stiffness also has a corresponding relative volume. A relative volume for each case consisted of the volume of one vertical leg member and two horizontal arm members, since there are twice as many arm members as leg members. Figure 5.15 shows the corresponding relative volume of the frame, for each size of the horizontal arm. Case five was the best case. This case used a square tube with two inch sides and 0.125 inches thick for the vertical leg and a horizontal arm thickness of 0.125 inches. For a 0.005 inch deflection, the arm size required was an equal-leg angle iron with 1.625 inch sides and 0.125 inches thick. This geometry had the lowest relative volume of 50.44 in^3 for the 0.005 inch allowable deflection. However, this case was not used for the frame, because its geometry was incompatible with the corner brackets. The geometry chosen for the frame was case four. This case had the next lowest relative volume of 59.5 in^3, where the vertical leg was a 1.5 inch square steel tube with a 0.25 inch wall thickness, and the horizontal members are 1.75 inch equal-leg angle iron with a thickness of 0.125 inches. The overall size of the frame is 39.37 inches (1m) square with a height of 21 inches. The computer program and a detailed derivation is located in appendix C.

5.6 Z Arm Guide Tube Groove Analysis

Two grooves, 180° apart on the outer surface of the vertical guide tube, are used to make the tube resist rotation. One track on each of the ball bushings is driven into the groove with a set screw. Thus, the outer guide tube may translate with no rotation. The parameter analyzed was the depth of the groove. A shallow groove was needed so that the strength of the guide tube would not be jeopardized. The distance that the ball bearing would protrude inward was measured as 0.0125 inch. The ball bearing manufacturer recommended a 0.012 inch "V" groove. Since a thin wall tube was to be used for the vertical guide tube, it was desirable to use a round groove, which can be made more shallow than a "V" groove. The recommended V-shaped groove depth of 0.012 inch corresponds to a round groove depth

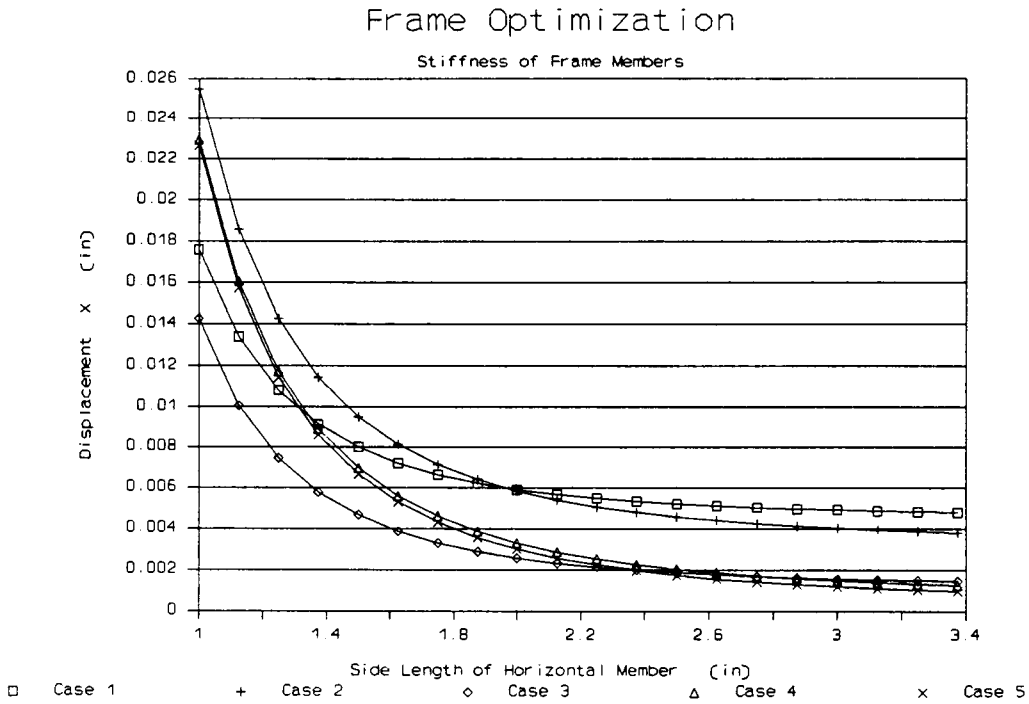

Case 1: Vertical leg 1x1x0.125.....Horizontal arm thickness 0.25
Case 2: Vertical leg 1x1x0.25.....Horizontal arm thickness 0.125
Case 3: Vertical leg 1.5x1.5x0.25.....Horizontal arm thickness 0.25
Case 4: Vertical leg 1.5x1.5x0.25.....Horizontal arm thickness 0.125
Case 5: Vertical leg 2x2x0.125.....Horizontal arm thickness 0.125

Figure 5.14: Stiffness of 2-D frame model with increasing frame arm inertia.

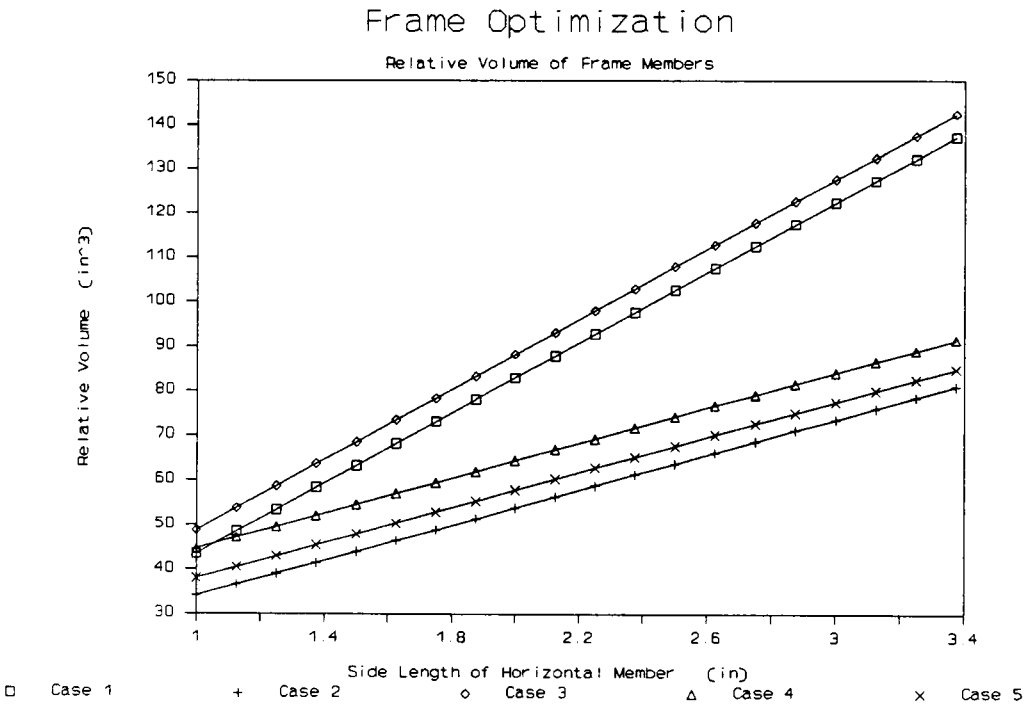

Case 1: Vertical leg 1x1x0.125.....Horizontal arm thickness 0.25
Case 2: Vertical leg 1x1x0.25.....Horizontal arm thickness 0.125
Case 3: Vertical leg 1.5x1.5x0.25.....Horizontal arm thickness 0.25
Case 4: Vertical leg 1.5x1.5x0.25.....Horizontal arm thickness 0.125
Case 5: Vertical leg 2x2x0.125.....Horizontal arm thickness 0.125

Figure 5.15: Relative volume of 2-D frame model with increasing frame arm inertia.

of only 0.008 inch. The maximum rated torque that the 3/4 inch bearing can withstand is 20 in-lbs. By using two bearings with two grooves, the maximum torque can be increased, since the bearings will share the load. The main consideration, however, was not the torque that the bearing could withstand but the force on the set screw that holds the balls in the groove. If the force is too high, the insert that holds the set screw could deflect the plastic tube that retains the bearings. A static analysis on the bearing showed that the force that the insert must provide to hold the ball in the groove, decreased 35 % by using a rounded groove instead of a V-shaped groove. For the round groove, the set screw moment arm is longer than for the V groove, so the force on the insert is less for the same applied torque on the guide tube.

Using the static analysis, a BASICA program was written to calculate the force on the insert that it must provide to hold the set screw, which holds the row of bearings in the groove. This force was termed the pull-out force, since inserts are classified in terms of the force required to extract the insert from the material they are imbedded in. The program was run for various torques and groove depths. Figure 5.16 shows the effects of increasing groove depth on the insert pull-out force, for various torques applied to the vertical drive tube. Note that the pull-out force becomes less dependent on groove depth as the groove depth increases. Although a deeper groove lowered the force on the insert, the force for a 0.008 inch deep groove was not unreasonably high, so this depth was used. For a torque of 5 in-lbs, the pull-out force on each insert is approximately 10.4 lbs. This torque exceeds the 2.6 in-lb holding torque of the 1.1 amp motor used for the Yaw rotation (appendix D).

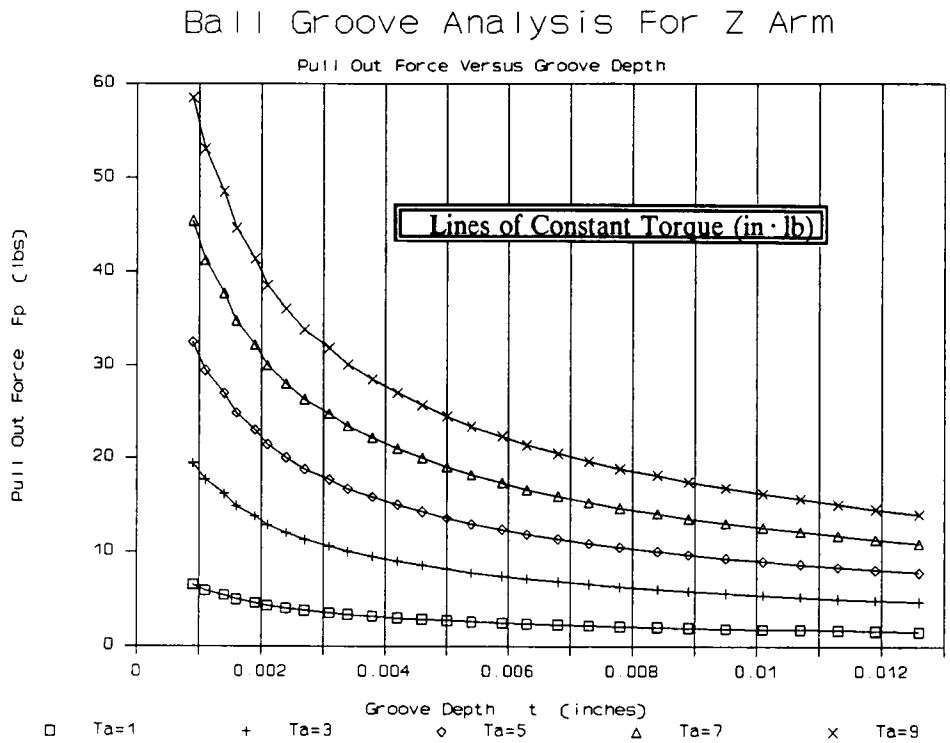

Figure 5.16: Insert pull-out force for increasing groove depth using selected applied torques.

CHAPTER 6

PERFORMANCE TESTING OF PROTOTYPE

6.1 Repeatability Test

The robot was tested for repeatability by programming it to execute a 27 inch move in the x-direction. After the move, the position of the end effector was measured from a datum point on the side of the frame. The movement and measurement were repeated 27 times. The data was averaged to find the mean and standard deviation. The standard deviation of the data was 0.00204 inches. Therefore, the robot will be within ± 0.0061 of an inch 99.99% of the time, or ± three standard deviations. The repeatability test data is shown in appendix E.

6.2 Z Arm Settling Time

Three tests were performed to determine if the settling time of the robot arm after performing a typical move met the performance criteria. The requirement by IBM was for the arm to settle to within ± 0.118 inches within 0.1 seconds. An accelerometer was attached to the wrist adaptor at the end of the Z Arm. The sensitivity of the accelerometer was 10.5 mV/G. The accelerometer's output over time was measured by a dual channel signal analyzer. The signal analyzer is digital and has the capability to integrate any input.

After the accelerometer was calibrated, the first test performed determined the acceleration over time of the fully extended, unloaded arm due to an impulse response. The arm was excited by giving it an initial displacement in the direction of the accelerometer, and then releasing the arm. The response of this test is shown in the top plot of Figure 6.1. The ordinate of the plot is in G's, and the abscissa is in seconds. The peak acceleration of the arm is approximately 13.5 G's. The other plots are the successive integrations of the acceleration. The middle plot of Figure 6.1 shows the velocity of the arm and the bottom one shows displacement. The ordinate of the displacement plot is in microunits. One unit equals one inch/G. The performance criteria was that the amplitude of vibration be within ± 0.118 inches after 0.1 seconds. The conversion of this displacement into the units on the plot is found

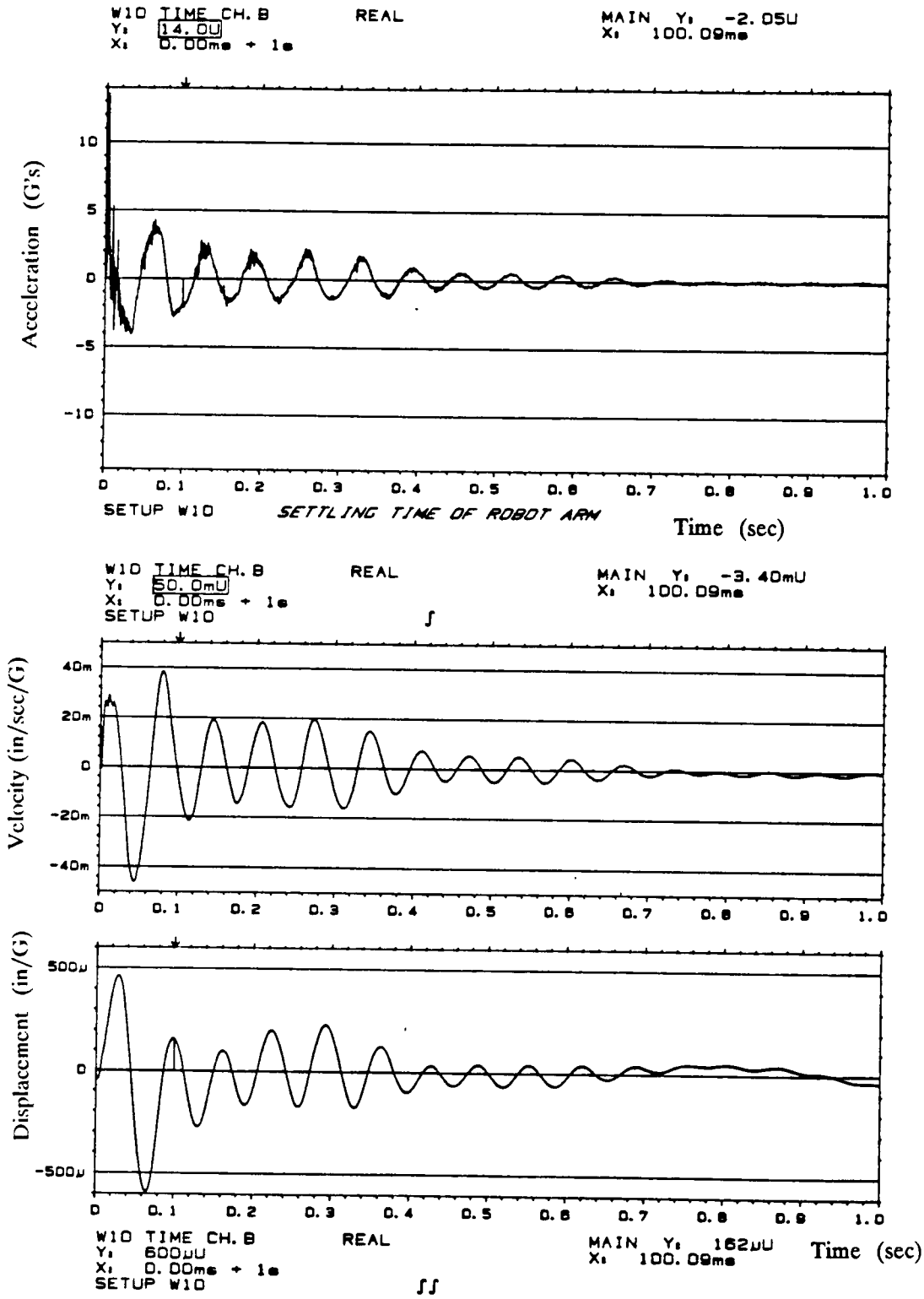

Figure 6.1: Impulse response of unloaded Z Arm and subsequent integrations.

by dividing 0.118 inches by 386 G's/unit , or 305 μunits. The first two oscillations of the arm are out of this range, but the third is in within specifications. Figure 6.2 shows the displacement plot again, but with the limits set at 310μ. Note that the two oscillations that are out of range occur before the 0.1 second cut off time. At 0.1 seconds, the amplitude of vibration is 162μ, or 0.0625 inches. Part of this movement is due to the 0.057 inch clearance of the vertical bearings that support the Z Arm. This clearance is equivalent to $\pm$148 μunits on the plot.

For the second test, the residual acceleration in the arm after the robot completed a move was measured. The point at which the motors stopped at the end of the move was determined by attaching the second channel of the signal analyzer to a coil that had the leads of one of the motors passing through it. This measured the voltage to the motors and showed when the motor cut off. A horizontal

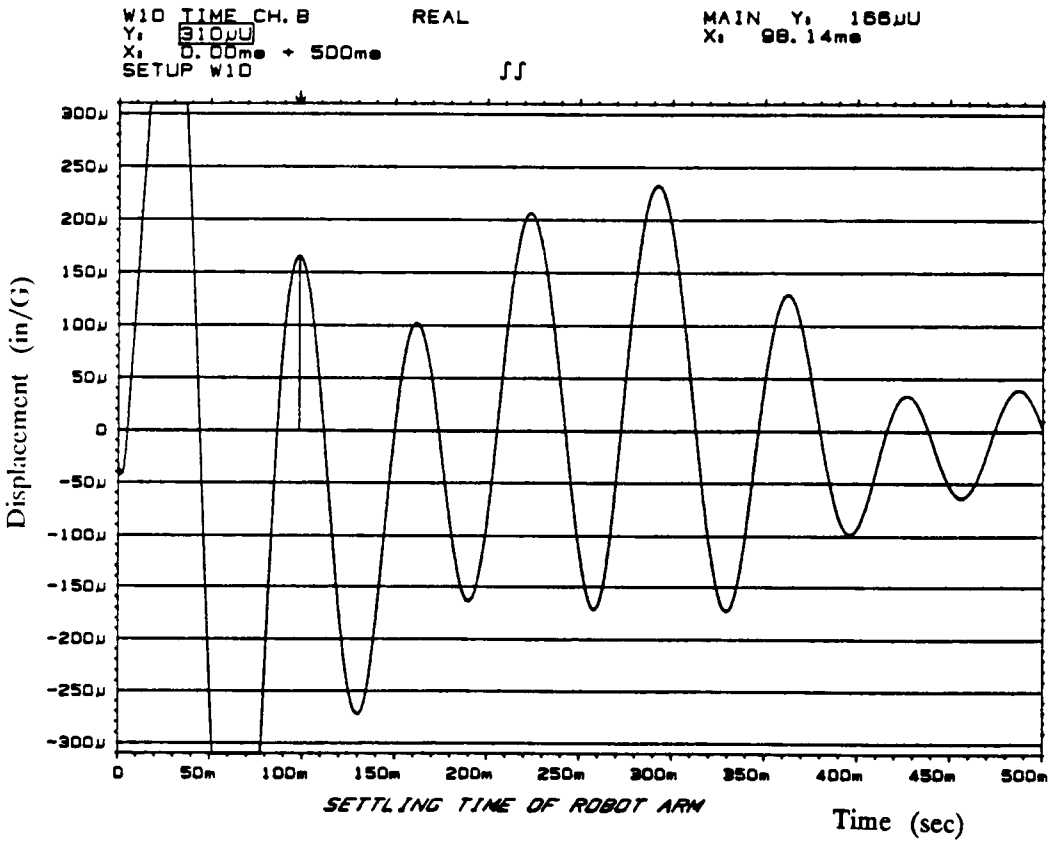

Figure 6.2: Z Arm displacement specification envelope.

dual axis move was used for this test, since this move produces the Z Platform's maximum speed of 48.2 in/sec. The robot moved from the home position to the center of its workspace. The motor voltage is shown in the upper plot of Figure 6.3, the lower plot shows the subsequent acceleration of the arm. The cut off point of the motor is at 659.17 msec. This value was used as the delay time for the accelerometer. Figure 6.4 plots the arm's acceleration after the motor cuts off. Note that the response is similar to that of the impulse response. High frequency noise was present at a frequency of 120 Hz. Attempts were made to find the amplitude of vibration for these accelerations, but when the signal was integrated, the displacements indicated by the signal analyzer were erroneous. The reason for this may be that the initial conditions effect the integration of the signal. However, an approximation of the displacement may

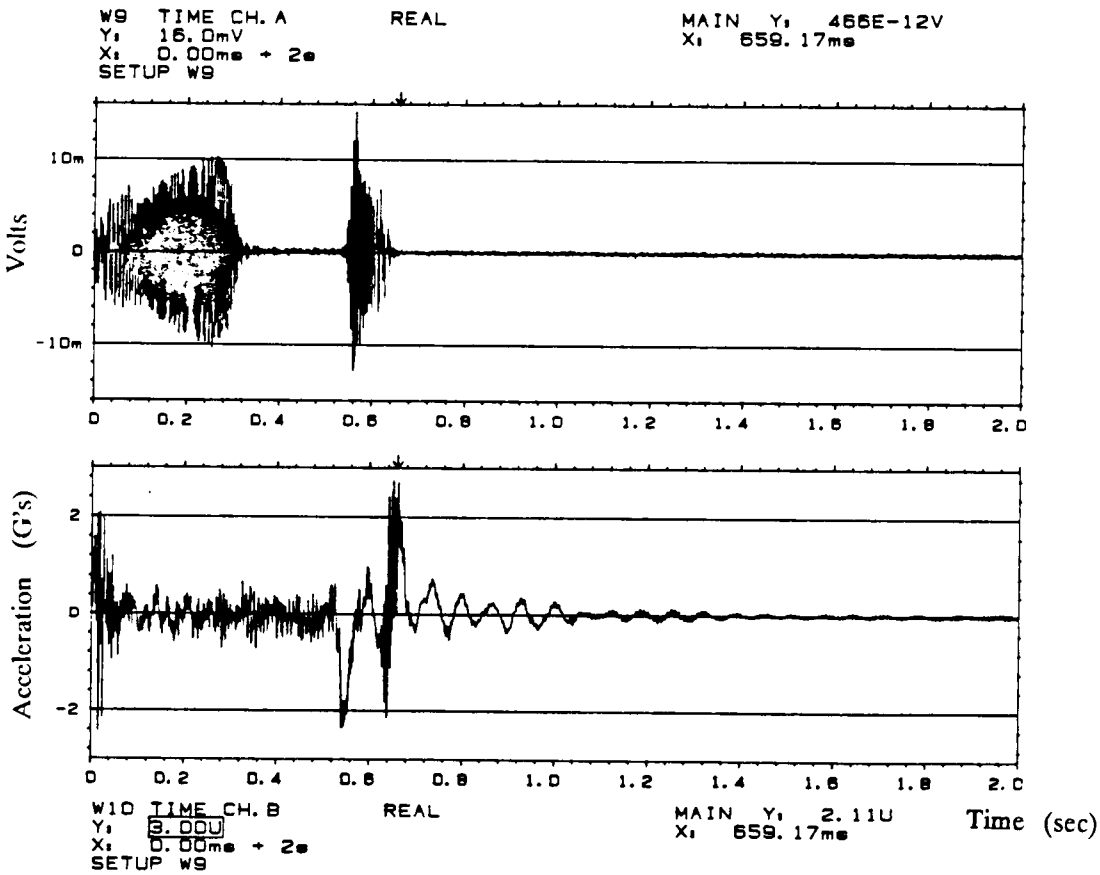

Figure 6.3: Dual channel output of motor pulse duration and Z Arm acceleration.

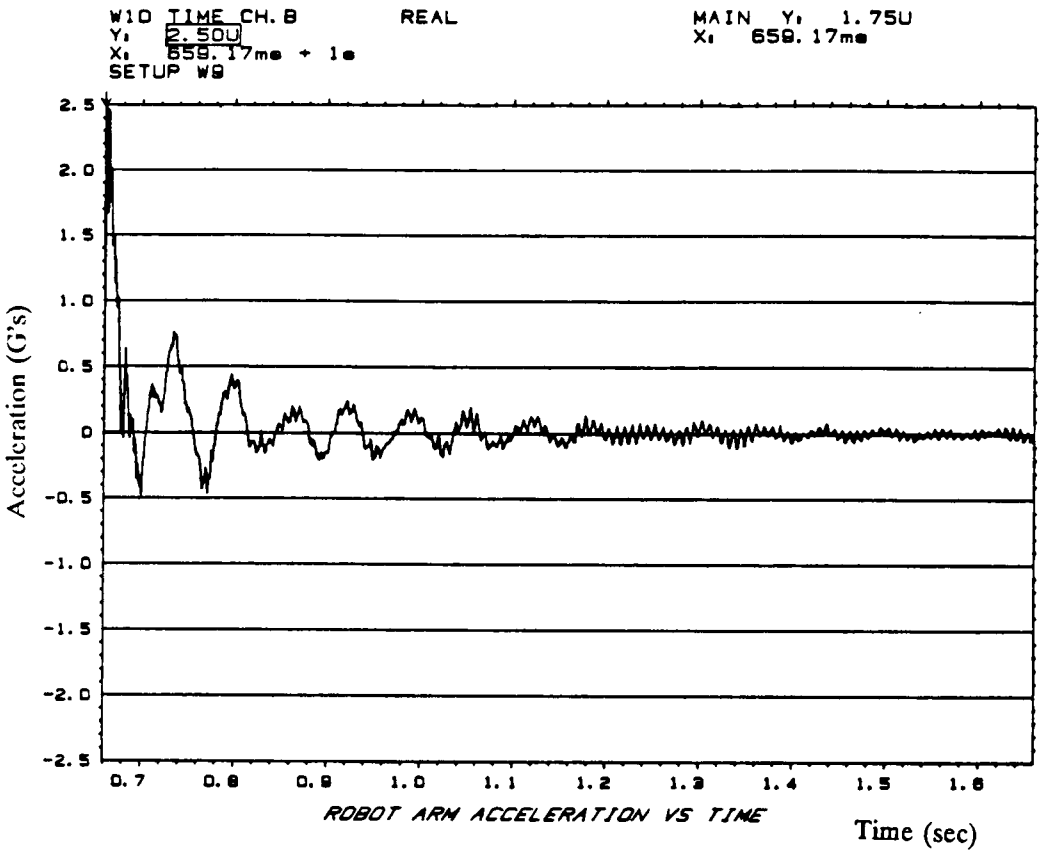

Figure 6.4: Z Arm residual vibration without payload.

be calculated by assuming that the motion is harmonic and the acceleration is proportional to the displacement,

$$a = -w^2X$$

Since the frequency and acceleration are known, the amplitude's magnitude may be solved for,

$$X = a/w^2$$

Performing this calculation on the first peak in Figure 6.4, with w = 94.25 rad/sec (15 Hz) and a = 2.46 G, the displacement X equals 0.107 inches. The logarithmic decrement was measured from this plot to find the damping ratio. Since the system is nonlinear, the damping ratio is not constant. The first damping ratio, found from the first four cycles, was 0.043. Over the next four cycles, the damping

ratio reduced to 0.025.

The final test was to add weight to the end of the arm to see how this effected the settling time. 2.6 pounds was added to the end of the arm. The frequency of vibration decreased with the added weight by 38 % to 9.3 Hz. The arm's acceleration also decreased, by the same amount, approximately equal to the ratio of the natural frequency of the arm with payload to the natural frequency of the arm without payload. A 3.5 lb weight was then added to the arm. This is in excess of the 3 pound payload required by IBM. The residual vibration after a move to the center of the workspace was measured for this case. Figure 6.5 shows the response of the arm. The frequency of vibration of the arm decreased with the added weight. Again, the displacement can be approximated, here w = 52.15 rad/sec (8.3 Hz) and the acceleration of the largest peak is a = -0.638G, so that the displacement equals 0.091 inches. Adding weight to the end of the arm decreased the damping ratio. For the first five cycles, the ratio was

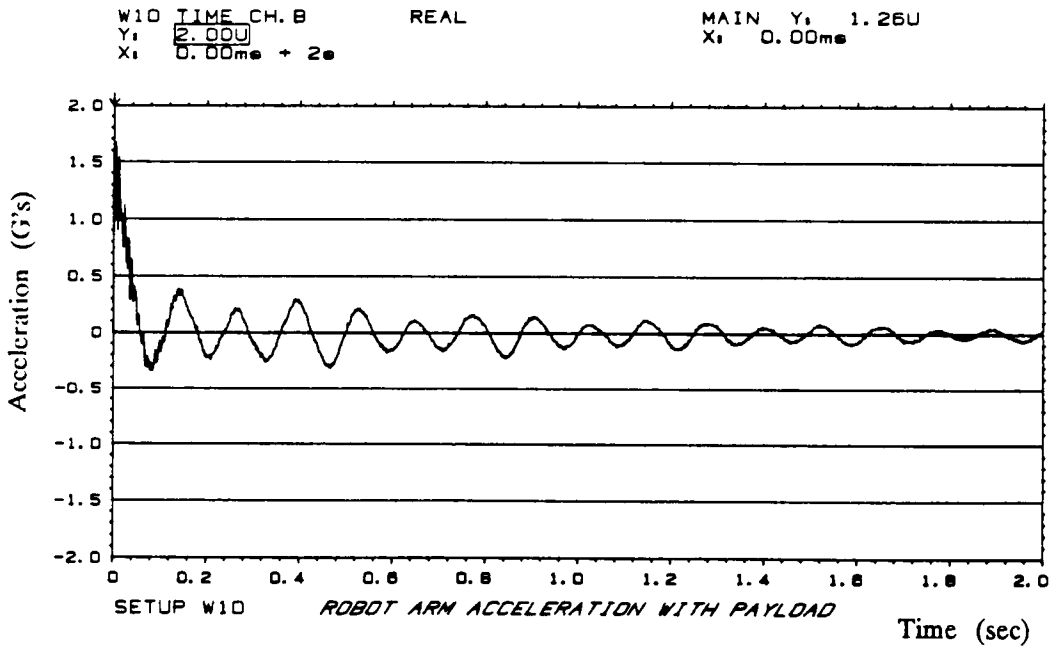

Figure 6.5: Residual vibration of Z Arm with 3.5 lb payload.

0.031. Over the next five cycles the damping ratio decreased to 0.022.

The measurements and calculations performed on the data shows that the Z Arm meets the requirement with the design payload of 3 pounds by settling to ± .118 inches within the 100 msec time. With the 3.5 pound payload, the arm is able to settle within the 0.1 second interval, to approximately half of the amplitude of the design goal. Table 6.1 shows the test data for the three different payloads. All of the data from the robot settling time tests is located in appendix F.

Table 6.1: Settling Time Test Results

Payload (lb)	Natural Freq. (Hz)	Max. Displ. (in)	Time (sec)	Damping Ratio (1st 5 cycles)	Damping Ratio (Next 5 cycles)
None	15	0.034	0.076	0.043*	0.025*
2.6	9.3	0.068	0.061	0.02	0.012
3.5	8.3	0.056	0.14	0.031	0.022

*These ratios were calculated using the first eight cycles.

6.3 Cyclic Testing

The reliability of the robot was tested in two continuous eight hour, cycle tests. The tests were run using the Stepper Motor Signal Generation (SMSG22) program developed by IBM, and were limited to moving only two axes at a time. The payload used during testing was 2.6 pounds added to the wrist adaptor.

The first test was for the X-Y Plus horizontal positioning mechanism. A bi-directional move was used to move the Z Platform horizontally, from one corner of the robot's workspace, at a 45° angle towards the center of the robot's workspace 14.43 inches away, and back to the corner. The move ramped the motors up to full speed (682 RPM) for 500 steps and then ramped them down. Since each slider was moving at 34.1 in/sec, this gave the Z Platform a maximum linear velocity of 48.2 in/sec. The test was run with the Z arm extended 10.5 inches. In the eight hour test, the robot performed the move 16,842 cycles without missing a step.

The Z Arm was tested in a bi-directional move with the z and x directions. The Z Arm achieved a velocity of 10 inches per second in a move from its upper position, to an extension of 10.5 inches. The x axis of the X-Y Plus system also moved during the test of the Z Arm. It received the same signals as the Z Arm's motor, but had a gear ratio of 1.5 times greater than that of the Z Arm. After eight hours, the robot had performed 10,476 cycles without missing a step.

X-Y Plus Cyclic Test Parameters

Run Time: 8 Hrs
Movement: Dual Axis, X and Y
Number of Moves: 16,842
Number of Motor Steps: 32.4 million
Total Travel Distance: 40,505 ft
Motorload (% of max capability): 70%
Timing Pulley Radius: 0.4775 inches (1/5" pitch, 15 teeth)
Robot Payload: 2.6 lbs
Ramp Up: 331 steps in 262 msec
Constant Velocity: 500 steps for 220 msec (34.1 in/sec)
Ramp Down: 131 steps in 123 msec
Maximum Velocity: sliders 34.1 in/sec Z Platform: 48.2 in/sec
Average Velocity: sliders: 16.87 in/sec Z Platform: 23.86 in/sec

Z Arm Cyclic Test Parameters

Run Time: 8 hrs
Movement: Dual Axis, Z and X
Number of Moves: 10,476
Number of Motor Steps: 22 million
Motorload (% of max capability): 70%
Robot Payload: 2.6 lbs
Ramp Up: 53 steps in 94.93 msec
Constant Velocity: 975 steps for 975 msec
Ramp Down: 22 steps in 54.5 msec

Parameter	X	Z
Total Travel Distance (feet)	27,500	18,333
Constant Velocity for 975 steps (in/sec)	15	10
Average Velocity (in/sec)	11.46	7.64
Timing Pulley Radius, 1/5" pitch (inches)	0.4775	0.3185

The cyclic testing revealed no new failure modes for the robot. The only evidence of wear was on the vertical guide tube of the Z Arm. Wear lines began to appear on the tube's outer surface where

it contacts the ball bushings. This is because this tube is made of stainless steel, instead of the recommended RC45 hardened tubing.

These tests also revealed that the stepper motors do not rely heavily on the ramp function. The same ramps were used for this test as were used on the first prototype of the X-Y Plus system that used the plastic sleeve bearings. These ramps were sufficient even though the loading on the motors changed with the reduction in friction and the increased weight of the system.

6.4 Failure Modes

The first failure that occurred during prototype operation was in the control tubes. The original control tubes were stainless steel. These proved to be an unreliable bearing surface for the linear ball bushings. Grooves a couple of thousandths of an inch deep on the control tubes began to appear shortly after the prototype became operational, even without any payload on the robot. The grooves probably would have reached a point where they would not get any deeper; as the groove deepens, its area increases and the stress on the tubes decreases. However, the grooves also created more bearing clearance, thereby decreasing the accuracy of the end effector. This condition was considered to be unacceptable, and the stainless steel control tubes were replaced with Thomson RC60 hardened steel tubes.

A more catastrophic failure occurred when the Z Platform inadvertently impacted against the slider at full speed. Even though rubber bumpers were in place, the Z Platform cracked at one of its bonded joints. This failure mode was counteracted by the addition of more ribs and by PVC welding all of the joints. Also, another o-ring bumper was added to help cushion the platform in case of another collision.

The Z Arm's lower internal snap ring that holds the spindle and bearing cartridge in place failed when it popped out of the internal groove in the vertical guide tube. This condition was repaired by deepening the groove by several thousandths of an inch. Also, the internal snap ring was slightly undersized, so it was prestressed for a tighter fit. This would not be necessary for the production model.

6.5 Prototype Performance Data

After testing the prototype it was concluded that the arm should not be fully extended during operation while having the full three pound payload on the arm. This constraint is recommended in order to reduce the stress on the Z Platform, since it has already broken once. The Z Arm travel is a maximum of 15.25 inches. The maximum recommended extension with a payload over 1.5 lbs is 70 % of this length, or 10.675 inches. This limitation is only for the prototype, it would not be necessary for the production model.

Table 6.2 contains performance data for the prototype in the first column. The second column is the design requirement requested by IBM. The presence of a dash in the table means there was no performance requirement specified.

Table 6.2: Robot Performance Data

Prototype Performance	Requirement
Degrees of freedom: 4	4
Step motors 2.1 Amp 200 step/rev	same
1.1 Amp 200 step/rev	same
Workspace (inches) X_{max} = 27.25, Y_{max} = 27.625, Z_{max} = 15.25	same
Motor linear resolution (inches/step) horizontal = 0.015	same
vertical = 0.01	same
Rotational resolution of yaw motor (degrees/step) = 1.8	1.8
Maximum speed of Z Platform (in/sec) horizontal: single axis = 34.1	-
dual axis = 48.2	-
Average horizontal speed of Z Platform over 12 inches (inches/sec): single axis = 19.7	39
dual axis = 27.8	39
Maximum speed of Z Arm: 10 (in/sec)	-
Theoretical Accuracy (inches) horizontal: 0.0788	0.118
vertical: 0.0016	-
rotational: 0.0154	-
Repeatability (inches) ± 0.006	-
Settling time to 0.118 inches: 0 sec	0.1 sec
Payload* (lbs) 3.0	3.0
Cost $1066	$600

*Note that the Z Arm should not be fully extended with this payload. This limitation is meant only for the prototype, not the production robot.

CHAPTER 7

COST ANALYSIS

The main design goal for the robot was a total cost (including electronics) of no more than $600, based on a projected production of 200,000 robots over 5 years. Table 7.1 gives a breakdown of the parts and their cost. The prices for the injection molded parts were estimated by a molding expert and are based on the molding costs and cycle time. Polycarbonate plastic was recommended as the molding material. The machining time for the components of the Z Platform and the frame were taken into account by assuming a $28 per hour labor cost. Materials cost were based on a one ton quantity of each item, but were quoted from a local vendor, not directly from a distributor. Table 7.2 is a breakdown of the parts that require machining time and the materials cost.

The total estimated cost of the robot was $1066, which is does not meet the cost requirement. The major cost contributors for the Z Arm assembly are the vertical guide tube and the mast. The machining costs alone for these two components were $168. The frame accounts for 17% of the total cost. The price quotes are referenced in Appendix I.

Table 7.1: Robot Costs

Part	Individual Cost	Quantity	Cost per Robot
X-Y Plus Positioning Mechanism			
Corner Bracket	1.00	4	4.00
Slider Bracket	5.00	4	20.00 (18,000, 50)**
Belt Gripper	1.00	4	4.00
2.1 Amp Stepper Motor/Driver	45.00	4	180.00
Guide Shaft	2.00/ft	12 ft	24.00
Control Tube	1.75/ft	5.875 ft	10.28
Linear Motion Bearings	17.79	4	71.16
Timing Gears	1.00	8	8.00
Timing Belt	3.00	4	12.00
Needle Bearings	1.45	4	5.80
Idler Shaft	2.00	4	8.00
Belt Tensioner[a]	2.00	4	8.00
Electrical Control	90.00	1	90.00
Hardware[a]	4.00	1	4.00
Total Cost of X-Y Plus Mechanism			$449.24
Z Platform Assembly			
Z Platform	9.50	1	9.50 (48,000, 55)**
Tube Mount	3.60	1	3.60 (23,000, 45)**
Belt Gripper	1.00	1	1.00
2.1 Amp Stepper Motor/Driver	45.00	1	45.00
1.1 Amp Stepper Motor/Driver	16.00	1	16.00
Vertical Guide Tube*	125.87	1	125.87
Drive Tube*	16.29	1	16.29
Drive Spindle*	22.48	1	22.48
Linear Motion Bearings	17.79	2	35.58
Self-Aligning Ball Bushings[b]	9.18	2	18.36
Radial Bearings[c]	13.87	2	27.74
Needle Bearing	1.45	1	1.45
Bearing Cartridge*	9.24	1	9.24
Motor Coupler*	9.24	1	9.24
Drive Plug*	9.24	1	9.24
Mast*	57.87	1	57.87
Mast Spacer*	4.65	2	9.30
Timing Gears	1.00	2	2.00
Timing Belt[d]	3.72	1	3.72
Wire Pivot	1.60	1	1.60 (9,000, 45)**
Wire Boom*	5.74	1	5.74
Hardware[a]	5.00	1	5.00
Total Cost of Z Platform Assembly			$435.82
Frame*	180.67	1	$180.67
Total Cost of Robot			$1065.73

[a]Estimate of total cost. [b]Price was based on a quantity of 50,000 bearings.
[c]Price was obtained by taking 30% off of the retail price of $19.82 per bearing.
[d]Price was based on a quantity of 100.
*See Table 7.2 for breakdown of machining time and materials cost.
**First item in parenthesis represents cost for a one cavity mold. Second number denotes cycle time in seconds.

Table 7.2: Machining Time Estimates and Materials Cost of Robot Parts

Part	Machining Time	Qty/Robot	Materials $	Total $
Mast Aluminum Square Tubing 1 in. sides 1/16 in. thick	2 hrs	1.72 ft 0.485 lb	1.09/ft	57.87
Vertical Guide Tube RC60 hardened tubing 0.75 in. OD 0.049 in. wall	4 hrs	1.875 ft 0.694 lb	7.40/ft	125.87
Drive Tube Aluminum Tubing 0.5 in. OD 0.035 in. wall	0.18 hrs	1.72 ft 0.106 lb	6.54/ft	16.29
Frame Square steel tubing 1.5x1.5x0.25 in.	5.67 hrs	7 ft 29.82 lb	0.73/ft	
Steel Equal-Leg Angle Iron 1.75x1.75x0.125 in.		26.25 ft 37.74 lb	0.64/ft	180.67
Wire Boom Stainless Steel Tubing 0.187 in. OD 0.035 in. wall	0.083 hrs	1.29 ft 0.074 lb	2.65/ft	5.74
Drive Spindle Stainless Steel Round Stock 0.652 in. DIA	0.75 hrs	0.238 ft 0.273 lb	6.22/ft	22.48
Drive Plug* Stainless steel round stock 0.5 in. DIA	0.33 hrs	0.0625 ft 0.042 lb		9.24
Motor Coupler* Brass round Stock 0.5 in. DIA	0.33 hrs	0.0625 ft 0.045 lb		9.24
Bearing Cartridge* Steel Tubing 0.656 in. OD 0.468 in. ID	0.33 hrs	0.0915 ft 0.052 lb		9.24
Mast Spacer* Steel Round Stock 0.375 in. DIA	0.167 hrs	0.146 ft 0.0276 lb		9.30

*Materials cost not included for these parts.

CHAPTER 8

RECOMMENDATIONS

8.1 Possible Molding Configurations

(a) More attention needs to be given to the method of attaching the timing belts to the sliders. The use of threaded studs to secure the belt gripper onto the timing belt is undesirable from an assembly standpoint (Figure 8.1,a). Threaded fasteners increase the number of parts and assembly time, and are therefore not cost effective. The original slider design used a molded belt gripper with teeth that meshed with the belt. A shelf was molded onto the slider with an internally threaded insert and set screw. The belt gripper meshes with the belt and is inserted into the shelf on the slider. The set screw is then tightened to secure the belt (Figure 8.1, b). The modularity of the slider requires that the part must be able to grip the timing belt from either side. Therefore, a shelf must exist on both sides of the slider. On the top side of the slider, the socket that holds the control tube creates an area for the shelf. The shelf on the other side of the slider, must protrude out by itself, in a cantilever position. This creates the possibility that the shelf would not provide enough rigidity to hold the belt. This design uses threaded fasteners, but not as many as were used for the prototype. Another pitfall is that the use of inserts increases molding costs due to set up cost and the cost of recovering the inserts from reject parts. One suggestion from IBM was that the insert could be eliminated by relying on an interference fit between the belt gripper and the shelf on the slider to secure the timing belt. This approach is the most cost effective method, but the design would have to be tested by actually molding the part to find out if it would work correctly. The final method investigated for securing the belts makes the use of a snap-fit of the belt gripper onto a boss on the slider. The problem of the cantilevered shelf is solved, since the boss that retains the belt gripper is the same on both sides of the slider. This method does away with the threaded fasteners, but is considerably more complicated to mold, and would actually have to be molded to see if it would be reliable (Figure 8.1, c).

(b) Another part that grips the timing belt is the motor mount for the 1.1 amp motor that performs

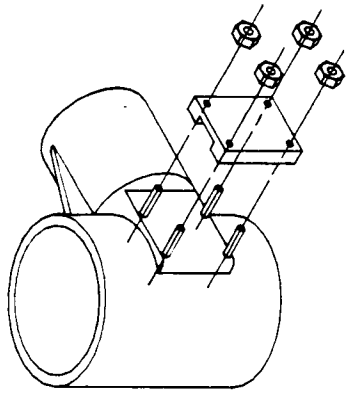

(a) Prototype method using self broaching studs.

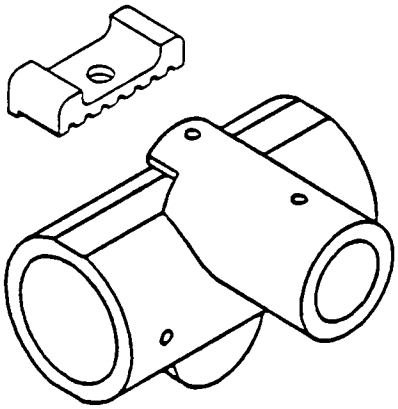

(b) Shelf design with insert and set screw.

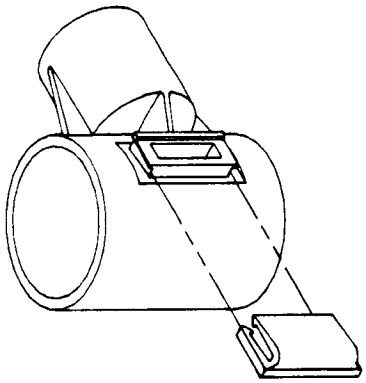

(c) Snap fit design.

Figure 8.1: Possible methods of timing belt attachment to sliders.

the yaw rotation. It would be advantageous to use the same belt gripper for the motor mount and for the sliders to reduce molding costs.

(c) Changes in the design of the corner brackets are needed to make them more suitable for molding. The design shown in Figure 8.2 has a non-uniform thickness and thick sections which are apt to develop sinks and voids when molded. Thick sections are also prone to have residual stresses and warping. In addition, the method of attaching the corner bracket to the frame is not optimal. The present design uses two bolts for each corner bracket to secure it to the frame. One way of eliminating the use of bolts would be to mold a socket into the corner bracket. The socket would slide onto a round post that is part of the frame. A set screw for at least one of the corner brackets would be needed, but the other bolts could be eliminated. A clay model of a redesigned corner bracket was created to help visualize the complex geometry and to minimize the amount of material. The model also uses corrugation and bosses, similar to the design of the Z Platform.

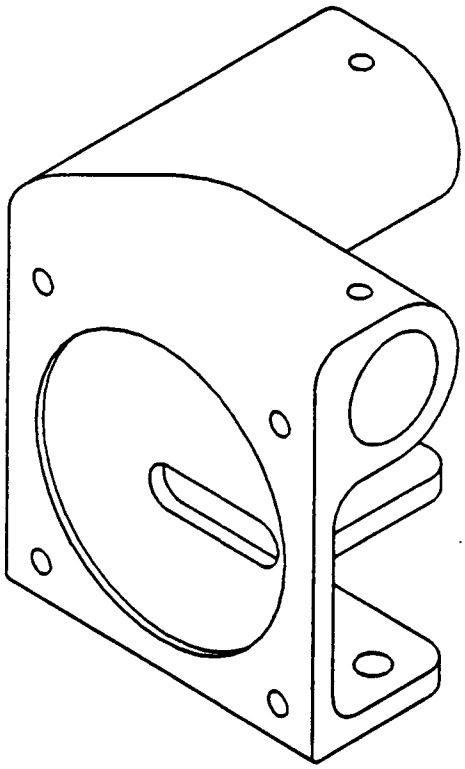

Figure 8.2: Present design of corner bracket.

8.2 Parts To Be Upgraded

(a) Steel, hardened to a minimum of RC 45, should be used for all of the bearing surfaces that are in contact with the Thomson ball bushings. This includes the outer guide shafts and the control tubes, used on the X-Y Plus system, and the vertical guide tube of the Z Arm. Hollow shafts hardened to RC60 were used for the control tubes on the prototype, which were heavy, stiff and too expensive for the production model. A thinner tube would allow the control tube to deflect rather than stall the motor if a bend in the tube were to exist. The thin-walled tube used for the prototype of the Z Arm's vertical guide tube is made of stainless steel and began to show wear lines during the cyclic tests.

(b) The Z Arm's vertical guide tube houses the bearings for the drive spindle. On the prototype, the bearings are separated by a cartridge. Two grooves inside the tube hold internal snap rings, which retain the cartridge inside the tube. An internally stepped tube would be a less expensive method of holding the bearings. This would eliminate the need for the upper internal snap ring. If the inner diameter of the tube matched the outer diameter of the spindle bearings, the bearing cartridge could be replaced by a plastic spacer (Figure 3.4, pg.15).

(c) The timing pulleys used on the prototype are made out of aluminum. It would be less expensive to use molded plastic pulleys. If the proper material was selected, the needle bearings in the idler pulleys could be eliminated by letting the plastic act as its own bearing.

(d) The ramps used to accelerate and decelerate the motors are not the optimum for the robot. The same ramps are being used on the second prototype as were used on the first one. These ramps were calculated based on the use of sleeve bearings, which have since been eliminated. The ramps could be modified to obtain a higher average velocity.

LIST OF REFERENCES

LIST OF REFERENCES

(1) Beer, Ferdinand P., and E. Russell Johnston, Jr. Mechanics of Materials. New York: McGraw-Hill Book Company, 1981.

(2) Design Handbook For DuPont Engineering Polymers, Module 1, General Design Principles, DuPont Corp.

(3) Linear Motion Designers Guide, Thomson Industries, Inc.

(4) The Design and Prototyping of the Horizontal Positioning Mechanism Used in a Low-Cost, High-Speed, Cartesian-Motion Robot. Mark L. Granger, June 1988.

(5) The Use of Embedded Microcontrollers in the Design of a Low-Cost Industrial Robot. Siak Thong Yeo, June 1988.

(6) Thomson, William T. Theory of Vibration With Applications. New Jersey: Prentice-Hall, Inc., 1981.

APPENDICES

APPENDIX A

Analysis of Critical Tolerances

The design requirement stated by IBM was that the end effector of the robot should be accurate to within 0.118 inches (3 mm). A tolerance study was performed on the robot to place limits on the maximum misalignments of the corner brackets and sliders. For case number one, where the corner brackets are misaligned horizontally, the expression for the misalignment in the y-direction is found from similar triangles,

$$Y_1 = Y_{cb}(L_1/L_{gs}) \tag{1}$$

When the control tubes are not orthogonal, the platform misalignment is given by,

$$Y_2 = Y_{sl}(L_2/L_{ct}) \tag{2}$$

The corner bracket elevation effects are,

$$Y_3 = L_3(Z_{cb}/L_{gs}) \tag{3}$$

$$Z_1 = Z_{cb}(L_1/L_{gs}) \tag{4}$$

The slop in the slider bearings creates the next positional errors,

$$Y_4 = L_3(d/L_{ct}) \tag{5}$$

$$Z_2 = d(L_2/L_{ct}) \tag{6}$$

The horizontal platform bearings contribution to misalignment is,

$$Y_5 = L_3(d/l) \tag{7}$$

The vertical platform bearings for the robot arm also creates a possible misalignment,

$$Y_6 = d(L_4/L_{vb}) \tag{8}$$

For the prototype,

L_1 = 32.5 in.
L_2 = 31.5 in.
L_3 = 20 in.
L_4 = 20.5 in.
L_{gs} = 39.37 in.
L_{ct} = 37.875 in.
d = 0.0015 in.
l = 1.5 in.

These values allow Y_4, Y_5 and Y_6 to be calculated. From equations (5), (7) and (8),

Y_4 = 0.0008 in.
Y_5 = 0.0200 in.
Y_6 = 0.0575 in.

Total = 0.0783 in.

The motor positional error is ± 3% of a step. There are 200 motor steps per revolution, or 1.8° per step. Three percent of this is 0.054° per step. Therefore, the motor linear positional error (MPE) is represented by,

$$MPE = 0.00094r \tag{9}$$

where r is the pulley radius in inches. For the prototype's horizontal motors, r = 0.4775 inches. Using this value in equation (9) gives a linear positional error of 0.00045 inches. Therefore, the amount of positional error available for the remaining inaccuracies is,

$$\text{Remaining inaccuracy} = 0.118 - 0.0783 - 0.00045 = 0.0392 \text{ in.}$$

This means that the remaining three cases of error must add up to 0.0392 inches.

By assuming a unit misalignment for each case, the cases may be weighed.

$$Y_{cb} = 27.64\ \%$$
$$Y_{sl} = 27.44\ \%$$
$$Y_{cb} = 44.92\ \%$$

$$\text{Total} = 100\ \%$$

The percentages are multiplied by the remaining allowable misalignment of 0.0392 inches to get the misalignments at the end of the robot arm.

$$Y_1 = 0.27643(0.0392) = 0.01084$$
$$Y_2 = 0.27438(0.0392) = 0.01076$$
$$Y_3 = 0.44919(0.0392) = 0.01761$$

$$\text{Total} = 0.03921 \text{ inches}$$

The maximum allowable misalignments may now be found by using equations (1), (2) and (3).

$$Y_{cb} = 0.01313 \text{ in.}$$
$$Y_{sl} = 0.01294 \text{ in.}$$
$$Z_{cb} = 0.03467 \text{ in.}$$

There are also inaccuracies in the vertical direction. The first one is where one corner bracket is elevated. This is given by equation (4). By substituting in the appropriate values,

$$Z_1 = 0.0286 \text{ inches}$$

The other significant contributor of vertical misalignment is due to the slop in the slider bearings, which will slant the control tubes. This expression is given by equation (6). Calculating this value,

$$Z_2 = 0.0013 \text{ inches}$$

The motor for the vertical motion also contributes to the overall inaccuracy. This motor is the same as that used for horizontal positioning, but the pulley radius is only 0.3185 inches. Using this value in equation (9) gives an error value of 0.0003 inches. Thus, the total vertical positioning error is the sum of these three values, or 0.0302 inches. The next five pages show the cases of misalignment due to bearing clearance and bracket misalignment.

The final source of positional error is in the yaw rotation. The tongue/groove arrangement has a clearance "c" of 0.002 inches. By similar triangles the rotational error "Φ" equals,

$$\Phi = c(2r_w/l) \tag{10}$$

where r_w is the radius of the wrist adapter, and l is the length of the tongue on the drive spindle. For the prototype, r_w = 1.5 inches and l = 0.411 inches. Using these values in equation (10) yields a rotational misalignment of ± 0.015 inches at the outer rim of the wrist adapter. The 1.1 amp motor used for the yaw rotation is accurate to ± 3 % of a step. Using the 1.5 inch radius of the wrist adapter in equation (9) gives an motor positional error (MPE) of 0.0014 inches. The sum of these two contributions gives a rotational positional accuracy at the periphery of the wrist adapter of ± 0.0164 inches.

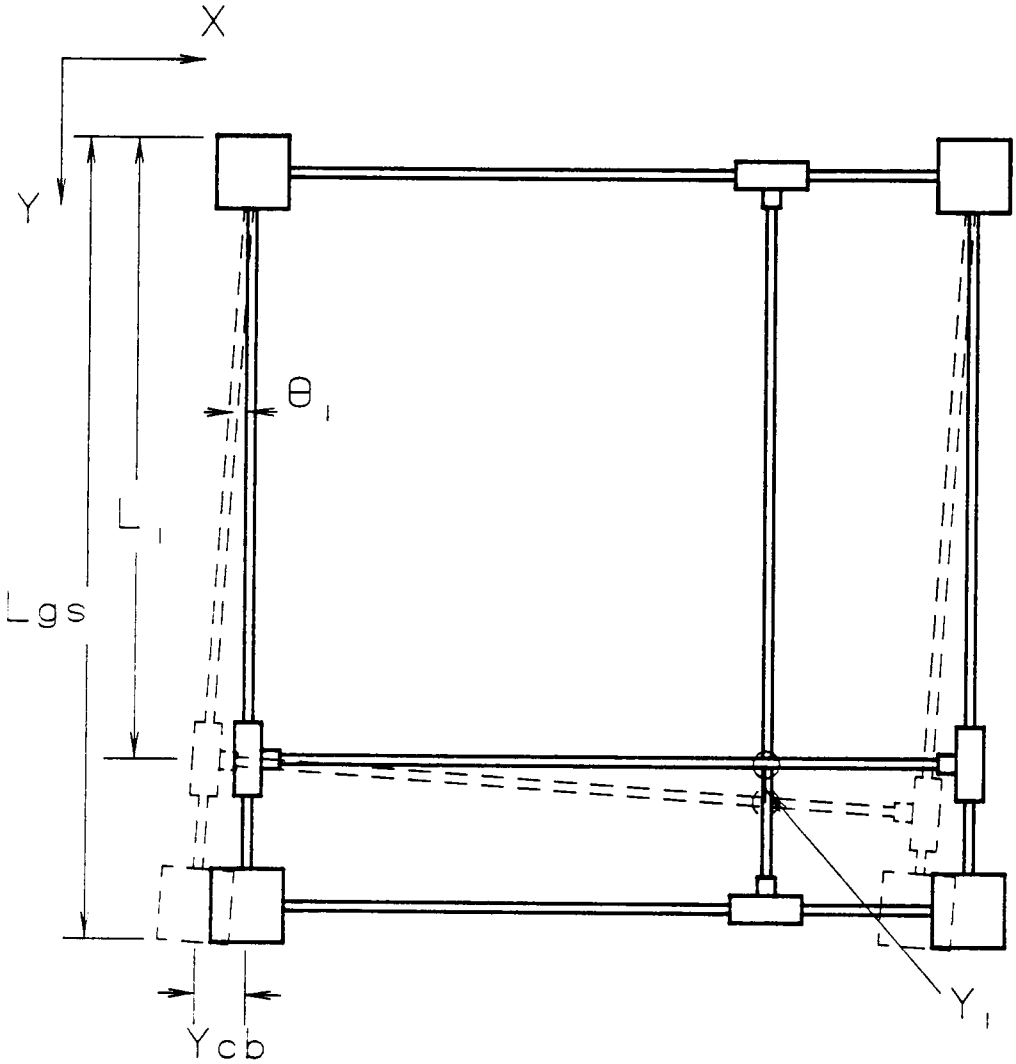

Lgs = Length of guide rod from corner to corner
Ycb = Distance of corner bracket misalignment
L_1 = Position of midpoint of upper platform bearing measured from corner
Y_1 = Inaccuracy of platform in y-direction due to corner bracket misalignment

Inaccuracy due to corner bracket misalignment.

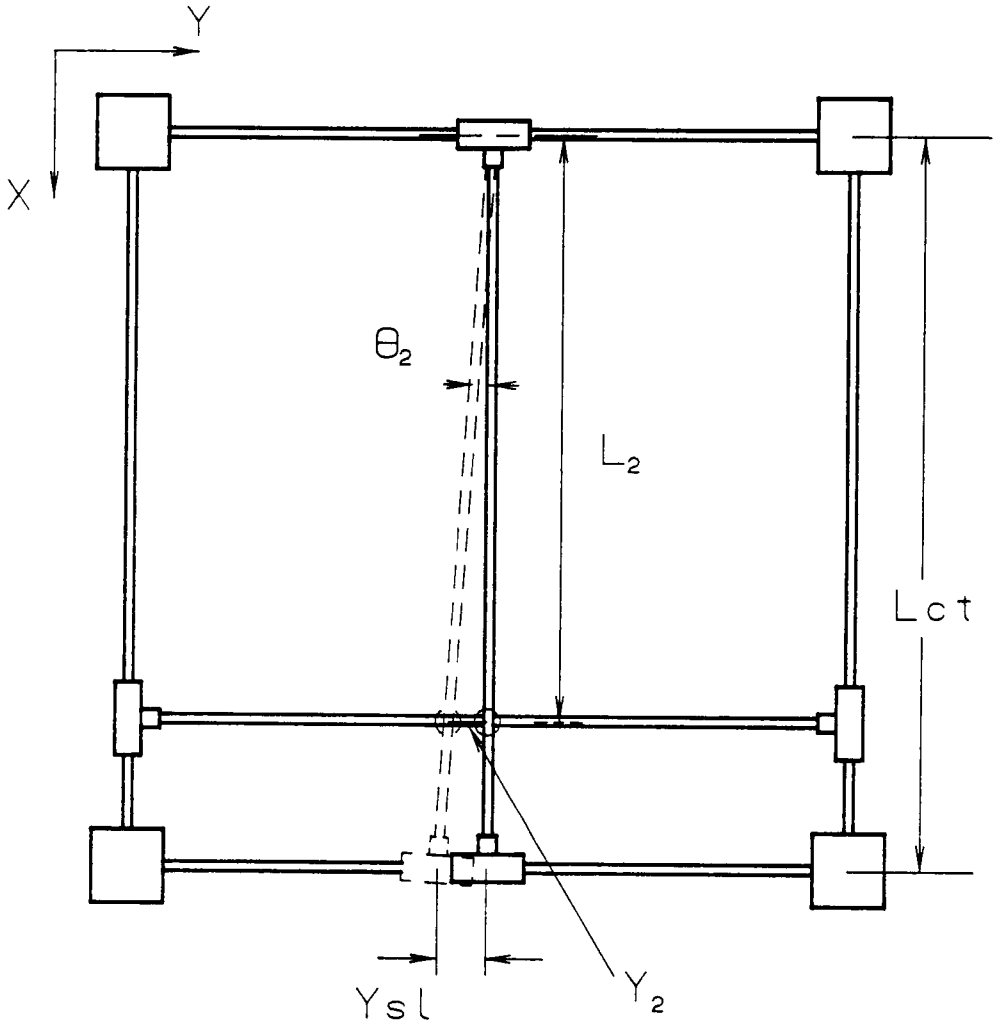

Lct = Distance between control tubes
Ysl = Slider misalignment
L_2 = Position of platform measured from control tube
Y_2 = Platform misalignment in y-direction due to non-orthogonal control tube

Case of non-orthogonal control tubes.

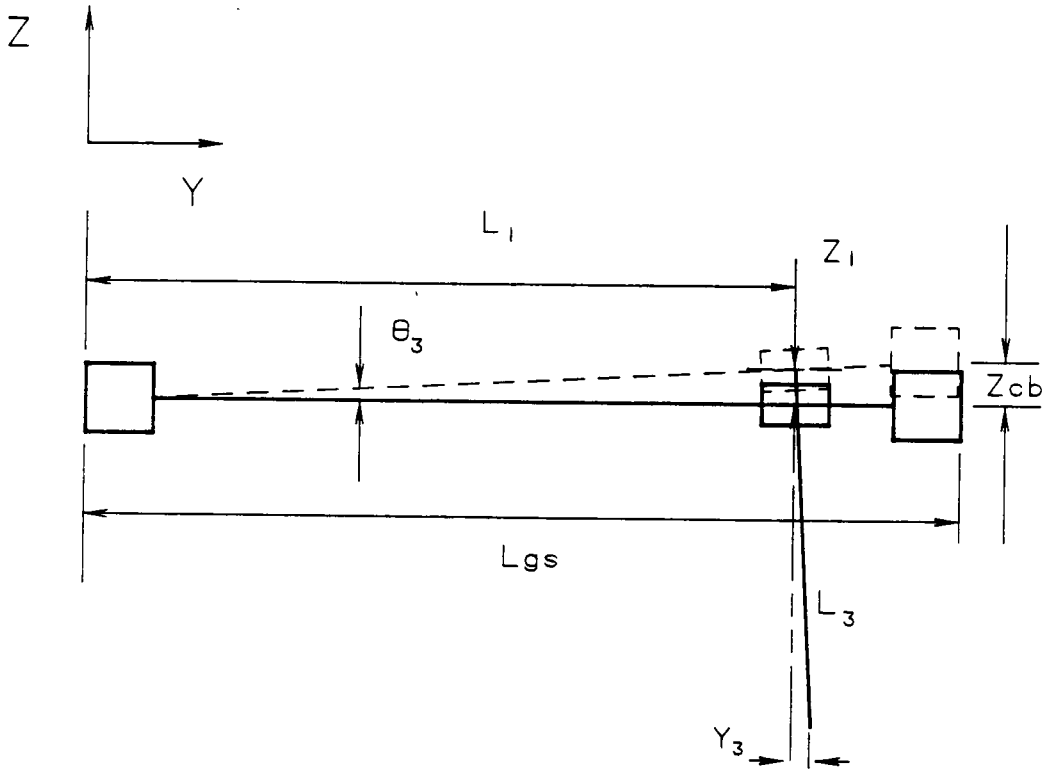

Lgs = Length from corner to corner
L_1 = Length from corner to midpoint of upper platform bearing
L_3 = Length from center of upper platform bearing to end of arm
Zcb = Vertical misalignment of corner bracket
Z_1 = Vertical misalignment of end of arm
Y_3 = Horizontal misalignment of arm in y-direction

Corner bracket elevation effects.

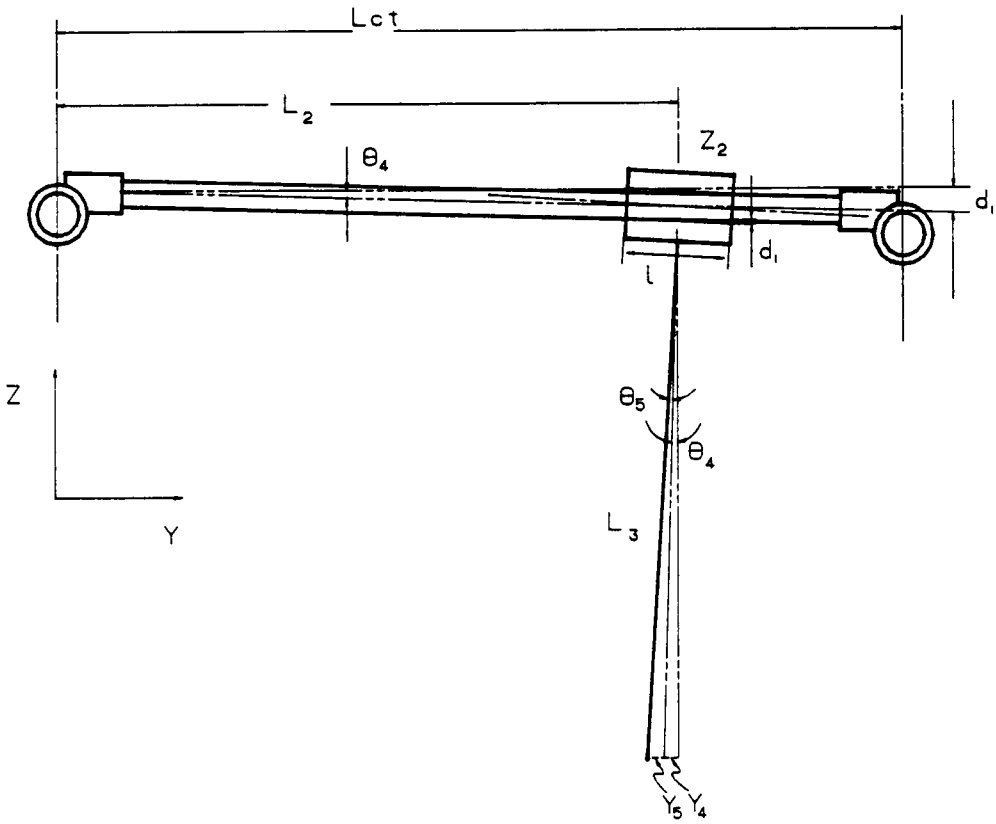

Lct = Length between control tube centers
L_2 = Position of midpoint of platform upper bearing measured from control tube
L_3 = Length of vertical guide tube measured from center of upper platform bearing
d_1 = Diametral clearance of 1" ball bushing
l = Length of bearing contact for 1" ball bushing
Y_4 = Horizontal misalignment of arm in y-direction due to slider bearings
Y_5 = Horizontal misalignment of arm in y-direction due to platform bearings
Z_2 = Vertical misalignment of platform at midpoint of upper bearing

Horizontal bearing clearance contributions.

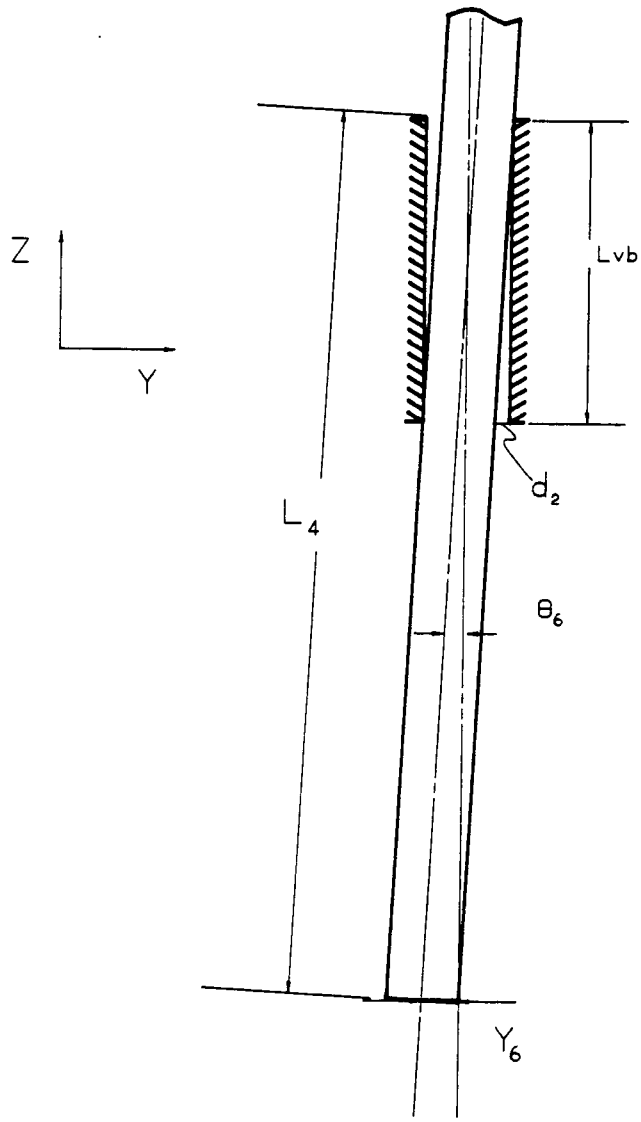

L_4 = Length of vertical arm measured from top of upper vertical bearing
Lvb = Sum of length between bearings and of bearing contact distance
d_2 = Diametral clearance of 3/4" self-aligning ball bushing
Y_6 = Horizontal play of arm in y-direction due to vertical bearing play

Vertical bearing clearance contributions.

APPENDIX B

Binding Analysis of Z Arm

A binding analysis was performed on the Z Arm. This was necessary because the timing belt for the vertical arm is offset from the center of the arm, which produces horizontal binding forces at the bearings. The free body diagram used for the analysis is shown below.

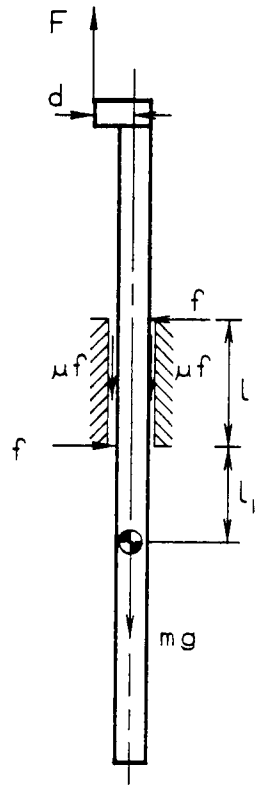

Free body diagram of Z Arm during upward travel.

Summing forces in the vertical direction gives an expression for the friction force f.

$$+\uparrow \Sigma F_v = F - mg - 2\mu f = ma$$

Solving for f,

$$f = (F - mg - ma)/2\mu \qquad (1)$$

Summing moments around the center of mass,

$$\Sigma M_{cm} = f(l+l_1) - fl_1 - Fd = 0$$

Substituting for f from equation (1) and solving for the acceleration

$$a_\mu = F(1 - 2\mu d/l)/m - g \qquad (2)$$

For the no friction case, equation (2) reduces to,

$$a_{\mu=0} = F/m - g \tag{3}$$

The ratio of these two accelerations is a measure of efficiency,

$$EFF_{acc} = a_{\mu}/a_{\mu=0}$$

The effects of the force offset distance d on the acceleration efficiency of the vertical arm was investigated by writing a BASICA program. The acceleration efficiency was calculated for various force offset distances, using various friction coefficients. A plot of this data is shown below. The coefficient of friction for the prototype is 0.004 and its force offset distance is 1.25 inches. This produces an acceleration efficiency of 99.2 %.

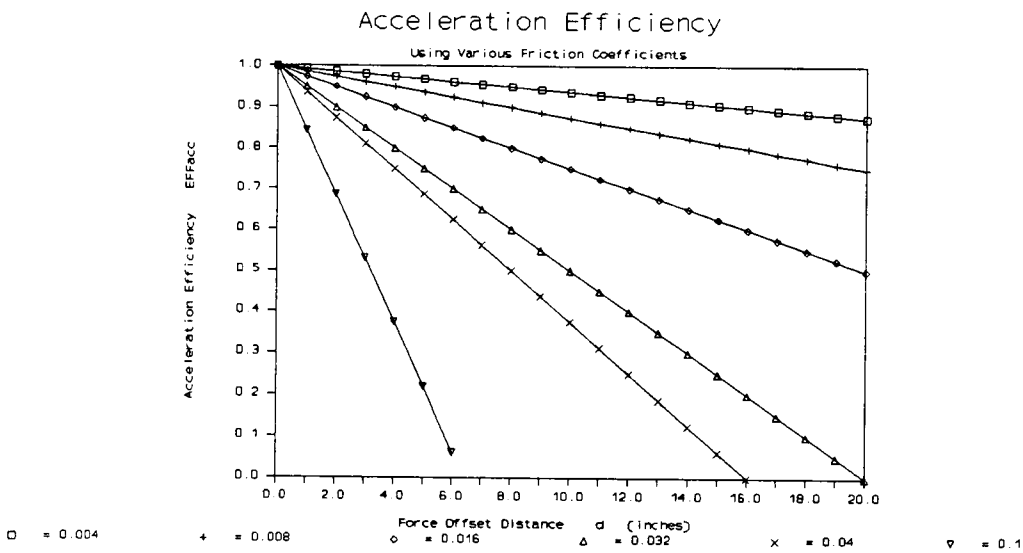

Z Arm efficiency with increased force offset distance using various friction coefficients.

APPENDIX C

Frame Analysis

The design criteria for the frame for the robot was to find the proper sizes for the vertical legs and the horizontal arms which produced adequate stiffness with minimal volume. The parts chosen for the frame were square tubing for the vertical legs and equal-leg angle iron for the horizontal arms. A 2-D model was used to model the frame as shown below. This simplified the analysis, but still gave the desired information on how the ratio of inertias of the vertical and horizontal members affected the stiffness. In the analysis, a horizontal load P was applied on the top of the frame. The dashed lines in

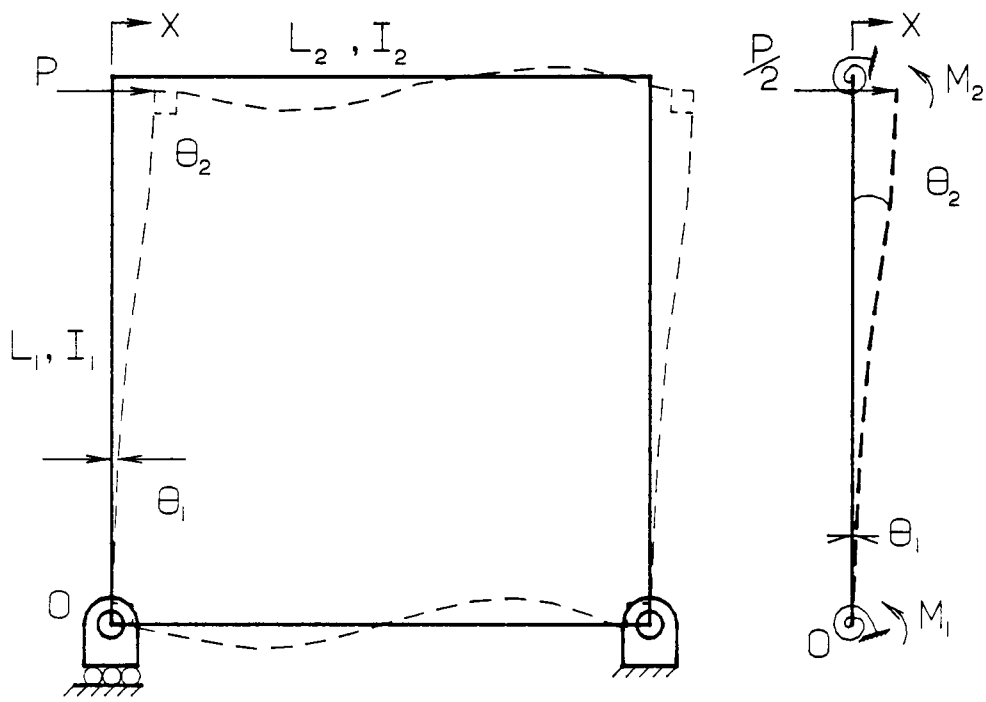

Two dimensional model of frame.

the figure show the exaggerated deflections of the frame under the loading. Since the frame is symmetric, the loading is shared equally by the two vertical legs. The contribution of the horizontal arms is a restoring moment at each end of the vertical leg. The restoring moments are equal to the angle of rotation Θ_n of the vertical leg times the stiffness K of the arms. This was modeled as a torsional spring at each end of the leg. The total deflection of the vertical leg at the point of the load is the contributions

of the load itself and of the restoring moments.

$$X = P(L_1)^3/3EI_1 + \Theta_1 L_1 - K\Theta_2(L_1)^2/2EI_1 \qquad (1)$$

Summing moments around point O,

$$\Sigma M_o = PL_1 - K\ {}_1 - K\Theta_2 = 0 \qquad (2)$$

Where K is the stiffness of the horizontal arms. This was modeled as a pinned beam with a moment at one end,

$$K = 3EI_2/L'$$

Due to the symmetry of the loading, there is no moment at the center of the arms. Therefore, the length used in determining K is half of the length of the horizontal arms. The final form of the stiffness equation is,

$$K = 6EI_2/L_2$$

Solving equation (1) for the angle of rotation at the point of the load,

$$\Theta_2 = P(L_1)^2/2EI_1 - K\Theta_2 L_1/EI_1 + \Theta_1 \qquad (3)$$

Combining these three equations into matrix form gives the relationships for the angles of rotation and the deflection at the point of the load, in terms of the frames geometry, stiffness and loading.

$$\begin{bmatrix} 1 & -L_1 & K(L_1)^2/2EI_1 \\ 0 & K & K \\ 0 & -1 & (1+KL_1/EI_1) \end{bmatrix} \begin{bmatrix} X \\ \Theta_1 \\ \Theta_2 \end{bmatrix} = \begin{bmatrix} P(L_1)^3/3EI_1 \\ PL_1 \\ P(L_1)^2/2EI_1 \end{bmatrix}$$

A BASICA program was written to vary the cross-sections of the horizontal members (equal-leg angle iron), while keeping a fixed cross-section of the vertical leg (square steel tubing). The program calculates the area, volume, and inertia of each member, and the horizontal deflection at the point of the load. A relative volume was defined that consisted of one vertical leg and two horizontal arms. A deflection of 0.005 inch was chosen as the maximum deflection. For each vertical leg size, there is a horizontal member size that will provide adequate rigidity for a 0.005 inch deflection. The combination of members with the minimum relative volume for this deflection and with a favorable geometry using stock sizes was chosen. Case five had the lowest relative volume for the 0.005 inch deflection, but did

not mate well with the cornerbrackets. The geometry chosen for the frame was case four. This case used a 1.5 inch square steel tube with a 0.25 inch wall thickness for the vertical legs, and a 1.75 inch equal-leg angle iron with a 0.125 inch thickness for the horizontal arms. The frame is one meter square and 21 inches high. The program and graphs obtained from the data are shown on the following pages.

```
10  'OPTFRAME.BAS  2/22/86  This program calculates the deflection of a
20  '               2-D frame with a side load at the top. Also
30  '               Calculated is area, volume and inertia of the members.
40  OPEN "xframe.dat" FOR OUTPUT AS #2
50  DIM C(50,50),L(50)
60      E=30*10^6:P=10        'modulus and load
70      LEN1=21:LEN2=39.37   'lengths of members
80  FOR J=1 TO 6
90      READ L1,T1,T2    'read vertical leg x-sect. and arm thickness
100     DL=0             'increment lengths of side of angle iron
110     FOR I=1 TO 20
120       L2=1+DL   'length of leg
130       A1=L1^2-(L1-2*T1)^2 'area of member 1
140       I1=1/12*(L1^4-(L1-2*T1)^4) 'inertia of member1
150       A2A=L2*T2:A2B=T2*(L2-T2):A2=A2A+A2B 'area of member 2
160       YBAR2=(A2A*L2/2+A2B*T2/2)/(A2A+A2B)
170       I2=1/12*T2*L2^3+T2*L2*(L2/2-YBAR2)^2+1/12*(L2-T2)*T2^3+(L2-T2)*T2*(T2/
2-YBAR2)^2 'inertia of member2
180       VOL=A1*LEN1+2*A2*LEN2 'volume
190 'calculating angles and deflection
200 '
210       K=6*E*I2/LEN2 'stiffness of horizontal member
220       A=1+K*LEN1/(E*I1):B=K*LEN1/(2*E*I1)
230       TH1=P*LEN1*(A-B)/(K*(A+1)) 'theta1
240       TH2=P*LEN1*(1+B)/(K*(A+1)) 'theta2
250       X=P*LEN1^3/(3*E*I1)+TH1*LEN1-K*TH2*LEN1^2/(2*E*I1) 'deflection
260       L(I)=L2
270       C(J,I)=X
280       DL=DL+.125
290     NEXT I
300   NEXT J
310   FOR J=1 TO 20
320     PRINT#2, USING " #.######## "#L(J),C(1,J),C(2,J),C(3,J),C(4,J),C(5,J),C(6
,J)
330   NEXT J
340 'data statements for various cases
350 DATA 1,.125,.25
360 DATA 1,.25,.125
370 DATA 1.5,.125,.25
380 DATA 1.5,.25,.125
390 DATA 2,.125,.125
400 DATA 2,.25,.125
```

OPTFRAME.BAS program for frame optimization.

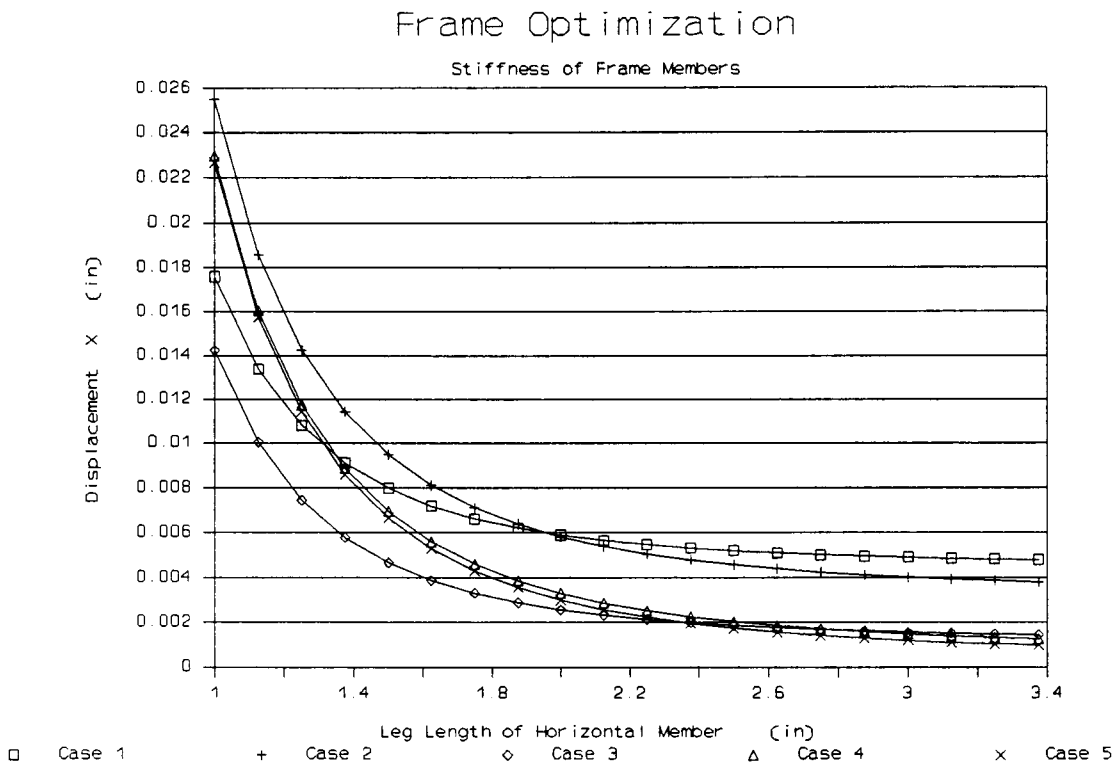

Case 1: Vertical leg 1x1x0.125.....Horizontal arm thickness 0.25
Case 2: Vertical leg 1x1x0.25.....Horizontal arm thickness 0.125
Case 3: Vertical leg 1.5x1.5x0.25.....Horizontal arm thickness 0.25
Case 4: Vertical leg 1.5x1.5x0.25.....Horizontal arm thickness 0.125
Case 5: Vertical leg 2x2x0.125.....Horizontal arm thickness 0.125

Stiffness of 2-D frame model with increasing frame arm inertia.

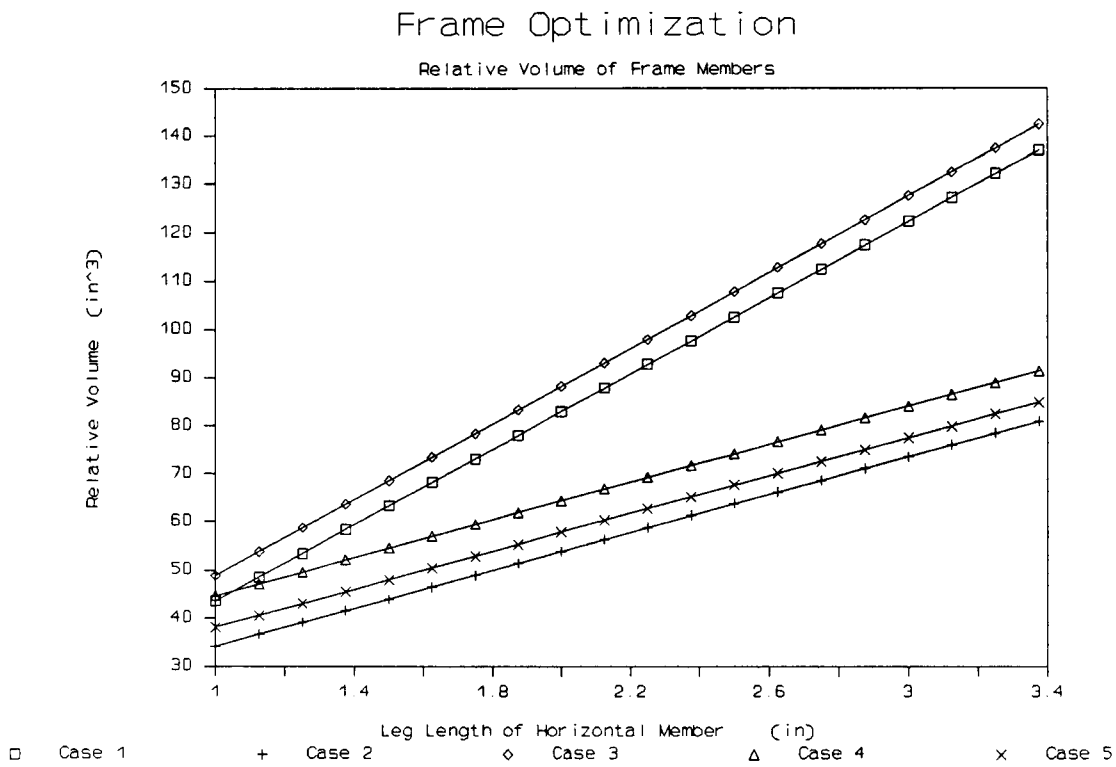

Case 1: Vertical leg 1x1x0.125.....Horizontal arm thickness 0.25
Case 2: Vertical leg 1x1x0.25.....Horizontal arm thickness 0.125
Case 3: Vertical leg 1.5x1.5x0.25.....Horizontal arm thickness 0.25
Case 4: Vertical leg 1.5x1.5x0.25.....Horizontal arm thickness 0.125
Case 5: Vertical leg 2x2x0.125.....Horizontal arm thickness 0.125

Relative volume of 2-D frame model with increasing frame arm inertia.

APPENDIX D

Z Arm Groove Analysis

The thin-walled tube used for the vertical guide tube in the Z Arm assembly, has two shallow grooves 180° apart, running along its length on the outer surface. The grooves make the outer guide tube to resist rotation by allowing one of the tracks on each of the two self-aligning ball bushings to be driven into the groove by a set screw. Since the vertical guide tube has a wall thickness of only 0.049 inches, a shallow groove was desired in order not to jeopardize the strength of the tube. However, a groove that was too shallow would allow the row of balls to pop out of the groove and allow the tube to turn. The manufacturer recommended a V-shaped groove 0.012 inches deep. It was decided to use a shallower round groove instead. Therefore, the 0.012 inch V groove was converted into a round groove of only .008 inches in depth as shown below (see diagram on pg. 81),

$$u = w/\tan\alpha \quad v = r\cos\beta \quad w = r\sin\beta$$

$$\begin{aligned} s &= u + v - r \\ &= r(1 - \sin\alpha)/\sin\alpha \end{aligned}$$

$$\begin{aligned} t &= d - s \\ &= d - r(1 - \sin\alpha)/\sin\alpha \end{aligned}$$

For $d = 0.012$ inches and $\alpha = 70°$

$$t = 0.008 \text{ inches}$$

Since two bearings are used for the vertical guide tube, one bearing can be used for each groove, thus increasing the maximum torque the bearings can withstand. The main consideration, however, was the force on the insert that holds the rows of balls in place. Two internally threaded inserts are imbedded into the plastic tube on the Z Platform. The inserts hold the set screws in place. If the force on the insert is too high, it could deflect the outer plastic tube of the Z Platform and allow the tube to rotate. A static analysis of the bearing in the groove, showed that the 0.008 inch deep round groove converted from the 0.012 inch V groove lowered the force on the insert by 35 % for a given torque. The moment arm of the set screw is longer for the round groove than for the V groove, so the force on the insert is lower for the same applied torque on the guide tube. A BASICA program used the static analysis to vary the groove depth for a given torque, to see how this influenced the force on the insert. Referring to the free body diagram of the bearing in the round groove on pg. 82,

$$b = 2r\sin\Theta \quad t = r(1-\cos\Theta) \tag{1}$$

Where Θ is the contact angle measure from the vertical centerline, b is the groove width, and t is its

depth. For an applied torque T_a, the force produced on the bearing is,

$$F = T_a/2(R + r\cos\Theta) \tag{2}$$

Where R is the radius of the vertical guide tube. Summing moments about point O,

$$\Sigma Mo = F_p\sin\Theta - F(r-t) = 0 \tag{3}$$

Using equation (1) for t and solving for the pull-out force F_p in equation (3),

$$F_p = F\cot\Theta \tag{4}$$

Although a deeper groove lowered the pull-out force, the force for the 0.008 inch deep groove, was not unreasonably high, so this depth was used. At the 2.6 in-lb holding torque of the 1.1 amp motor used for the yaw rotation, the force on each insert is calculated to be 5.4 lbs. Page 83 shows a plot of the pull-out force variation as groove depth increases, for selected applied torques.

```
10  'GROOVE.BAS  9/9/88  This program finds the pull out force created by an
20  '            an applied torque to the vertical guide tube of the Z Arm.
30  '            The groove depth is varied for each selected torque.
40  DIM TORQ(100),FP(100),T(100)
50  OPEN "scrn:" FOR OUTPUT AS #1
60  OPEN "groove.dat" FOR OUTPUT AS #2
70  BRAD=1/16:PI=3.1415927#:R=3/8  'ball radius, pi, tube radius
80  PRINT#1, TAB(15) "THETA          t          b          Ta          F            Fp"

90  PRINT#1, TAB(12) "-------------------------------------------------------
--------"
100  FOR TA = 1 TO 9 STEP 2       'vary applied torque
110    PRINT#2, USING "  ##.#  ";TA
120    FOR A= 10 TO 45 STEP 1     'vary groove depth defined by angle theta
130      THETA=A*PI/180
140      T = BRAD*(1-COS(THETA)):B=2*BRAD*SIN(THETA)  'groove depth and width
150      F = .5*TA/(R+BRAD-T)    'force due to torque
160      FP = F/TAN(THETA)       'pull out force
170      PRINT#1, TAB(12) USING " ###.####  "; A,T,B,TA,F,FP
180      PRINT#2, USING " .####  ##.##  ";T,FP
190    NEXT A
200 NEXT TA
```

GROOVE.BAS program for calculating pull out force for increasing groove depth.

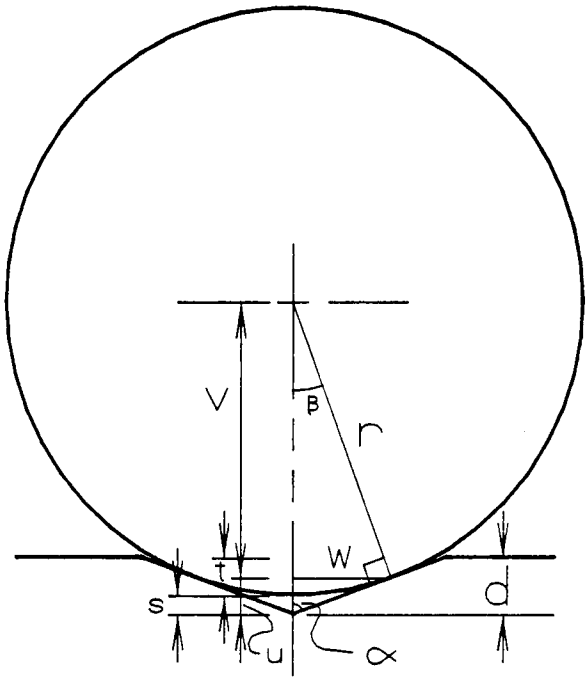

d = Depth of V groove
α = Angle of V groove measure from the vertical (= 70°)
ß = Contact angle
r = Radius of ball bearing for 3/4" super ball bushing
t = Depth of round groove
s,u,v,w = intermediate variables

Ball groove conversion geometry.

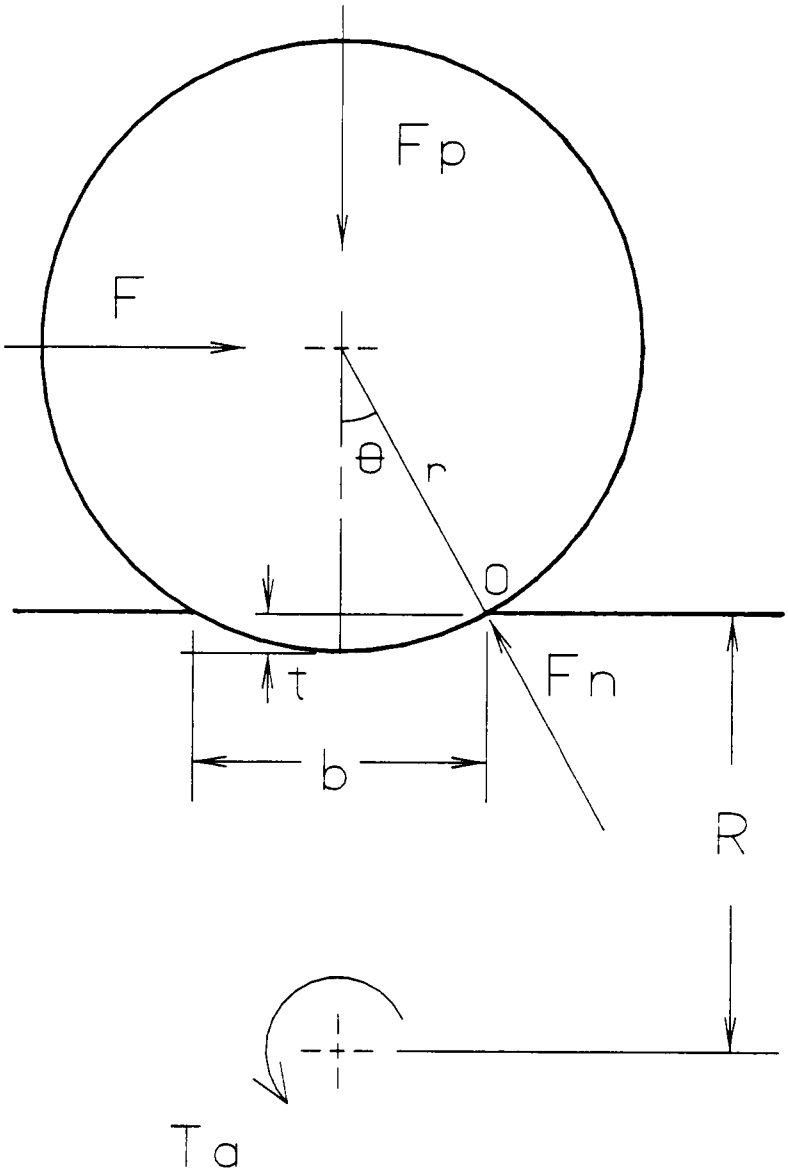

b = Groove width
t = Groove depth
r = Ball bearing radius
R = Vertical guide tube radius
O = Contact angle measured from vertical centerline
T_a = Torque applied to vertical guide tube
F = Force on bearing due to torque T_a
F_p = Force insert must exert on bearing (pull-out force)

Free body diagram of bearing in round groove.

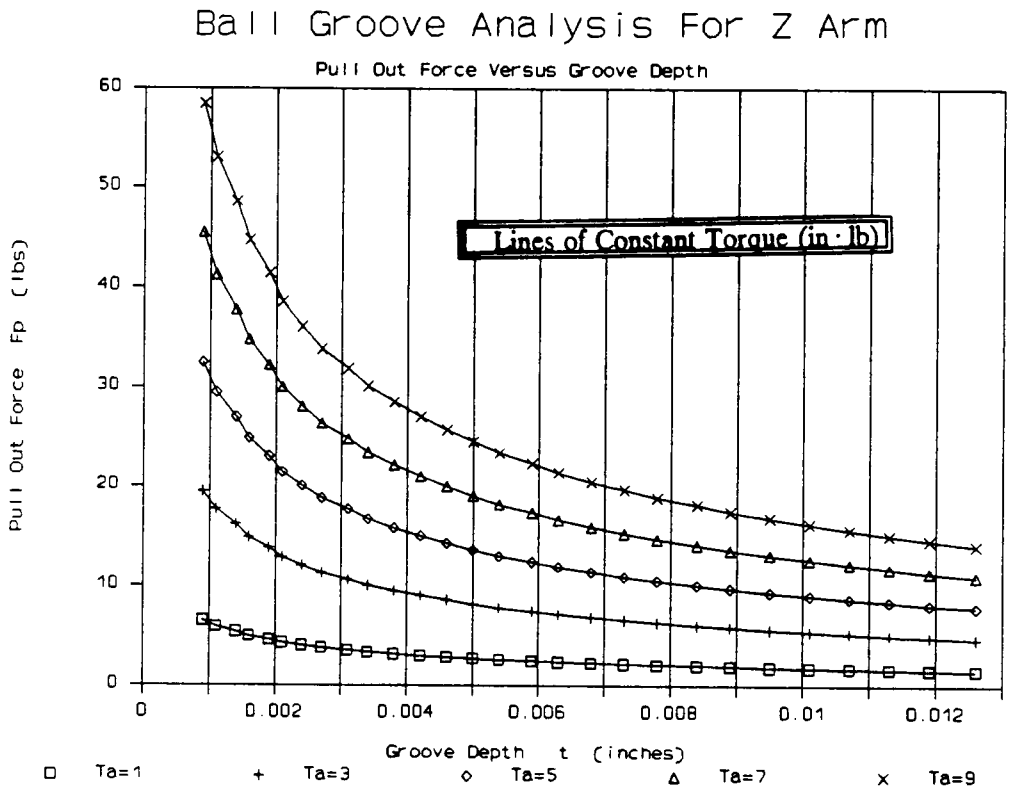

Insert pull-out force for increasing groove depth using selected applied torques.

APPENDIX E

Repeatability Test of Z Arm

A repeatability test was performed on the robot to see how much variation exists in the arm's horizontal positioning. The test was conducted by having the robot execute a horizontal move in the x-direction over and over and over, measuring its position from a fixed reference after each move. A parallel was attached to the side of the frame as the measuring datum. Each time after the robot moved from its home position, to 27 inches away in the x-direction, the distance from the robot wrist adaptor to the parallel was measure with a vernier caliper. After a delay time of 30 seconds the robot would then return home and immediately repeat the move for another measurement. This was repeated 27 times. From this data the standard of deviation was found to be 0.00204 inches. This means that the arm is repeatable to a point in its workspace to within ± 0.0061 inches, or ± 3σ. The worksheet shown below contains the test data and the preliminary calculations to obtaining the standard of deviation.

#	Xi	Sum Xi	Xm	(Xi-Xm)^2		Sigma
1	6.264	169.164	6.265333	0.000001	0.000112	0.002036
2	6.266		6.265333	0.000000		
3	6.265		6.265333	0.000000		
4	6.267		6.265333	0.000002		
5	6.265		6.265333	0.000000		
6	6.266		6.265333	0.000000		
7	6.263		6.265333	0.000005		
8	6.264		6.265333	0.000001		
9	6.267		6.265333	0.000002		
10	6.261		6.265333	0.000018		
11	6.265		6.265333	0.000000		
12	6.267		6.265333	0.000002		
13	6.266		6.265333	0.000000		
14	6.266		6.265333	0.000000		
15	6.266		6.265333	0.000000		
16	6.266		6.265333	0.000000		
17	6.266		6.265333	0.000000		
18	6.267		6.265333	0.000002		
19	6.265		6.265333	0.000000		
20	6.265		6.265333	0.000000		
21	6.266		6.265333	0.000000		
22	6.268		6.265333	0.000007		
23	6.267		6.265333	0.000002		
24	6.263		6.265333	0.000005		
25	6.265		6.265333	0.000000		
26	6.269		6.265333	0.000013		
27	6.259		6.265333	0.000040		

Worksheet of Z Arm repeatability test data.

APPENDIX F

Settling Time Test of Z Arm

Three tests were performed on the robot to determine the settling time of robot arm. The requirement stated by IBM is that the robot arm should settle to within 0.118 inches (3mm) within 0.1 seconds (100 msec). The output of an accelerometer, attached to the wrist adaptor at the end of the Z Arm, was recorded by a dual channel signal analyzer. The sensitivity of the accelerometer was 10.5 mV/G. The signal analyzer is digital and has the capability to store and manipulate any input.

The first test was to measure the arm's acceleration over time when subjected to an impulse response. The arm was fully extended without any payload attached to the wrist adaptor. The arm was given an initial displacement and plucked. The acceleration was measured for one second. The peak acceleration for was 13.5 G's. This signal was then integrated by the signal analyzer to produce the velocity and displacement of the end of the arm. The maximum displacement of the arm was approximately 0.232 inches, which occurred 0.065 seconds after the arm was plucked. At 0.1 seconds, the displacement was reduced to 0.0625 inches. This value is below the 0.118 inch requirement. The natural frequency for the arm when fully extended and no payload is 94.25 rad/sec, or 15 Hz. The damping ratio for the first six cycles was 0.046. Over the next five cycles the damping ratio increased to 0.073.

The plots from the signal analyzer for this test are shown on the next three pages.

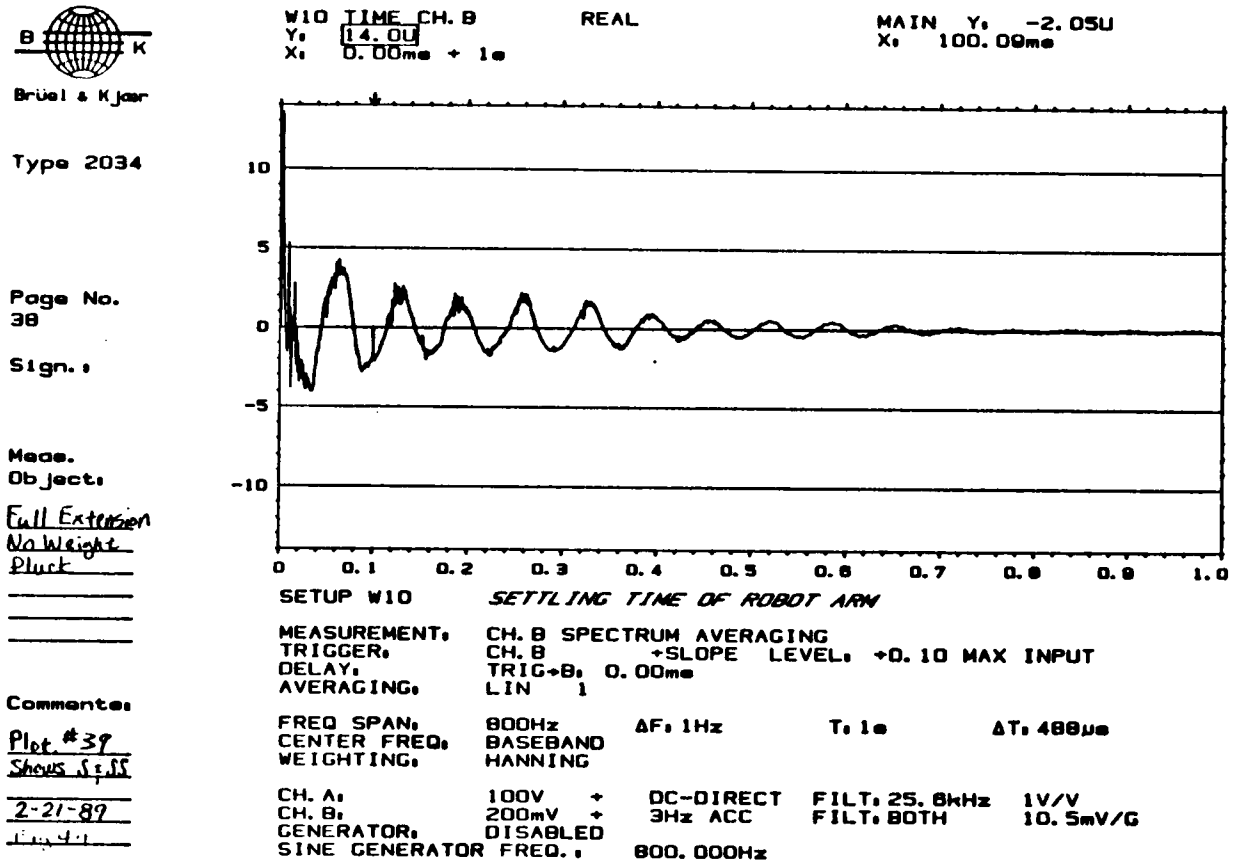

Z Arm acceleration over time due to an impulse response.

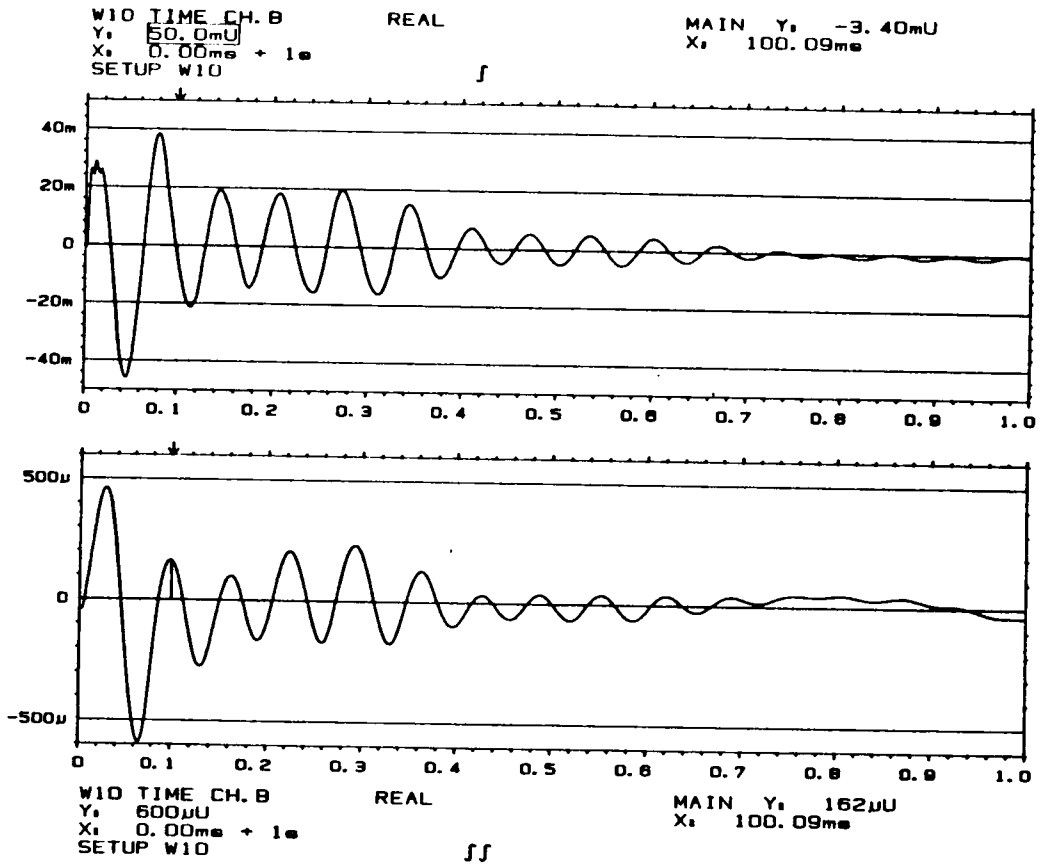

Integrated velocity and displacement due to impulse response.

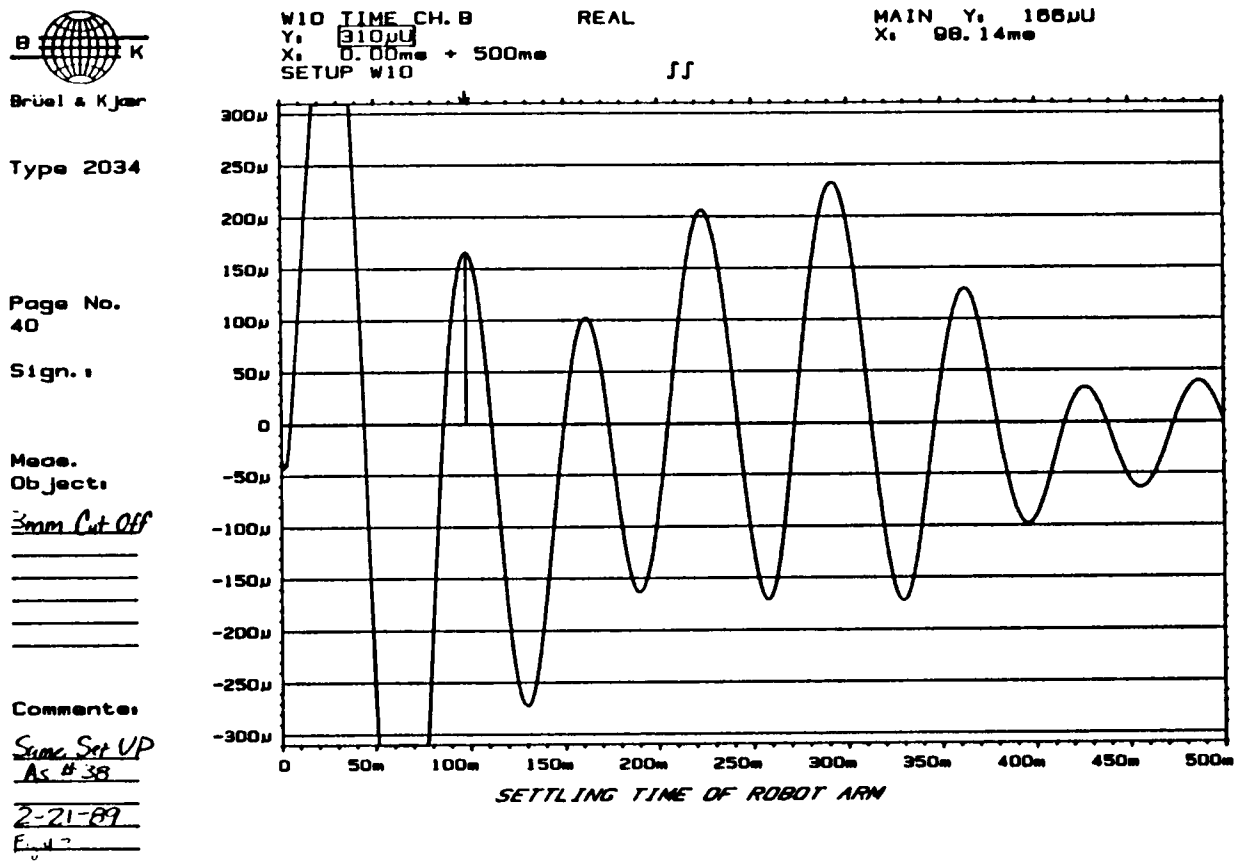

Z Arm displacement specification envelope.

The second settling time test was to use both channels of the signal analyzer to measure the output of the motor voltage, while simultaneously measuring the acceleration of the arm. The robot was programmed to move at top speed, from the home position to the center of the workspace and stop. The motor output voltage during this move indicated at what point the motors cut off. The time period after the motors cut off was the residual vibration of the arm. The time at which the motors stopped for this particular move was 659.17 msec. Therefore, this time was used as the delay time to trigger the accelerometer. The natural frequency of the arm did not change from this test, but the accelerations were 80 % lower than the accelerations of the impulse response test. This is due to the motor's ramping down to decelerate the system, therefore, lowering the vibration.

The integrations of this signal were erroneous. The reason for this may be that the initial conditions effect the integration of the signal. By assuming that the motion of the arm is harmonic, the displacement is proportional to the acceleration by the relation,

$$X = -a/w^2$$

Where "a" is the acceleration of the arm in inches/sec^2, and "w" is the frequency of vibration in rad/sec. Performing this calculation on the first peak with a = 0.78G and w = 94.25 rad/sec, the displacement equals 0.034 inches. Therefore, the arm is never beyond the desired specification of 0.118 inches.

The damping ratio for the first five cycles was 0.043. Five cycles later, the damping ratio decreased to 0.025. The plots taken for this test are shown on the next four pages.

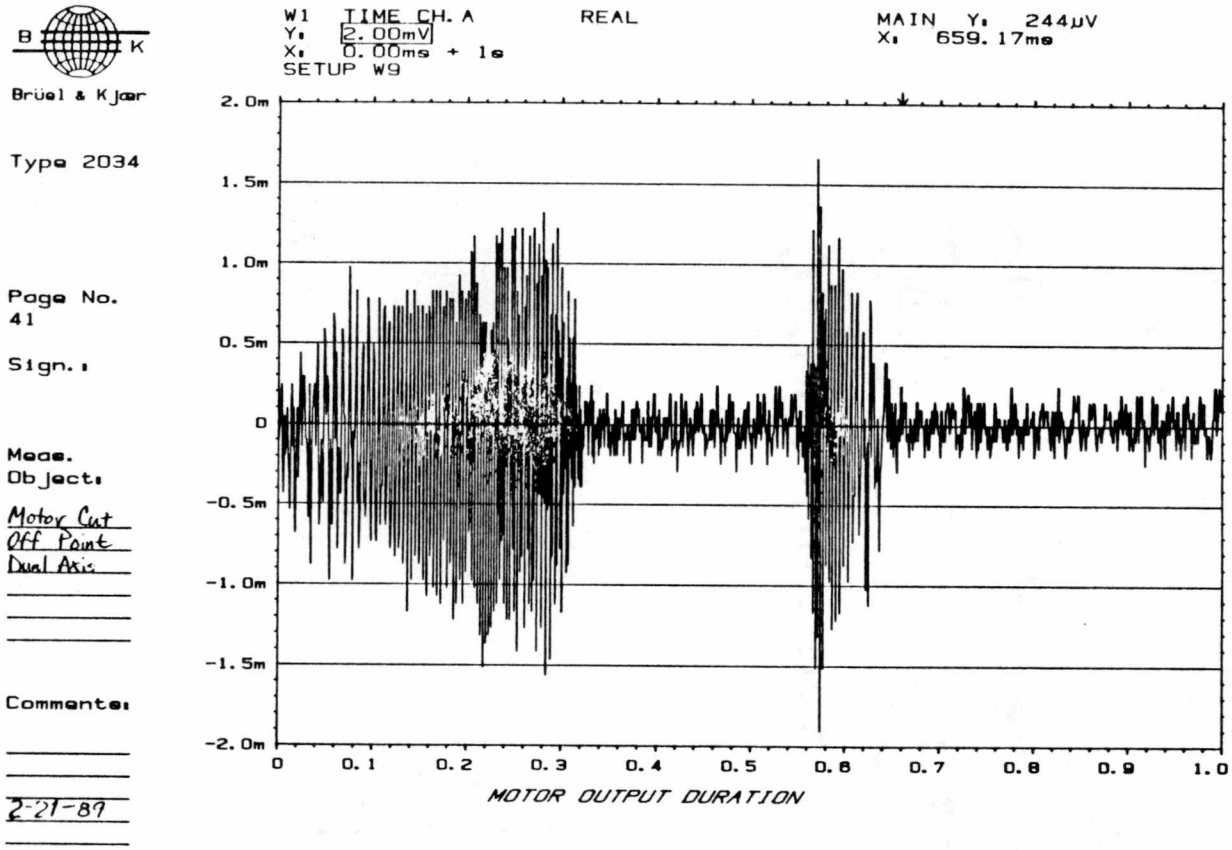

Motor pulse duration during move.

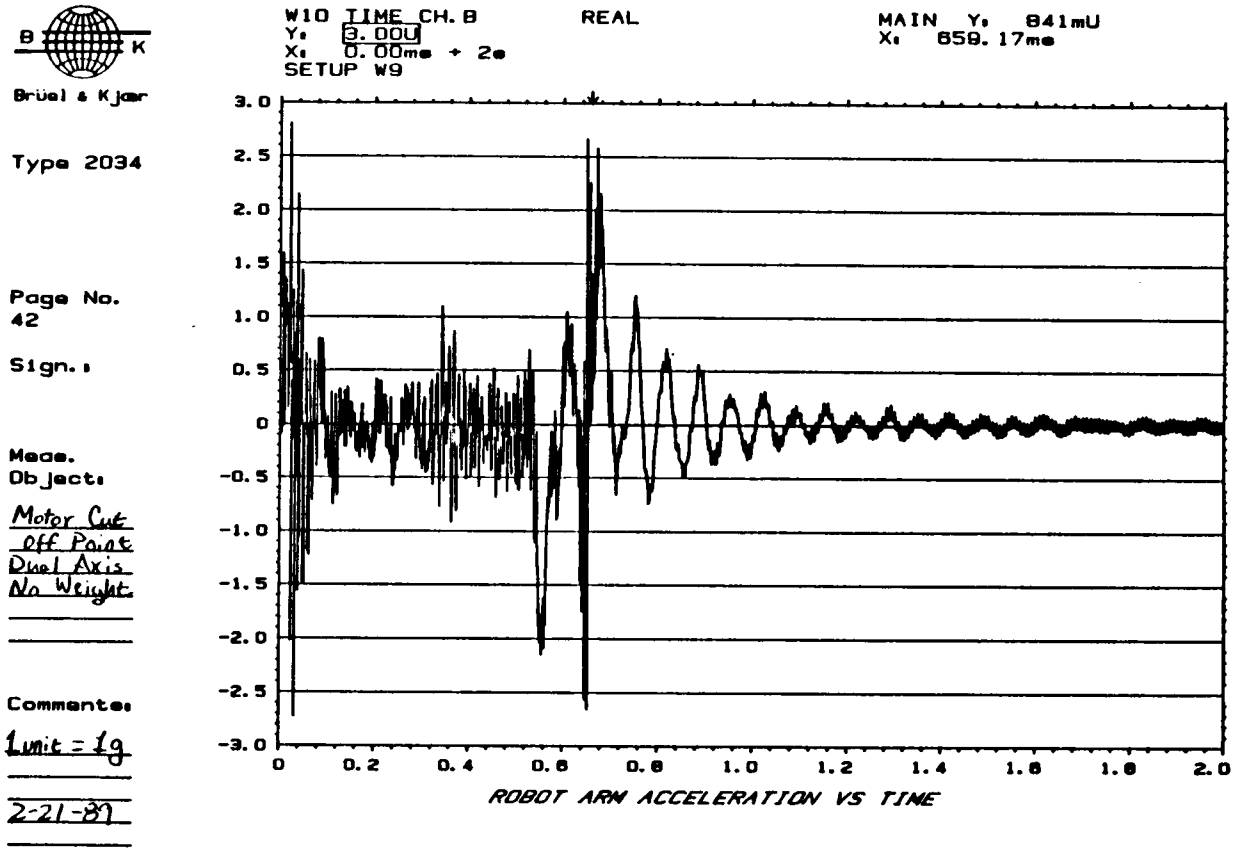

Z Arm acceleration over time during move to center.

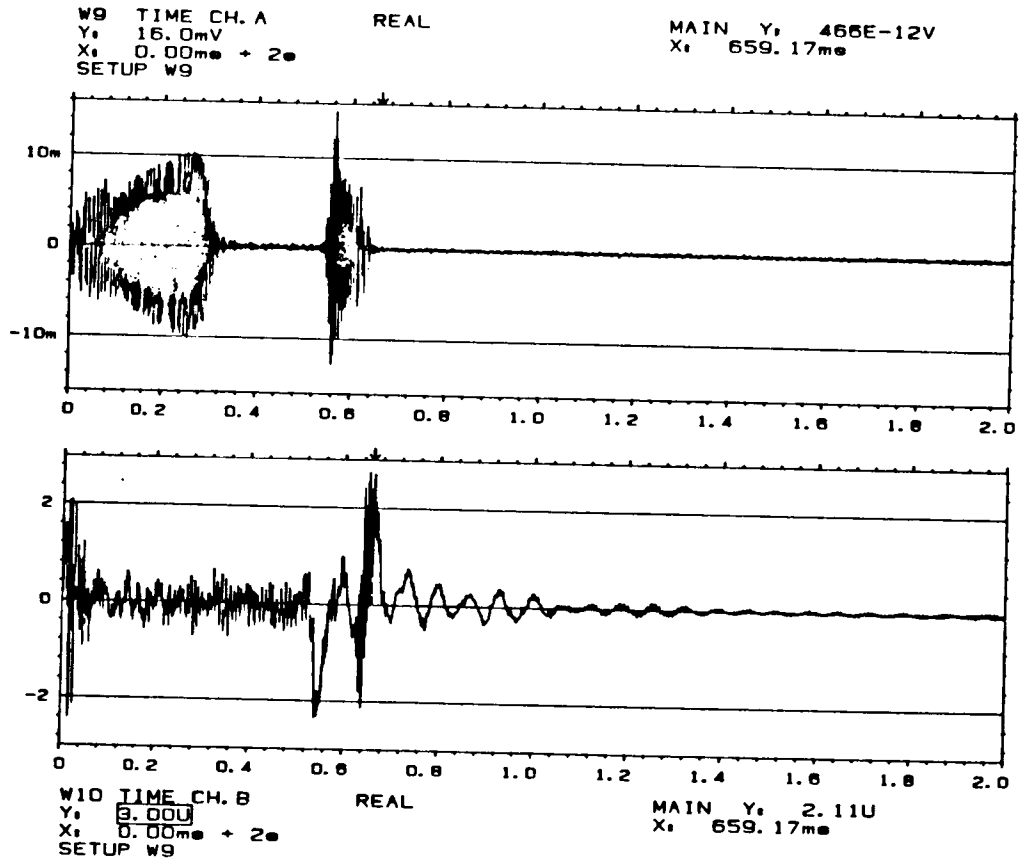

Dual channel output of motor pulse and Z Arm acceleration.

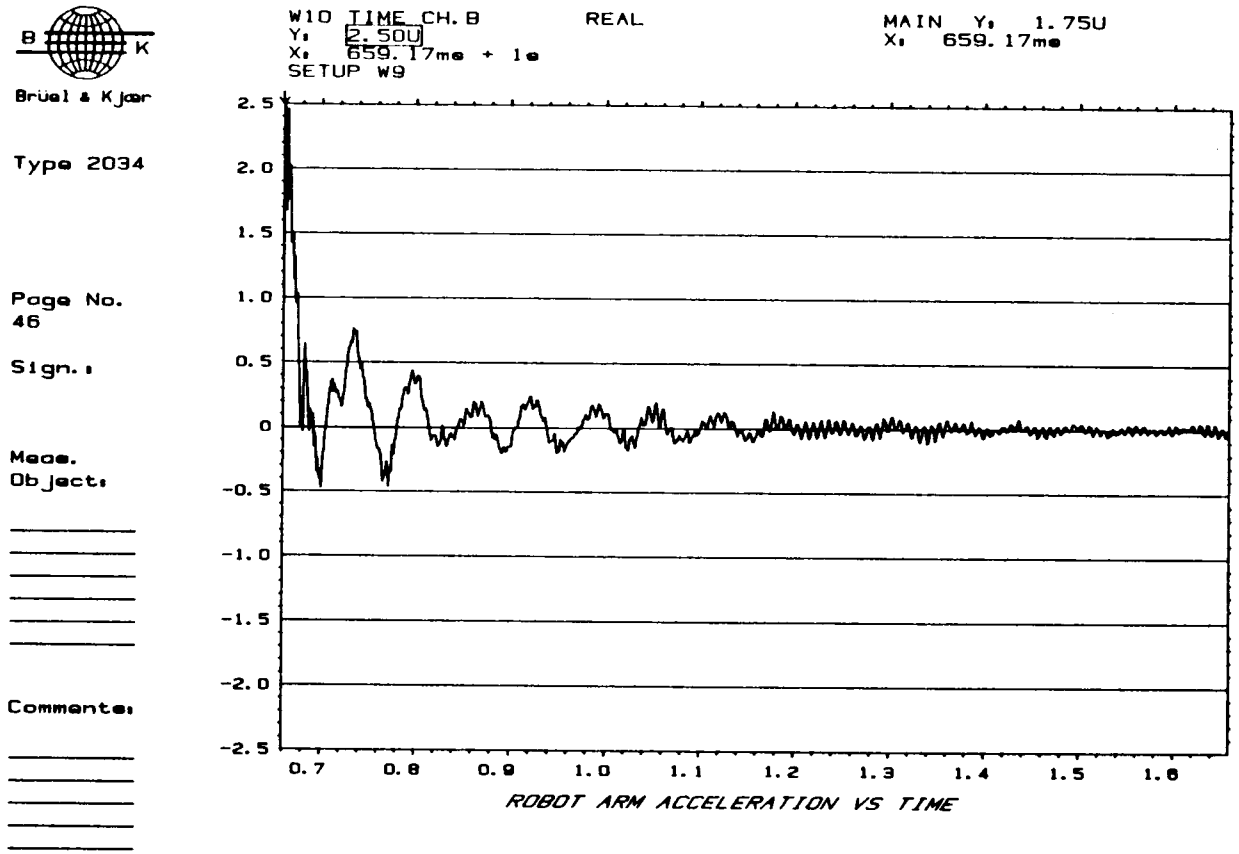

Residual vibration of Z Arm following motor cutoff time.

The final test was to use the delay time for the accelerometer, found in the previous test, to measure the residual vibration of the arm. This test consisted of two runs, both with the arm fully extended, but with increasing weight added to the wrist adaptor. The first run was with 2.6 pounds added to the wrist adaptor. High frequency noise was present at a frequency of 120Hz. The addition of weight reduced the frequency of vibration by 38 %, to 58.43 rad/sec, or 9.3 Hz. The accelerations of the arm were also lower, approximately by the ratio of the natural of the arm with payload to that of the arm without payload. The damping ratio for the first five cycles was 0.02. This decreased to 0.012 over the next five cycles.

The displacement of the arm can be approximated. The first peak had an acceleration of, $a = 0.6G$. For $w = 58.43$ rad/sec, the displacement equals 0.068 inches. The plot from the first run is shown on the next page.

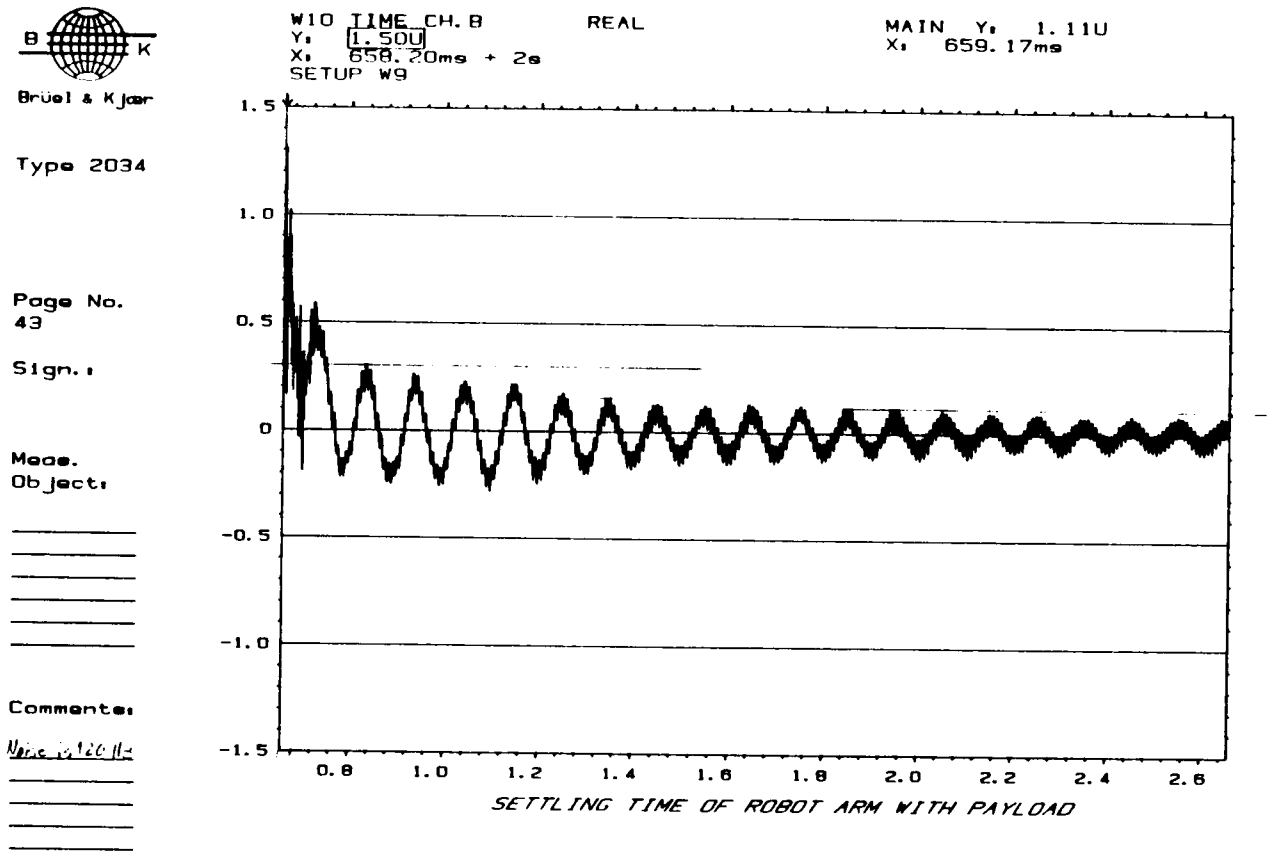

Z Arm residual vibration with 2.6 pound payload.

The final run was to measure the residual vibration of the arm, with a 3.5 pound payload. The frequency was lower for this test, 52.15 rad/sec, or 8.3 Hz. The damping ratio for the first five cycles was 0.031. This ratio decreased to 0.022 over the next five cycles.

The displacement of the first peak of the residual vibration was calculated to be 0.056 inches, where the acceleration was 0.396G. The next page shows the plot generated from this test.

The results form the settling time tests show that the arm meets the desired performance criteria of settling to within an amplitude of ±0.118 inches with 0.1 second.

The results from the tests are tabulated below.

Settling Time Test Results

Payload (lb)	Natural Freq. (Hz)	Max. Displ. (in)	Time (sec)	Damping Ratio (1st 5 cycles)	Damping Ratio (Next 5 cycles)
None	15	0.034	0.076	0.043*	0.025*
2.6	9.3	0.068	0.061	0.02	0.012
3.5	8.3	0.056	0.14	0.031	0.022

*These ratios were calculated using the first eight cycles.

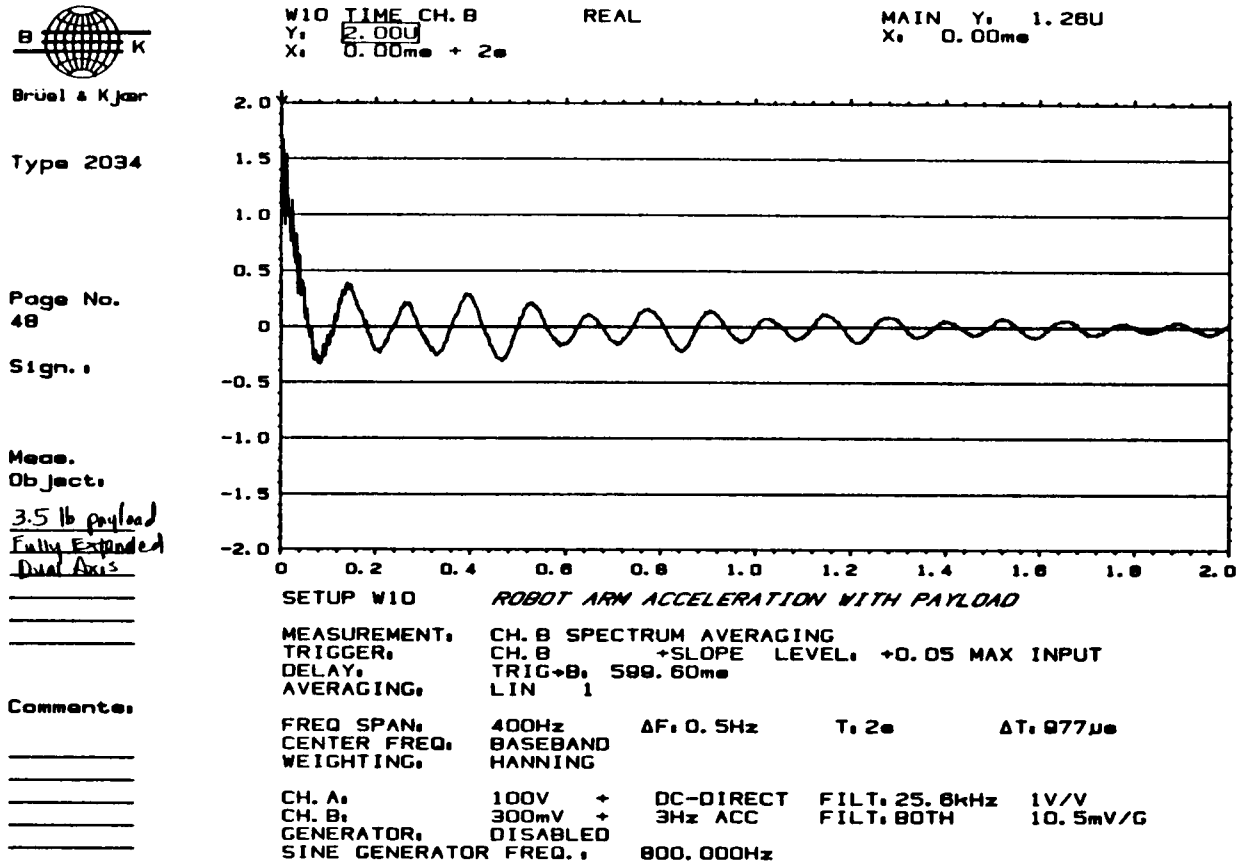

Acceleration versus time for the arm with a 3.5 pound payload.

APPENDIX G

PVC Pull Test Data

The PVC plastic used for the prototype to model injection molded parts was bonded together with PVC cement. The strength of the cement was tested in five pull tests, using an Instron tensile tester equipped with a strip recorder. The tests used strips of PVC, 7/8 of an inch wide and 3/16 of an inch thick. Four specimens, were made to test the cement's strength in a lap joint and a butt joint of the PVC strips.Two samples were made to test a lap joint of the PVC. The glue area was 0.875 in^2. One of the lap joints was filed before cementing, to roughen its surface, while the second specimen's surface was prepared by using only the PVC primer. The strip chart from the test is shown on the next page. The chart speed was two inches per minute, with 1000 lbs full chart scale. The filed lap joint sample, failed at a load of 572 pounds. The pull rate was 0.2 in/min. The shear stress for the specimen is given by,

$$\begin{aligned} \tau &= P/A \\ &= 572/0.875 \\ &= 654 \text{ psi} \end{aligned}$$

The test on the second lap joint sample had the same glue area as the first sample. The pull rate of the tester was reduced to 0.1 in/min. This joint withstood 800 lbs before failure, which produced a shear stress of 914 psi.

The next two tests of the cement was to bond the PVC strips together using a butt joint. Both samples were primed with the PVC primer before they were bonded together, but the first specimen was also filed to roughen its surface. The pull rate of the tester was 0.1 in/min. The area of the butt joints was 0.137 in^2. Both samples failed when the axial load reached 170 pounds. This produced a stress of,

$$\begin{aligned} \sigma &= P/A \\ &= 170/.137 \\ &= 1243 \text{ psi} \end{aligned}$$

The final test was to pull a solid piece of PVC with a 0.137 in^2 cross-sectional area until it failed. The pull rate for this test was 0.1 in/min, with 5000 pounds full chart scale. The strip of PVC failed at 1275 lbs. This produced an axial stress of 9306 psi. A typical area of one of the Z Platform's joints is 0.375 in^2. If the stress on the joint was 654 psi, the force on the joint 245 lbs. This force is approximately a factor of 10 greater than the expected loads on the robot. Therefore, the PVC cement was used to bond together the plastic parts. The strip chart from the pull tests is shown on the next page.

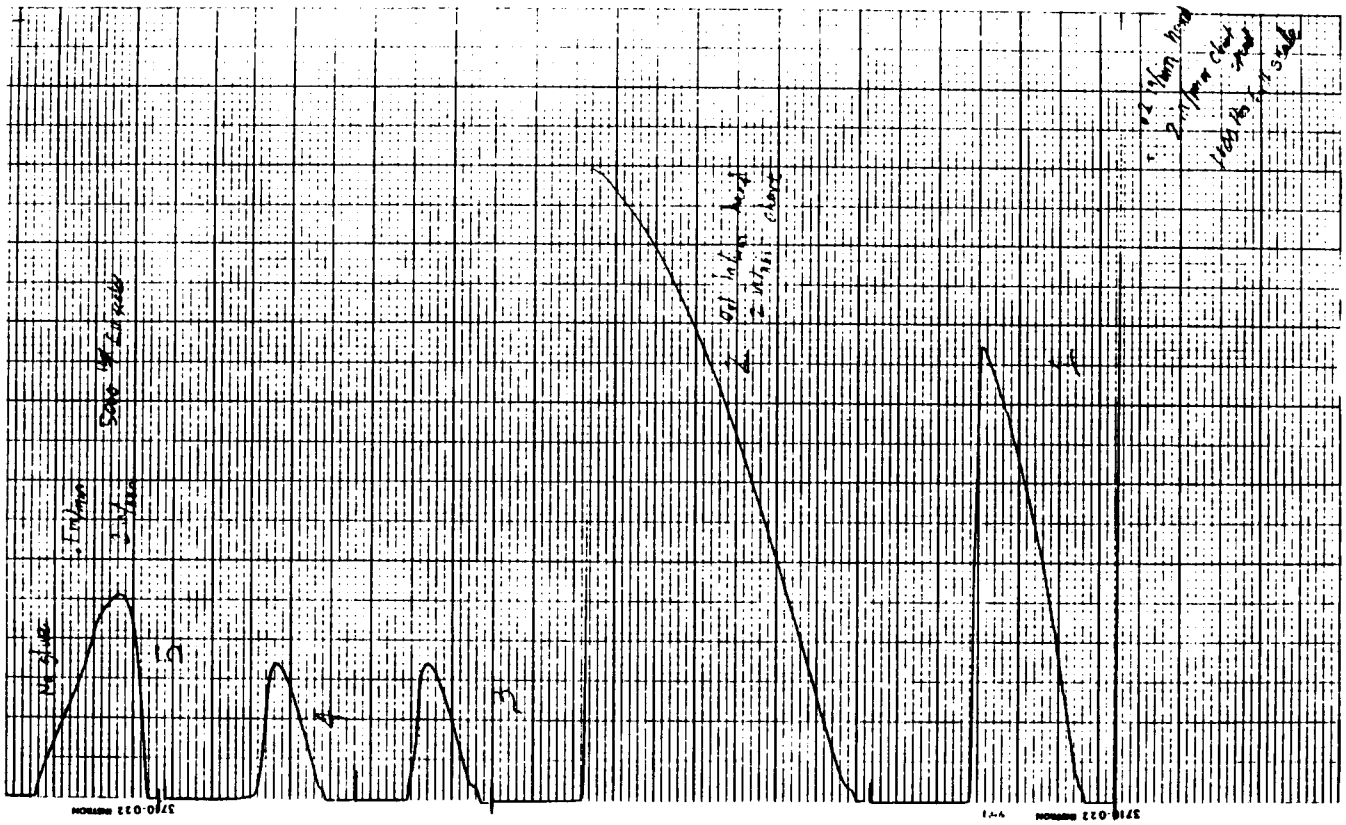

Instron strip chart from PVC pull test.

APPENDIX H

Prototype Pictures

The next four pages contain photographs taken of the prototype.

(1) View of robot showing the X-Y Plus system and frame.

(2) Corner view showing how sliders set the control tube spacing.

(3) Overhead view of the Z Platform assembly.

(4) Close-up view of Z Platform.

(5) Close-up view of the Z Arm assembly.

(6) Home position showing corner bracket, stepper motors, photocells and belt tensioners.

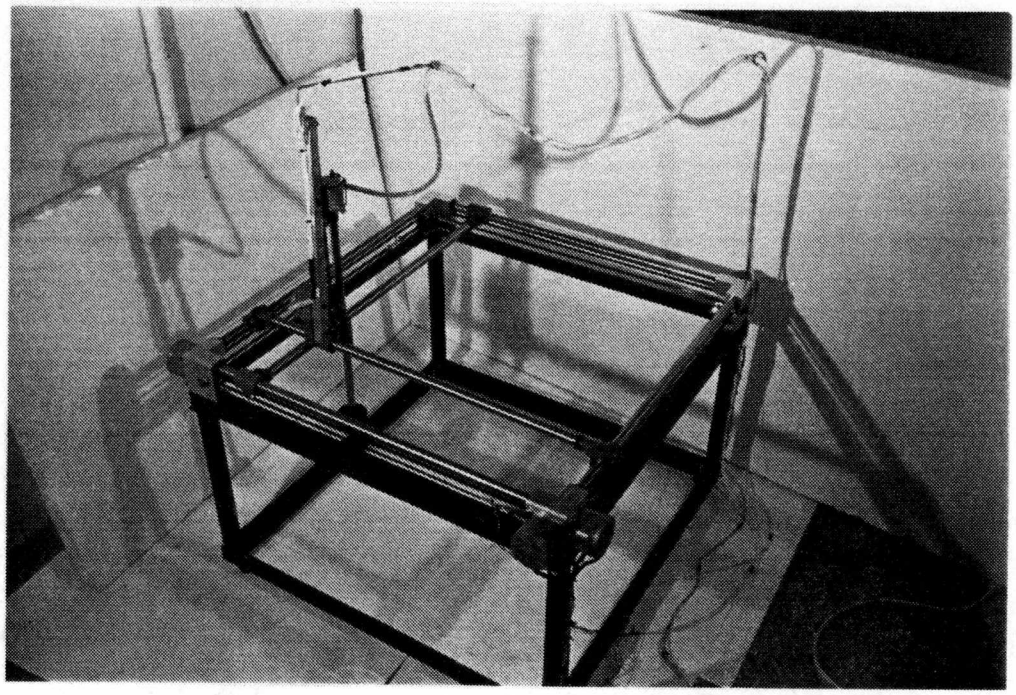

View of robot showing the X-Y Plus system and frame.

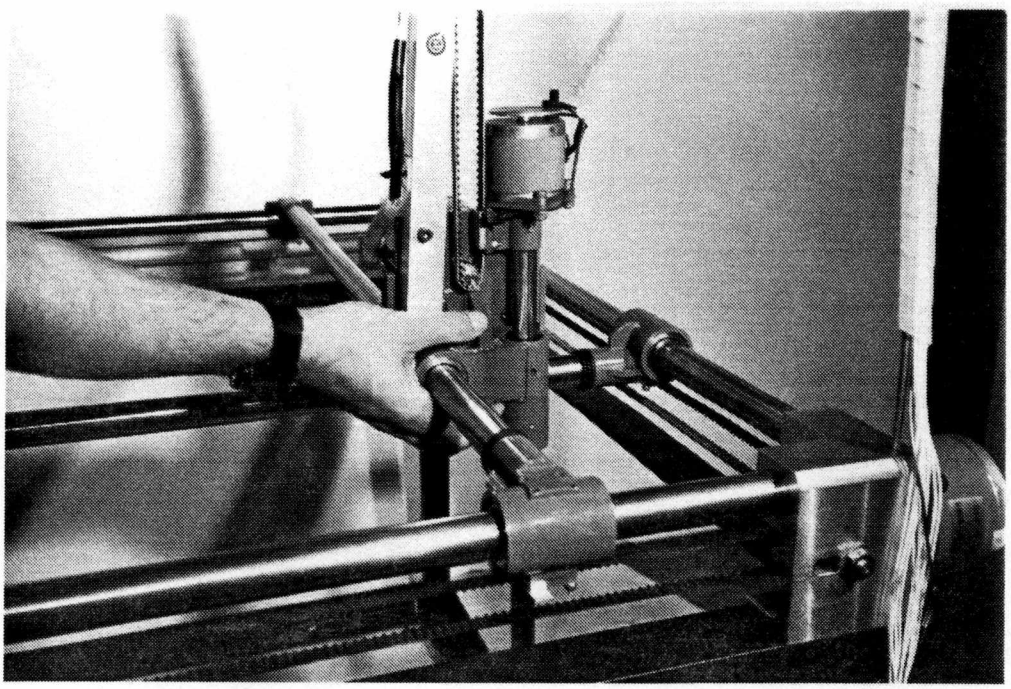

Corner view showing how sliders set the control tube spacing.

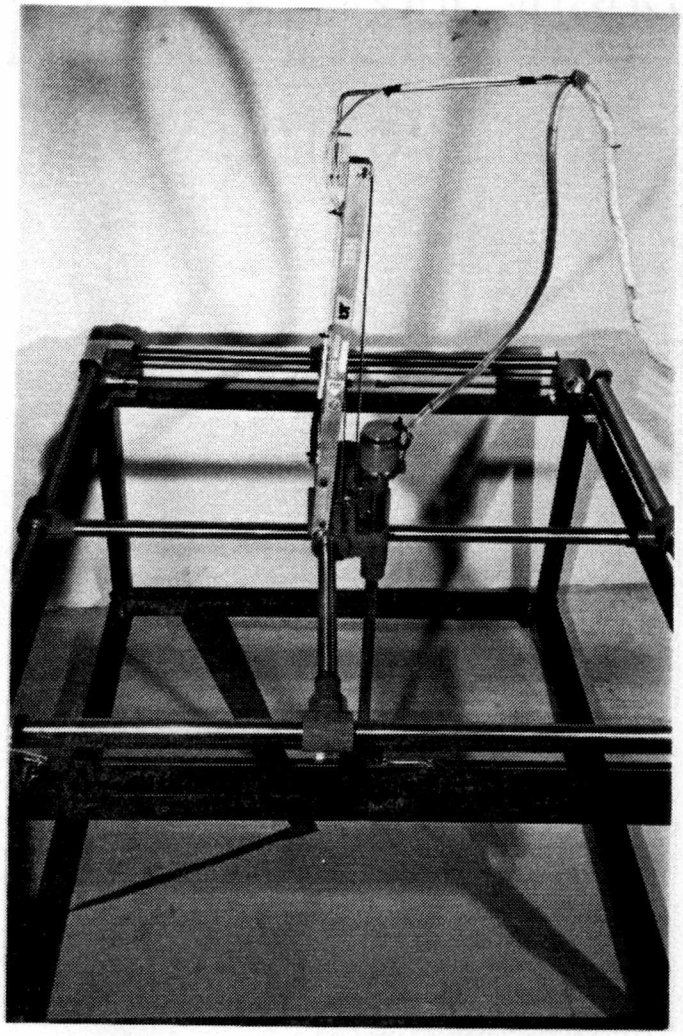

Overhead view of the Z Platform assembly.

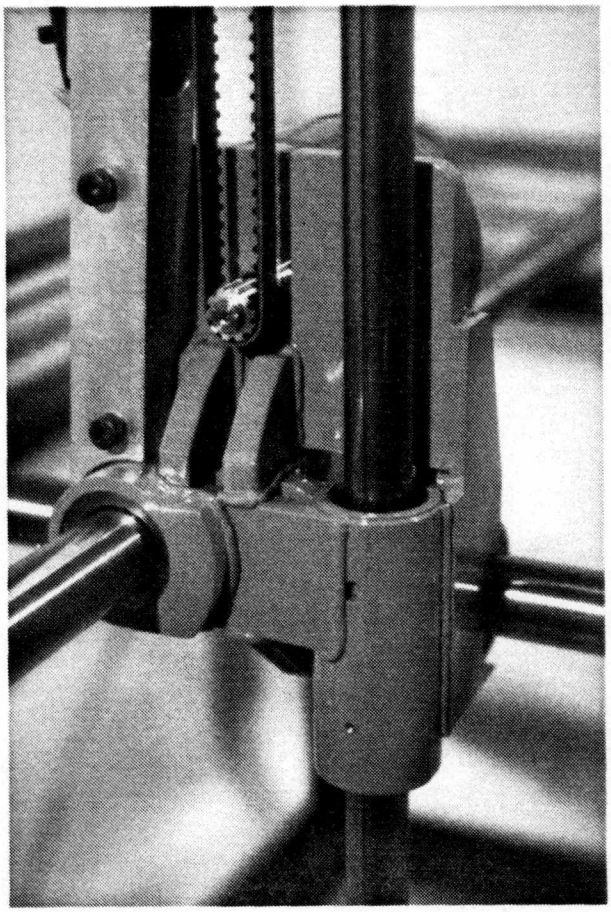

Close-up view of the Z Platform.

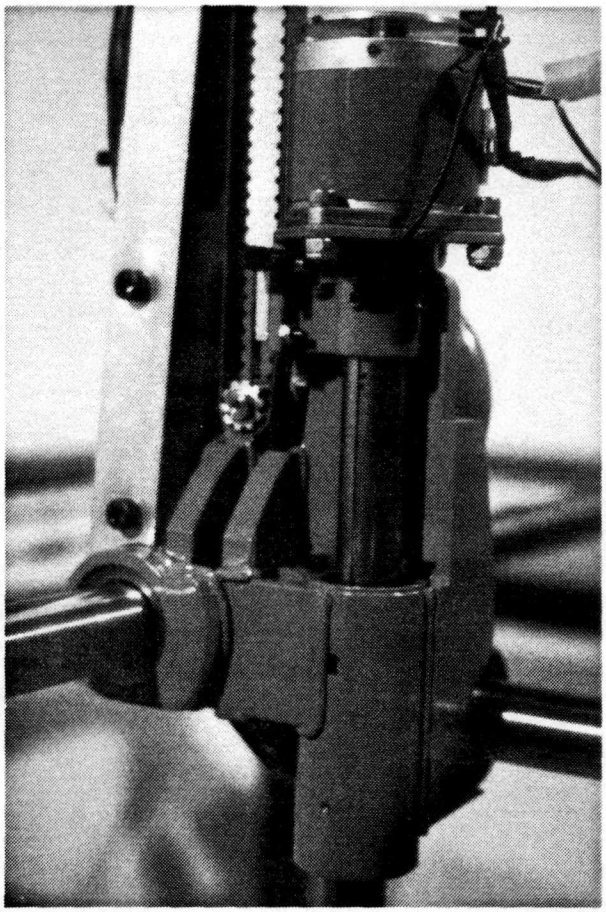

Close-up view of the Z Arm assembly.

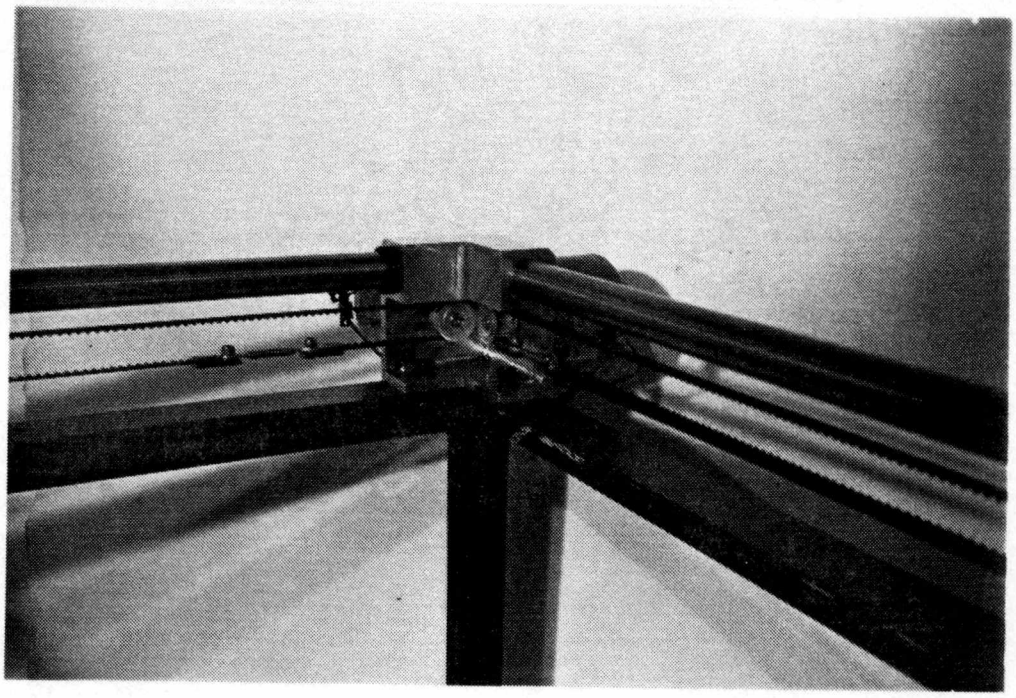

Home position showing corner bracket, stepper motors, photocells and belt tensioners.

APPENDIX I

Vendors and Price References

VENDORS

Product	Address	Contact
Self-Clinching Fasteners	Lee Limited P.O. Box One Bethania, NC 27010 (919) 924-8245	Robert E. Lee III
Linear Motion Bearings	Thomson Industries, Inc. Manhasset, NY 11030 (516) 883-8000	Jamie Dekorte
Structural Steel	Blount Steel Supply 409 Home Avenue Maryville, TN (615) 637-7583	Greg Russell

ROBOT PRICE REFERENCES

The price references for the X-Y Plus positioning mechanism and the Z Platform are listed below.

Part	Individual Cost	Quantity	Price Reference
X-Y Plus Positioning Mechanism			
Corner Bracket	1.00	4	P. Hackenworth-IBM
Slider Bracket	5.00	4	R. Mansur-IBM
Belt Gripper	1.00	4	P. Hackenworth-IBM
2.1 Amp Stepper Motor/Driver	45.00	4	Sanyo Step-Syn
Guide Shaft	2.00/ft	12 ft	Motion Industries
Control Tube	1.75/ft	5.875 ft	Motion Industries
Linear Motion Bearings	17.79	4	Dixie Bearing
Timing Gears	1.00	8	Matt Galatha-IBM
Timing Belt	3.00	4	Matt Galatha-IBM
Needle Bearings	1.45	4	Stock Drive
Idler Shaft	2.00	4	Matt Galatha-IBM
Electrical Control	90.00	1	Siak Yeo-UT
Hardware	4.00	1	Mark Granger-UT
Z Platform Assembly			
Z Platform	9.50	1	R. Mansur-IBM
Tube Mount	3.60	1	R. Mansur-IBM
Belt Gripper	1.00	1	Matt Galatha-IBM
2.1 Amp Stepper Motor/Driver	45.00	1	Sanyo Step-Syn
1.1 Amp Stepper Motor/Driver	16.00	1	Sanyo Step-Syn
Vertical Guide Tube*	125.87	1	Blount Steel
Drive Tube*	16.29	1	Blount Steel
Drive Spindle*	22.48	1	Blount Steel
Linear Motion Bearings	17.79	2	Dixie Bearing
Self-Aligning Ball Bushings	9.18	2	Dixie Bearing
Radial Bearings	13.87	2	Berg
Needle Bearings	1.45	1	Stock Drive
Mast*	57.87	1	Blount Steel
Timing Gears	1.00	2	Matt Galatha-IBM
Timing Belt	3.72	1	Motion Industries, Inc.
Wire Pivot	1.60	1	R. Mansur-IBM
Wire Boom	5.74	1	Blount Steel
Hardware	5.00	1	Lawrence Garrett-UT
Frame*	180.67	1	Blount Steel

*Machining time estimates provided by Daniel Graham, Machinist at the Department of Mechanical Engineering, University of Tennessee, Knoxville.

APPENDIX J

Robot Assembly Procedures

ROBOT ASSEMBLY PROCEDURES

A list of the tools required to completely assemble the robot is given below. The part(s) for which the tool is needed is listed in parentheses.

(1) 9/16 socket with driver (corner bracket locknuts)

(2) 5/8 open end wrench (corner bracket idlers)

(3) 9/16 open end wrench (frame feet)

(4) 7/16 open end wrench (z motor mounts)

(5) 3/8 open end wrench (mast idler, yaw motor mounts)

(6) 1/4 box end wrench (timing belt hangers)

(7) Wide slot head screwdriver (z motor mounts)

(8) Narrow slot head screwdriver (belt tensioners)

(9) Allen keys needed:

- (a) 5/16 (corner bracket bolts)
- (b) 1/4 (frame bolts)
- (c) 3/16 (mast bolts)
- (d) 5/32 (yaw motor mount bolts)
- (e) 1/8 (wrist adaptor set screw, z-idler)
- (f) 3/32 (tube mount screws)
- (g) 5/64 (x-y pulley set screws)
- (h) 0.05 (bearing set screws)

(10) Two wooden blocks 2 3/4 inches high

(11) Level

(1) Frame Assembly Instructions

The frame is bolted together by matching the appropriate letters and numbers that are stamped on the vertical legs to those stamped on the horizontal members. The letters are on the top side of the

frame. Care should be taken to ensure that each bolt is tight. The frame should then be leveled by adjusting the rubber feet that the frame rests on. The following page is a plot of the robot assembly showing the proper alignment.

(2) X-Y Plus Assembly and Alignment Procedure

Once the frame is assembled, the X-Y positioning system is aligned on top of the frame.

(a) Locate the corner bracket that is stamped "C".

(b) Place this corner bracket in the corner of the frame stamped "C". Bolt the corner bracket down using the two 3/8 inch bolts and the nylon locknuts, making sure that it is square with the corner of the frame. This is the datum corner, to which the remainder of the X-Y Plus System will be aligned.

(c) Locate the outer guide shaft and the corner bracket that are stamped "D", and one of the two sliders that lower the control tube below the level of the outer guide shafts. (Note that the timing belt attachment point is always pointing down on all of the sliders).

(d) Insert the end of guide shaft "D" into the "C" corner bracket and slide on the selected slider onto the guide shaft. Place the "D" corner bracket on the other end of the guide shaft, making sure that the corner bracket is in the correct corner of the frame marked "D". Do not bolt down this corner bracket yet, but insert one of the bolts to hold it in position.

(e) Locate the outer guide shafts marked "A" and "C". Place the "A" shaft into the "D" corner bracket, and the "C" shaft into the "C" corner bracket.

(f) Find the two matching sliders that raise the control tubes, and one of the control tubes. Slide the Z Platform onto the control tube, using its upper bearing. Make sure that front of the Z Platform is facing the rubber bumpers on the control tube. Place the matching sliders onto the ends of the control tube.

(g) With the front of the Z Platform facing left, slide this assembly onto the two

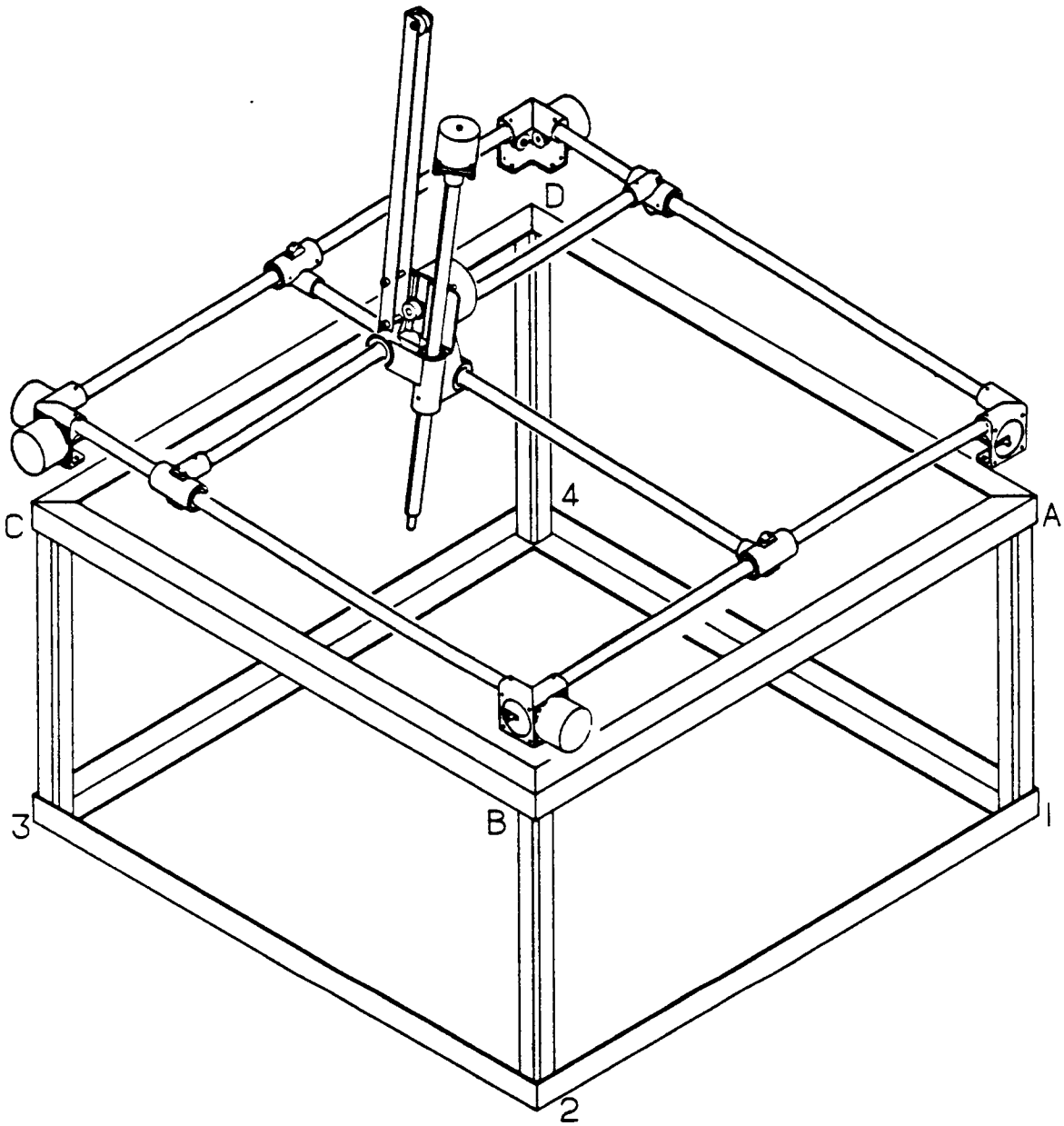

Robot assembly showing alignment marks.

guide shafts that are sticking out of the corner brackets. (Note that the Z Platform will have to be rotated sideways in order to clear the frame, if it has already been assembled. Also the center of mass of the Z Platform is very near its upper bearing when the Z Arm is fully extended).

(h) Slide the assembly about one foot down the guide shafts, and chock the ends of the guide shafts using the two wooden blocks.

(i) Locate the remaining control tube and insert the end without the rubber bumpers through the lower bearing in the Z Platform and into the socket of the slider on the opposite side.

(j) Make an assembly out of the remaining two corner brackets, the fourth guide shaft and the last slider. Make sure that the rubber bumpers are on the side of the "B" corner bracket, and that the slider is inserted with the timing belt underneath the outer guide shaft.

(k) Offer up this assembly, with the "B" corner bracket on the left, to the free ends of the guide shafts. Once the corner brackets begin to slide onto the shafts, place the free end of the control tube into the slider. Now the assembly can be pushed all the way in until the guide shafts bottom out on the corner brackets.

(l) With the system complete, align the corner brackets to their respective holes and insert the remaining bolts, but do not tighten. Check to see if the system is aligned by moving each control tube by hand. With a light push, each control tube should move freely from one end to the other. If this is not the case, adjust the corner brackets with the bolts still in place. Once the robot moves freely and effortlessly, secure each corner bracket to the frame.

(3) Z Platform Assembly Instructions

(a) Place the motor with its timing gear into its mounting face on the back of the Z Platform. Mount the motor to the platform, using the two flat head machine screws that fit into the two holes on the right side of the Z Platform.

(b) With the timing belt already attached to the Z Arm (see Part 4), Loop the timing belt through the idler pulley, insert the shoulder bolt through the mast, spacer and idler, then secure with the nylon lock nut.

(c) Insert the Z Arm into its bearings with the belt gripper facing the center of the motor. Make sure that the two bearing's ball tracks, that are under the set screws, are in their respective grooves. Adjust the bearings by tightening the two bearing set screws on the Z Platform, until the bearings bind. Then loosen the set screws until the arm begins to move freely.

(d) Loop the timing belt over the motor drive gear, and extend the Z Arm until the tube mount comes into contact with the Z Platform.

(e) Mount the mast onto the platform by first lining up its holes with the Z Platform, and then inserting one of the cap head screws into the upper mounting hole. Place the lock nut on the back side of the motor and tighten until the mast is tight, but can still rotate about the screw.

(f) Insert the lower bolt through the mast and tighten the lock nut until it begins to bottom out.

(g) Tighten the timing belt by placing the upper end of the mast on a table with the timing belt side against the table. Tighten the two locknuts while pushing the Z Platform down to tension the belt.

(h) Slide the wiring boom with its pivot onto the end of the mast.

(4) Z Arm Assembly Instructions

(a) Slide the tube mount onto the vertical guide tube. Line up the hole in the vertical guide tube that is on the groove, with the hole in the tube mount that places the belt mount surface parallel to the plane of the grooves. Secure the tube mount onto the guide tube with the two set screws.

(b) Insert the drive spindle into the bearing cartridge, and insert this into the lower end of the vertical guide tube, with the tongue of the drive spindle inside the guide tube.

(c) Insert the lower internal snap ring into the end of the vertical guide tube. Slide the snap ring spacer onto the drive spindle, until it clears the groove on the shaft for the external snap ring. Place the external snap ring onto the drive spindle.

(d) Align the punch mark on the side of the drive spindle with the groove that has the set screw. Align the red dots on the side of the calibration disk and the Yaw motor. Insert the motor with is drive tube through the tube mount. If the red dots are in line with the punch mark on the drive spindle, the motor will become flush with the mounting surface on the tube mount. Secure the Yaw motor to the tube mount.

(e) Secure the timing belt onto the Z Arm by meshing the belt gripper onto the timing belt and securing the four locknuts. Make sure that the photocell for the vertical home position is secured to the tube mount.

VITA

Lawrence Mancil Garrett was born on December 23, 1963 in Huntsville, Alabama. In 1968, he moved to Oak Ridge, Tennessee. A graduate of the Oak Ridge School System in 1981, he entered the University of Tennessee in Fall of 1981, and received his Bachelor of Science degree in December 1986. He then entered graduate school with an emphasis in machine design. A graduate teaching assistantship at the Engineering Computer Center, the University of Tennessee, Knoxville, involved teaching students to use CADAM, and being a system operator for a PRIME 750 computer. This work included writing an operators manual, and creating training exercises for MEDUSA CAD software. Another project included using ANSYS and Mtab/SAP86 finite element packages to perform a stress analysis on a plastic automobile part.

He received his Master of Science in Mechanical Engineering in May 1989. Larry's interests include numismatics, automobile restoration, bicycling, and flying disc sports.